

*Ph.D Thesis*

**A Beacon based Localization System for Autonomous  
Mobile Robots and its Applications in Traffic and  
Transport Control**

*Submitted to*

**Cochin University of Science and Technology**

*In partial fulfilment of the requirements for the award of the degree of*

**Doctor of Philosophy**

*by*

**JAMES KURIAN**

*Under the guidance of*

**Dr. P. R. SASEENDRAN PILLAI**

**DEPARTMENT OF ELECTRONICS  
FACULTY OF TECHNOLOGY  
COCHIN UNIVERSITY OF SCIENCE AND TECHNOLOGY  
COCHIN, INDIA 682 022**

OCTOBER 2008

# **A Beacon based Localization System for Autonomous Mobile Robots and its Applications in Traffic and Transport Control**

**Ph.D Thesis in the field of Mobile Robotics**

## **Author**

**JAMES KURIAN**

Department of Electronics  
Cochin University of Science and Technology  
Cochin,  
Kerala,  
India 682 022  
Email:james@cusat.ac.in

## **Research Advisor**

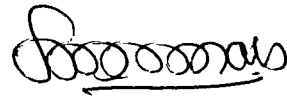
**Dr. P. R. SASEENDRAN PILLAI**

Professor  
Department of Electronics  
Cochin University of Science and Technology  
Cochin,  
Kerala,  
India 682 022  
Email:prspillai@cusat.ac.in

OCTOBER 2008

## CERTIFICATE

This is to certify that this thesis entitled “**A Beacon based Localization System for Autonomous Mobile Robots and its Applications in Traffic and Transport Control**” is a bona fide record of the research work carried out by **Mr. James Kurian** under my supervision in the Department of Electronics, Cochin University of Science and Technology. The results presented in this thesis or parts of it have not been presented for the award of any other degree(s).



**Dr. P. R. Saseendran Pillai**

(Supervising Guide)

Professor

Department of Electronics

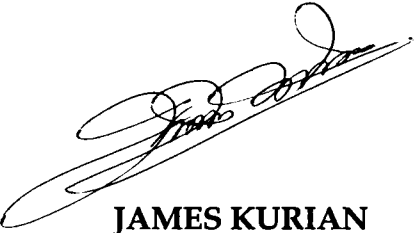
Cochin University of Science and Technology

Cochin\_22  
20-10-2008

## DECLARATION

I hereby declare that the work presented in this thesis entitled **“A Beacon based Localization System for Autonomous Mobile Robots and its Applications in Traffic and Transport Control”** is based on the original research work carried out by me under the supervision of **Dr. P. R. Saseendran Pillai**, Professor, in the Department of Electronics, Cochin University of Science and Technology. The results presented in this thesis or parts of it have not been presented for the award of any other degree.

!



**JAMES KURIAN**

Cochin - 22

20.10.2007

## ACKNOWLEDGEMENTS

I would like to express my heartfelt gratitude to my research guide Dr. P. R. Saseendran Pillai, Professor, Department of Electronics, Cochin University of Science and Technology for his guidance, support and timely advice. I could not have completed the thesis without his encouragements and valuable suggestions.

Let me express my sincere gratitude to Prof. (Dr.) K. Vasudevan, Head of the Department for his encouragements and support extended to me.

My heartfelt debt and thanks goes to my teachers and former heads of the department Prof. (Dr) K. G. Nair and Prof. (Dr) K. G. Balakrishnan, for their advice and encouragements to move forward.

It is also the time to acknowledge my personal debts to my teachers Prof. (Dr) C. S. Sridhar, and Prof. (Dr) K. Poulose Jacob for their love and encouragements during the past years.

I would like to express my thanks and appreciation to Dr. V. P. N. Namboori, International School of Photonics for the fruitful discussions.

My special thanks to Dr. K. T. Mathew, Dr. P. Mohanan, Dr. Tessamma Thomas, Dr. C. K. Anandan and all other colleagues, friends and research scholars who helped me in various ways.

Let me also remember at this moment my friends Dr. P. Ramakrishnan, Dr. Babu P. Anto, Dr. N. K. Narayanan and Dr. K. K. Narayanan for their love and companionship.

I would also like to express my thanks to Dr. T. K. Mani and Girish. G for their support and help.

I thank all the library and administrative staff of the department for their co-operation and support.

I also take this opportunity to thank all the technical staff, M.Tech and M.Sc students of the department for their help.

I would like to thank all of the people who have helped, encouraged and supported me during the period of my research work.

I remember the most valuable support from my wife Mariamma, thank you for your constancy in love, support and understanding.

# ABSTRACT

## A Beacon based Localization System for Autonomous Mobile Robots and its Applications in Traffic and Transport Control

ACCURATE sensing of vehicle position and attitude is still a very challenging problem in many mobile robot applications. The mobile robot vehicle applications must have some means of estimating *where they are* and in *which direction they are heading*. Many existing indoor positioning systems are limited in workspace and robustness because they require clear lines-of-sight or do not provide absolute, drift-free measurements.

The research work presented in this dissertation provides a new approach to position and attitude sensing system designed specifically to meet the challenges of operation in a realistic, cluttered indoor environment, such as that of an office building, hospital, industrial or warehouse. This is accomplished by an innovative assembly of infrared LED source that restricts the spreading of the light intensity distribution confined to a sheet of light and is encoded with localization and traffic information. This Digital Infrared Sheet of Light Beacon (**DISLiB**) developed for mobile robot is a high resolution absolute localization system which is simple, fast, accurate and robust, without much of computational burden or significant processing. Most of the available beacon's performance in corridors and narrow passages are not satisfactory, whereas the performance of **DISLiB** is very encouraging in such situations. This research overcomes most of the inherent limitations of existing systems.

The work further examines the odometric localization errors caused by over count readings of an optical encoder based odometric system in a mobile robot due to wheel-slippage and terrain irregularities. A simple and efficient method is investigated

and realized using an FPGA for reducing the errors. The detection and correction is based on redundant encoder measurements. The method suggested relies on the fact that the wheel slippage or terrain irregularities cause more count readings from the encoder than what corresponds to the actual distance travelled by the vehicle.

The application of encoded Digital Infrared Sheet of Light Beacon (DISLiB) system can be extended to intelligent control of the public transportation system. The system is capable of receiving traffic status input through a GSM (Global System Mobile) modem. The vehicles have infrared receivers and processors capable of decoding the information, and generating the audio and video messages to assist the driver. The thesis further examines the usefulness of the technique to assist the movement of differently-able (blind) persons in indoor or outdoor premises of his residence.

The work addressed in this thesis suggests a new way forward in the development of autonomous robotics and guidance systems. However, this work can be easily extended to many other challenging domains, as well.



# CONTENTS

<b>ABSTRACT</b>	<b>XIII</b>
<b>LIST OF FIGURES</b>	<b>XIX</b>
<b>ABBREVIATIONS</b>	<b>XXV</b>
<b>Chapter 1 Introduction</b> .....	<b>1-12</b>
1.1 Background and Motivation	2
1.1.1 Mobile Robot Localization	4
1.1.2 Autonomous Localization Systems	5
1.2 Thesis Roadmap	8
1.3 Practical Systems	11
1.4 Summary	12
<b>Chapter 2 Review of Localization Systems</b> .....	<b>13-60</b>
2.1 Sensors for Mobile Robots	14
2.1.1 Proprioceptive Sensors	15
2.1.2 Exteroceptive Sensors	15
2.2 Tactile Sensors	16
2.3 Odometric Sensors	17
2.3.1 Optical Encoders	17
2.4 Electronic Compasses	18
2.5 Inertial Navigation Sensors	21
2.5.1 Accelerometers	22
2.5.2 Gyroscopes	24
2.5.2.1 Mechanical Gyroscope	24
2.5.2.2 Optical Gyroscope	26
2.5.2.3 MEMS Gyroscope	27
2.6 Beacon based Localization	31
2.6.1 Localization Techniques	32
2.6.1.1 Trilateration	33
2.6.1.2 Triangulation	35

2.6.2 Global Positioning System	36
2.7 Active Ranging Systems	42
2.7.1 Time-of-Flight Active Ranging	42
2.7.1.1 <i>The Ultrasonic Rangefinder (Sonar)</i>	43
2.7.1.2 <i>Laser Rangefinder (Lidar)</i>	45
2.7.1.3 <i>Radar Devices</i>	48
2.7.2 Structured light sensor	52
2.8 Motion Sensors	53
2.8.1 Doppler Effect-based Sensing (Radar or Sonar)	54
2.9 Vision-based Sensors	55
2.9.1 Visual Ranging Sensors	55
2.9.2 Stereo-Vision	56
2.9.3 Visual Guidance System	57
2.10 Map Based Positioning	57
2.11 Summary	60

## **Chapter 3 Methodology..... 61-67**

3.1 Mounting Assembly	62
3.2 The Development Support Systems	62
3.3 Beacon Transmitter	64
3.4 Beacon Receiver	64
3.5 DISLiB System	65
3.6 Beacon Networking	65
3.7 Error Reduction	66
3.8 Traffic Control	66
3.9 Visually Impaired Support	66
3.10 Summary	67

**Chapter 4 Digital Infrared Sheet of Light Beacon System ..... 69-96**

4.1 Brief History of Indoor Localization	71
4.2 Sheet of Light Beacon	73
4.2.1 Principle of operation	74
4.2.2 The beacon transmitter	79
4.3 Vehicle Localization	81
4.3.1 Method of Installation	82
4.3.2 The Beacon Receiver and Controller	83
4.3.3 The Beacon Performance and Evaluation	87
4.4 Resolution Enhancement	89
4.5 Position and Attitude update	91
4.6 Summary	96

**Chapter 5 Odometric Error Reduction System ..... 97-113**

5.1 The Odometric System	99
5.1.1 Position Measurement	99
5.1.2 Speed/Velocity Estimation	100
5.2 Position and Attitude Estimation	103
5.2.1 Position Updates from Encoder Data	103
5.2.2 The Error Reduction Technique	104
5.3 Implementation	106
5.3.1 The Sine/Cosine Module	107
5.3.2 The Realization Details	111
5.4 Summary	113

**Chapter 6 Applications of DISLiB System ..... 115-133**

6A Traffic and Transport Control	116
6A.1 Introduction	116

6A.2 Outline of Traffic Control System	118
6A.3 Infrared Sheet of Light Beacon	120
6A.4 The Beacon Receiver and Vehicle Unit	123
6A.5 Installation and Working	123
6B Differently-able Assistance	126
6B.1 Introduction	126
6B.2 Localization of the visually impaired	128
6B.3 The Beacon Receiver	129
6B.4 Position and heading	130
6C Summary	133
<b>Chapter 7 Conclusions</b>	<b>135-141</b>
7.1 Contributions	135
7.2 Highlights of the Work	136
7.3 Strengths and Limitations	138
7.4 Future Research	141
7.5 Summary	141
<b>Appendix</b>	<b>143-156</b>
A1.1 Introduction	144
A1.2 Robotic Workcell	146
A1.3 Robot Controller Design	147
A1.4 Control Program and User Interface	149
A1.5 Web Control Module	152
A1.6 Exercises	154
A1.7 Summary	156
<b>REFERENCES</b>	<b>157-169</b>
<b>LIST OF PUBLICATIONS</b>	<b>171-175</b>
<b>INDEX</b>	<b>177-179</b>

## LIST OF FIGURES

Figure 1.1	<i>A block diagram showing the general arrangement of a mobile robot Localization system.</i>	5
Figure 1.2	<i>The photographs of (a) <b>enon</b> and (b) <b>ASIMO</b></i>	11
Figure 2.1	<i>A quadrature encoder disc and the resulting channel A and B pulses.</i>	18
Figure 2.2	<i>Block diagram of a digital flux gate compass.</i>	20
Figure 2.3	<i>A commercially available Electronic Compass SP3003D from Sparton Electronics (2008).</i>	21
Figure 2.4	<i>Basic components of a one degree of freedom accelerometer.</i>	23
Figure 2.5	<i>A mechanical gyroscope Model.</i>	25
Figure 2.6	<i>Basic components of a fiber optical gyroscope.</i>	27
Figure 2.7	<i>Basic Structure of MEMS Gyro.</i>	29
Figure 2.8	<i>Functional block diagram of ADIS16251.</i>	30
Figure 2.9	<i>(a)The bias vs. time and (b) The sensitivity vs. angular rate at <math>\pm 80</math> degree per sec. range of ADIS16251.</i>	30
Figure 2.10	<i>Photograph of an iMEMS gyro chip</i>	31
Figure 2.11	<i>The estimation process</i>	33
Figure 2.12	<i>Trilateration method to obtain location of a mobile robot <math>P_4</math> from its distance from three stations located at <math>P_1</math>, <math>P_2</math> and <math>P_3</math></i>	34
Figure 2.13	<i>The basic triangulation problem on three observations <math>O_1</math>, <math>O_2</math> and <math>O_3</math></i>	35
Figure 2.14	<i>GPS Satellite signals.</i>	38
Figure 2.15	<i>The schematic of the GPS sub system.</i>	41
Figure 2.16	<i>Photograph of the GPS sub system studied.</i>	42
Figure 2.17	<i>UBG-05LN laser scanner from Hokuyo Automatic Company.</i>	47
Figure 2.18	<i>Block diagram of a MMW RADAR transceiver.</i>	49
Figure 2.19	<i>76GHz Millimeter Wave Automobile Radar using Single Chip MMIC.</i>	51
Figure 2.20	<i>Basic Structured Light Setup.</i>	53
Figure 2.21	<i>Architecture of a visual guidance system.</i>	57
Figure 2.22	<i>Block diagram of the concurrent map-based localization.</i>	59

Figure 3.1	<i>Photograph of the PIC Microcontroller Development Board</i>	63
Figure 3.2	<i>Photograph of the fabricated three wheeled prototype vehicle</i>	64
Figure 4.1	<i>Functional block diagram of a mobile robot vehicle control system.</i>	73
Figure 4.2	<i>The infrared LED of the beacon transmitter mounted on the structural assembly made up of sand blasted metal plates, which act as Lambertian scattering surfaces providing a sheet of light.</i>	75
Figure 4.3	<i>Variation of effective light sheet thickness against the mounting height of the beacon (<math>h</math>). The sheet thickness varies nearly linear above a height of two metres.</i>	76
Figure 4.4	<i>The schematic diagram of the beacon transmitter for the characterization of the assembly and the transmitter.</i>	77
Figure 4.5	<i>Photograph of the prototype of the beacon (DISLiB) implemented using PIC 12F675 microcontroller with three micro switch inputs for configuration.</i>	78
Figure 4.6	<i>The schematic diagram of the portable beacon receiver for the characterization of the assembly and the transmitter</i>	78
Figure 4.7	<i>Functional block diagram of the beacon transmitter consisting of a microcontroller, which generates the encoded signal for driving the infrared LED mounted inside the special assembly and an RS485 network for establishing communication with a host computer.</i>	79
Figure 4.8	<i>The scheme of the scaled version of SIRC communication protocol format which uses 12-bits for location encoding, one parity bit for error detection and appropriate start pulse.</i>	80
Figure 4.9	<i>Schematic diagram of the USB to RS485 Bridge.</i>	81
Figure 4.10	<i>Photograph of the USB to RS485 bridge module.</i>	81
Figure 4.11	<i>A typical workspace showing the beacon positions (<math>B</math>) and mounting of the same vertically above the tracks <math>Tr1, Tr2</math> etc. at a height of <math>h</math> metres.</i>	83
Figure 4.12	<i>Block diagram of the beacon receiver and controller consisting of PIC 18F4550 microcontroller, which manages motor control, RF link with host using CYWM6935 wireless module operating at 2.4GHz ISM band, 20X4 LCD display, optical incremental encoders attached to the wheels and the beacon receiver interface</i>	84
Figure 4.13	<i>Schematic diagram of the motor drive using LMD18200 H-bridge</i>	85
Figure 4.14	<i>Functional block diagram of the monitoring and control station</i>	86
Figure 4.15	<i>Photograph of the prototype of the beacon receiver and controller</i>	87

Figure 4.16	<i>3-D surface plots showing the role of vehicle speed, beacon receiver's reading time and Effective Light Sheet Thickness (ELST) against the resolution of the system. (a) indicates the variation of resolution with respect to speed and reading time (b) the variation of resolution with respect to speed and ELST.</i>	88
Figure 4.17	<i>Flowchart showing the implementation details of the resolution enhancement Algorithm</i>	91
Figure 4.18	<i>Kinematic scheme of the three wheeled mobile robot vehicle and the footprint of the effective light sheet width <math>d</math>. The attitude <math>\theta</math> is the angle between the absolute reference frame <math>OXY</math> and the mobile reference frame <math>PUV</math>. The origin <math>P</math> is attached to the mid point of the axes joining the rear wheels and the sensors <math>S_1</math> and <math>S_2</math>. The time delay <math>t_d</math> between the encoded signals reaching the sensors is also shown.</i>	93
Figure 5.1	<i>Functional block diagram of the optical incremental Encoder Pulse Processing Module (EPPM), which computes the velocity information in period mode and pulse mode depending upon the current speed of the vehicle. It also provides the incremental position (distance) update of the wheel.</i>	100
Figure 5.2	<i>3-D surface plot showing the role of (a) quantization error plotted against encoder pulse per revolution and observation time window in pulse counting mode and (b) relative error plotted against encoder pulse per revolution and oscillator clock frequency in period counting mode.</i>	102
Figure 5.3	<i>The Kinematic scheme of the three wheeled mobile robot vehicle having attitude <math>\theta</math>, which is the angle between the absolute reference frame <math>OXY</math> and the mobile reference frame <math>PUV</math>. The origin <math>P</math> is attached to the midpoint of the axes joining the rear wheels and the axis of symmetry of the vehicle. <math>\phi</math> is the steering angle.</i>	103
Figure 5.4	<i>Plan view of three typical postures of a vehicle over a hump show an error condition of over counts when (a) both the rear wheels are over the hump, (b) when one of the rear wheels and (c) the front wheel is over the hump.</i>	105
Figure 5.5	<i>The simplified functional diagram of the FPGA sub system which computes two sets of position increments and two attitude values. The switching, control and communication blocks are also shown.</i>	106
Figure 5.6	<i>A unit vector rotated to angle <math>\theta</math> using iteration.</i>	108

Figure 5.7	<i>The 3-D plot showing the variations in residual angle which is a measure of computational error against input angle and the number of iterations.</i>	110
Figure 5.8	<i>Screen shot showing the various wave forms with the system clock of 50MHz of encoder pulse processing module.</i>	112
Figure 5.9	<i>Screen shot showing the various results of computation along with the control and status signal associated with the sequential CORDIC module.</i>	112
Figure 5.10	<i>Photograph of the sub system implemented in Altera Cyclone-II EP2C70F672-G6 FPGA development board.</i>	113
Figure 6.1	<i>A traffic signaling installation using an encoded infrared sheet of light beacon.</i>	119
Figure 6.2	<i>The infrared LEDs of the beacon transmitter mounted on a structural assembly made up of sand blasted metal plates, which act as Lambertian scattering surfaces providing a sheet of light.</i>	121
Figure 6.3	<i>Variation of effective light sheet thickness against the mounting height of the beacon (<math>h</math>).</i>	122
Figure 6.4	<i>Functional block diagram of the beacon transmitter consisting of a microcontroller, which generates the encoded signal for driving the Infrared LEDs mounted inside the special assembly and a GSM Modem for establishing the communication with a traffic management center.</i>	122
Figure 6.5	<i>Block diagram of the vehicle unit consisting of the infrared receiver module, a microcontroller and its associated components</i>	123
Figure 6.6	<i>Photograph of the prototype of the Vehicle Unit</i>	125
Figure 6.7	<i>Block diagram of the beacon receiver consisting of PIC18F2550 microcontroller, which manages the audio record play back ChipCorder</i>	130
Figure 6.8	<i>A typical posture of the shoulder unit and the footprint of the effective light sheet thickness (ELST) <math>d</math>. The heading angle <math>\alpha</math> is the angle between the ELST and the axis joining the beacon sensors <math>S_1</math> and <math>S_2</math>. The time delay <math>t_d</math> between the encoded signals reaching the sensors is also shown.</i>	131
Figure 6.9	<i>Typical mounting scheme of the guidance and support system with an ear phone (shoulder unit).</i>	132
Figure 6.10	<i>Photograph of a typical shoulder unit with an LCD display for debugging.</i>	133
Figure A1.1	<i>Functional diagram of the setup</i>	146
Figure A1.2	<i>Block diagram of the robot controller</i>	148



<b>Figure A1.3</b>	<b><i>Screen shot in play mode</i></b>	<b>149</b>
<b>Figure A1.4</b>	<b><i>Details of the online control mode</i></b>	<b>150</b>
<b>Figure A1.5</b>	<b><i>The GUI for the file/offline control mode</i></b>	<b>151</b>
<b>Figure A1.6</b>	<b><i>A typical file structure of the control program</i></b>	<b>152</b>
<b>Figure A1.7</b>	<b><i>Block diagram of the Ethernet web control/server module</i></b>	<b>152</b>
<b>Figure A1.8</b>	<b><i>The Control Web page for the file/offline control mode</i></b>	<b>153</b>
<b>Figure A1.9</b>	<b><i>Photographs of the finished view and inside view of the controller and a typical workcell</i></b>	<b>155</b>

## ABBREVIATIONS

ACC	Adaptive Cruise Control
AGV	Automated Guided Vehicles
ASCII	American Standard Code for Information Interchange
BIN	Beacon Identification Number
C/A	Coarse Acquisition
CAD	Computer Aided Design
CCD	Charge Coupled Device
CMOS	Complimentary Metal Oxide Semiconductor
CORDIC	COordinate Rotational DIgital Computer
DGPS	Differential Global Positioning System
DISLiB	Digital Infrared Sheet of Light Beacon
DSSS	Direct Sequence Spread Spectrum
ELST	Effective Light Sheet Thickness
<i>enon</i>	<i>exciting nova on network</i>
EPPM	Encoder Pulse Processing Module
FMCW	Frequency Modulated Continuous Wave
FOG	Fiber Optical Gyroscope
FPGA	Field Programmable Array
GPS	Global Positioning System
GSM	Global System Mobile
GUI	Graphical User Interface,
INS	Inertial Navigation System
IP	Internet Protocol
ISM	Industrial, Scientific and Medical
LCD	: Liquid Crystal Display

LED	Light Emitting Diode
LGA	Land Grid Array
MEMS	Micro Electro-Mechanical System
MMIC	Monolithic Microwave Integrated Circuit
MMWR	Millimeter Wave Radar
NMEA	National Marine Electronics Association
PC	Personal Computer
PI	Proportional Integral
PID	Proportional Integral Derivative
PSoC	Programmable System on Chip
PWM	Pulse Width Modulation
RAM	Random Access Memory
RF	Radio Frequency
RFID	Radio Frequency Identification
RTC	Real Time Clock
SCARA	Selective Compliance Articulated Robot Arm
SD card	Secure Data card
SIRC	Sony Infrared Remote Control
SLAM	Simultaneous Localization And Map building
SPI	Serial Peripheral Interface
UART	Universal Asynchronous Receiver Transmitter
USB	Universal Serial Bus
VGS	Visual Guidance System
Wi-Fi	Wireless Fidelity
XR4	: eXperimental Robot 4

# INTRODUCTION

Chapter 1

---

- 1 Background and Motivation ..... 2
  - Mobile Robot Localization
  - Autonomous Localization Systems
- 1.2 Thesis Roadmap ..... 8
- 1.3 Practical Systems ..... 11
- 1.4 Summary ..... 12

---

In this modern age the autonomous or semi autonomous robot vehicles find applications in automated inspection systems [1], floor sweepers [2], hazardous environments [3], autonomous truck loading systems [4], agriculture tasks, delivery in establishments like manufacturing plants, office buildings, hospitals [5], etc. and providing services for the elderly [6]. In addition to this, autonomous vehicles are widely utilized in undersea exploration and military surveillance systems [7, 8]. Automated Guided Vehicles (AGVs), such as the cargo transport systems are heavily used in industrial applications. Mobile robots are also finding their way into a growing number of homes, providing security, automation [9, 10], and even entertainment. In each of these tasks, some type of positioning system is essential. A variety of technologies have been developed and used successfully to provide position and attitude information. However, many of these existing positioning systems have

inherent limitations in their workspace. These limitations generally fall into two main categories: line-of-sight restrictions and insufficient resolution/precision as they require multiple clear lines-of-sight and absolute drift-free measurements.

In mobile robot applications, two basic position estimation methods are employed concurrently, viz., the *absolute* and *relative* positioning [11]. *Absolute* positioning methods usually rely on the use of appropriate exteroceptive (external) sensing techniques, like navigation beacons [12,13], active or passive landmarks[14], map matching [15], or satellite-based navigation [16] signals. Navigation beacons and landmarks normally require costly installations and maintenance, while map-matching methods are usually slower and demand more memory and computational overheads. The satellite-based navigation techniques are used only in outdoor implementations and have poor accuracy, of the order of a few metres. Relative position estimation is based on proprioceptive (internal) sensing systems like odometry [17], inertial navigation system (INS) [18] or optical flow techniques [19]. The vehicle performs self localization by using relative positioning technique, called dead reckoning. For implementing a navigational system many indoor mobile robots use active beacons [13] together with traditional inertial navigation systems employing gyros and accelerometers or position odometric system or both. The latter provides accurate and precise intermediate estimation of position during the path execution.

## **1.1 Background and Motivation**

Autonomous navigation and autonomous mobile Robots/Vehicles specifically, are currently of great interest to the scientific, industrial, and military communities. Such systems have the potential to improve human-safety and performance in various applications like hazardous environments, industrial establishments, guiding differently able personnel, autonomous highway driving, automated traffic and transport control system and Robotic Army that may fight in

the battlefields. The ability of a mobile robot to determine its location in space is a fundamental competence for autonomous navigation. Knowledge of self-location, and the location of other places of interest is the basic foundation on which all high level navigation operations are built. It enables strategic path planning for tasks such as goal reaching, exploration and obstacle avoidance, and makes the following of these planned trajectories possible. Without a notion of location, a robot is limited to reactive behavior based solely on local stimuli and is incapable of planning actions beyond its immediate sensing range.

The knowledge of position and attitude information is not exclusive to the realm of mobile robots. Information about the location of an inanimate object, for example a cargo pallet, can streamline inventory and enable warehouse automation. Unmanned vehicles promise to allow often dangerous tasks to be performed from remote locations in a range of application domains such as mining, defense and sub sea exploration. With the advent of newer technologies, including a host of relatively cheap sensors and increase in computational speed, there has been a recent push to increase the level of autonomy with which remote agents are allowed to operate. This is seen in numerous application domains where the systems are required to operate for long periods with little or no input from a human operator. From the landing of spacecraft on distant planets [21] to submersible vehicles operating too deep in the oceans [22], there is a need for systems capable of making decisions and performing controls in an independent manner.

A number of groups around the world have been concentrating their efforts on the development of field deployable robots and these are being taken up in a variety of industrial sectors. The deployment of autonomous systems in field environments demands high levels of robustness and system integrity. As

technology advances the autonomous mobile robot vehicles can navigate at higher speeds with high resolution and precision. The need for reliable, high resolution localization system for indoor autonomous navigation has resulted in a considerable amount of research.

### **1.1.1 Mobile Robot Localization**

This section briefly describes the features of localization schemes commonly used in mobile robot vehicles. Relative position estimation or dead reckoning is based on proprioceptive (internal) sensing systems, where the error growth rates are usually unacceptable. This is the most basic form of localization, which is simply estimation of the vehicle pose by integrating estimates of its motion by the help of inertial sensors and encoder-based odometry. The problem with dead reckoning is that each change-in-pose estimate includes a component of error and these errors accumulate as part of the integration process. Thus, uncertainty in the pose estimate increases monotonically with time and one cannot prevent this increase. The error growth rates of these systems are usually unacceptable. Pose estimation with bounded uncertainty is only possible through the availability of *absolute* rather than incremental pose measurements.

Inertial Navigation System (INS) is complex and expensive and requires more information processing for extracting the required position and attitude information. The localization based on INS uses accelerometers or gyros, where the accelerometer data must be integrated twice to yield the position information, thereby making these sensors extremely sensitive to drift. A very small error in the rate information furnished by the INS can lead to unbounded growth in the position errors with time and distance. Rate information from the gyros can be integrated to estimate the position and yields better accuracy than accelerometers. Though the odometric system is simple, inexpensive and accurate over short distances, it is

prone to several sources of errors due to wheel slippage, variations in wheel radius, body deflections, surface roughness and undulations. For better traction, most of the mobile robots use rubber tyres, which have unevenness in their diameter and these tyres compress differently under asymmetric load distribution or load imbalances, causing further position and attitude errors.

### 1.1.2 Autonomous Localization Systems

The general arrangement of a mobile robot localization system is shown in figure 1.1. From the proprioceptive sensors' data the pose and velocity of the vehicle can be estimated. The system also takes measurements from one or more exteroceptive sensors and uses this information to provide corrections to the estimated values. Depending upon the sensor type and its quality the resolution and precision of the estimated position and attitude varies. Various algorithms and filtering techniques are utilized for the extraction of best estimate from the available information.

Navigation beacons and landmarks normally require costly installations and maintenance, while map-matching methods are usually slower and demand more memory and computational overheads. The satellite-based navigation techniques are used only in outdoor implementations and have poor accuracy, of the order of a few metres.

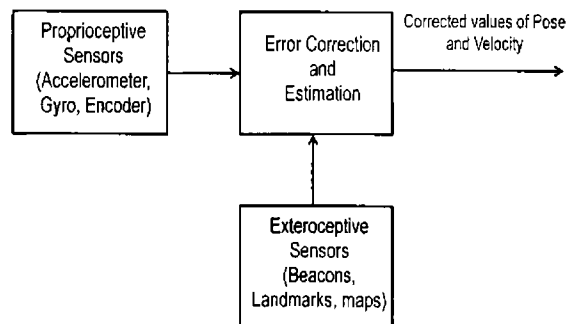


*Figure 1.1: A block diagram showing the general arrangement of a mobile robot localization system.*



For outdoor applications Differential Global Positioning System (DGPS) based localization techniques provide adequate resolution, whereas for indoor use, this resolution is insufficient and moreover the satellite signals may be obstructed, which further aggravate the situation. Another technique is map based localization where the map of the environment defined by the locations of distinct landmarks provides a source of absolute position information. Thus, given an ability to sense its surroundings, the robot can obtain absolute pose estimates by registering sensed information with the map. The problem with *a priori* map based localization is the need to have explored the environment in advance, and to have surveyed the landmark locations before the robot can begin to navigate autonomously. Construction of an *a priori* map may be a difficult operation and a new map must be built for each new environment. Moreover, the resulting map is static and cannot adapt to changes in the environment or grow with exploration into regions beyond the original map bounds. The geometric feature extraction or map based navigation methods are highly environment dependant and sometimes it is too difficult to derive the pose.

Substantial research works are going on in the area of Simultaneous Localization and Map building (SLAM) [20] using various sensing systems. The motivation for SLAM is to overcome the need for *a priori* maps as a mechanism for bounded pose uncertainty, and to enable map construction that is extensible and adaptive to environmental change. SLAM is performed by storing landmarks in a map as they are observed by the robot sensors, using the robot pose estimate to determine the landmark locations, while at the same time, using these landmarks help to improve the robot pose estimates. As the landmarks are repeatedly re-observed, their locations become increasingly certain and the map converges, eventually acquiring the rigidity of an *a priori* map. The complexity of the SLAM estimation problem is potentially huge, which require more memory and

computational overhead for feature extraction. Further, the structure of the SLAM problem is characterized by monotonically increasing correlations between landmark estimates. For these reasons, there has been a significant drive to find computationally effective SLAM algorithms. This has been achieved through the development and use of the Kalman and extended Kalman filter as the estimation algorithms of choice in SLAM algorithms.

The errors in kinematic and environmental parameters will lead to poor estimation of positions during the path execution and this necessitates the need for frequent absolute localizations. For indoor applications like localization of personnel, products and vehicles in warehouses as well as production environments, where a stable and accurate localization system is necessary, the ultrasonic, infrared, [23] radio frequency [24] and laser techniques [25] are commonly used. The use of ultrasonic sensors [26,27] is limited to the proximity because of poor system characteristics like moderate axial resolution, low lateral resolution, and high rate of inaccuracies in measurements resulting from multiple reflections, environmental complexity and the aperture cone. Radio frequency systems are very expensive and are susceptible to reflections from metallic objects. These localization systems, which utilize triangulation or trilateration techniques [28], have high uncertainty in position estimations, incurring extra computational overheads, resulting possibly in slowing down the path execution process of the vehicle.

Most of the high resolution systems are complex and costly. A cost effective commercially available infrared Beacon System used for indoor robot localization application is the *Northstar* from Evolution Robotics Inc. [29]. This system requires a reflecting roof for its functioning, which is not always feasible in an industrial or warehouse environment. The reflective characteristics as well as the

indoor lighting system may affect its performance. Here also the computational overhead due to the triangulation method exists.

For the successful navigation and path planning of indoor mobile robots, a well-defined and structured workspace is required. This can provide high-rate of precise positioning and attitude information for reliable estimation of the vehicles' localization and navigation map.

This thesis investigates the localization problem in the context of 2-D (planar) environments, so that the location of the robot is given by its *pose* (i.e., position  $(x, y)$  and orientation  $\theta$ ).

## 1.2 Thesis Roadmap

The thesis deals with the necessary background by discussing common localization methods available for the detection of position and attitude measurement of mobile robot vehicles. The robotic systems have utilized various sensing techniques and processing algorithms for the extraction of information. The various sensing techniques reported for mobile robot localization are examined.

Some sensors are simple but some others are sophisticated and equipped with complex and costly processing electronics, which can be used to acquire information about the robot's environment or even to directly measure a robot's absolute position. As the mobile robot moves around, it will frequently encounter unforeseen environmental characteristics, and therefore such sensing is particularly critical. General classification of sensors used for localization of robots and their features are discussed. Examples of different types of sensors and the information they provide are also presented. Various beacon based systems and their merits and demerits in the application of localization of autonomous mobile robots are

examined. Odometric sensors, INS and active ranging sensors are thoroughly discussed. Complex systems like vision based localization and SLAM are also briefly explained.

The methodology of design, construction and experimental details of a beacon system and receiver developed for the absolute localization of autonomous robot vehicle is discussed.

The development of a cost effective, accurate and reliable system, utilising an infrared sheet of light, which minimizes position errors during the path execution is presented. The encoded digital infrared sheet of light beacon (DISLiB) construction, method of installation and its implementation using a microcontroller are explained. Results of the characteristics study of the beacon transmitter are given. A resolution enhancement algorithm developed is described and the variations of the same with the environmental parameters are plotted. The position and attitude updating for a three wheeled mobile vehicle with one driving-steering wheel and two fixed rear wheels in-axis is also discussed. The characteristics, merits and realization details of the system are thoroughly explored.

The realization details of an odometric error reduction system, which can be utilized as part of all wheeled mobile robot vehicles, are discussed. The various factors causing errors to the odometric system are examined. A simple and efficient method and its implementation in FPGA for reducing the odometric localization errors caused by over count readings of an optical encoder based odometric system in a mobile robot due to wheel-slippage and terrain irregularities is also discussed. The detection and correction is based on redundant encoder measurements. The standard quadrature technique is used to obtain four counts in each encoder period. The CORDIC algorithm is used for the computation of sine and cosine terms in the update equations. The necessary hardware is designed and developed for the

independent computation and comparison of the position and attitude values from the rear wheel and front wheel encoder data. The digital comparators manage the switching of multiplexers that selects the least values among the computed values. The results presented demonstrate the effectiveness of the technique.

The suitability of DISLiB system to applications where localization and guidance are of great importance, like intelligent control of the public transportation system as well as guidance of differently-able personnel are envisaged. The adaptive traffic control system ensures safe and smooth traffic flow and informs the drivers about the traffic status. The guidance and obstacle avoidance systems for the visually impaired personnel provide less body gear and adequate information about the environment. The installation and realization of these systems are explained. A novel technique to reduce the traffic congestions and location identification is introduced. The need for an intelligent traffic control for the modern public transportation system is well illustrated. The realization details of a traffic and transport control system using existing GSM network are discussed. The design of a flexible and friendly driver support system for the vehicle is also proposed. The diverse ways of position estimation and support systems for differently-able people that are already in use are briefed. The **DISLiB** based visually impaired personnel support system is simple, cost effective and provides less body gear without much computational burden or significant processing. The natural language assisting capability of the system by incorporating a chipCorder is addressed.

A comparison of the merits and demerits of the system has also been carried out. This research work is carried out with an aim of developing a robust, cost effective and absolute position update system without any computational burden. The proposed absolute localization method has been realized and tested.

Suggestions for improving the system performance are also proposed. The extension of the use of the system to other applications is also suggested. The major contributions of the work are also listed.

### 1.3 Practical Systems

There is a great demand for the practical use of service robots in a wide range of applications, to enable a more enriched society, in view of declining birthrates, unwillingness of people to join army and aging populations in many countries. Fujitsu Frontech and Fujitsu Laboratories Ltd, have introduced a new service robot, *enon* (*exciting nova on network*) [30] that can assist in such tasks as providing guidance, escorting guests, transporting objects, and security patrolling. The robot is able to autonomously cater the customers' requirements while being linked to a network (Wireless LAN (802.11a/11b/11g) [30].

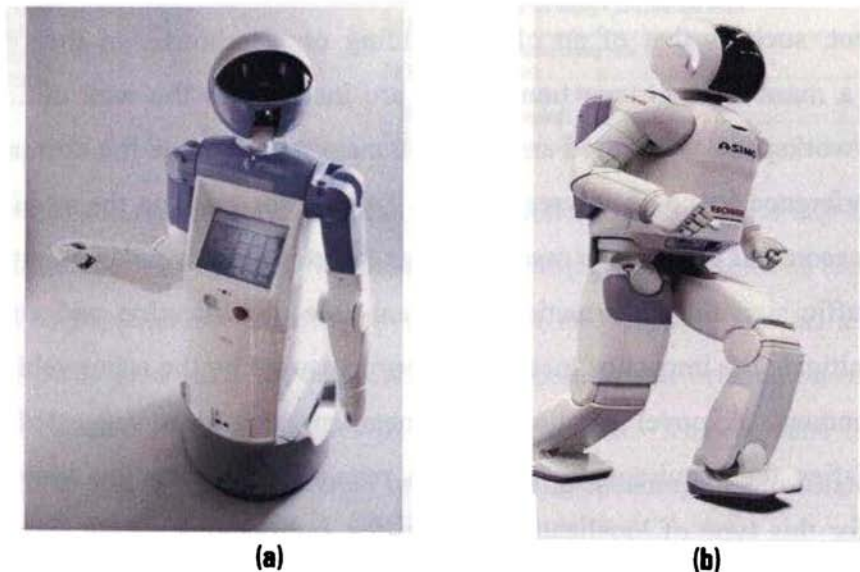


Figure 1.2 The photographs of (a) *enon* and (b) *ASIMO*

Honda engineers has created an advanced humanoid robot *ASIMO* with 34 degrees of freedom that help it walk and perform tasks much like a human [31].

These degrees of freedom act much like human joints for optimum movement and flexibility. ASIMO is designed to operate in the real world, where people need to reach for things, pick things up, navigate along floors, sidewalks, and even climb stairs. Its abilities to run, walk smoothly, climb stairs, communicate, and recognize people's voices and faces will enable *ASIMO* to easily function in real world and truly assist humans [31]. The photographs of *enon* and *ASIMO* are shown in figure 1.2.

## 1.4 Summary

This thesis describes the development of an accurate and reliable localization system for autonomous mobile robot navigation, utilising an infrared sheet of light, which minimizes the position and attitude errors during the path execution. This provides a cost effective position and attitude sensing system designed specifically to face the challenges in a realistic, cluttered indoor environment, such as that of an office building or warehouse. In the proposed approach, a number of beacon transmitters are installed in the well defined and structured workspace as required and all the transmitters provide the estimates in a common reference frame or universal frame. Two sensor units on the mobile robot read the beacon and process the measurements to determine its position, attitude as well as traffic signaling information. The real-time identification and correction methods mitigate the impact of localization errors caused by the robot vehicles and the environment. A novel resolution enhancement algorithm suggested in this thesis satisfies the requirements of a high resolution localization system. The potential for this type of localization system for autonomous robots operating in structured indoor environments is enormous.

## REVIEW OF LOCALIZATION SYSTEMS




---

2.1 Sensors for Mobile Robots .....	14
• Proprioceptive Sensors • Exteroceptive Sensors	
2.2 Tactile sensors .....	16
2.3 Odometric Sensors .....	17
• Optical encoders	
2.4 Electronic Compasses .....	18
2.5 Inertial Navigation Sensors .....	21
• Accelerometers • Gyroscopes	
2.6 Beacon based Localization .....	31
• Localization Techniques • Global Positioning System	
2.7 Active Ranging Systems .....	42
• Time-of-flight active ranging • Structured light sensor	
2.8 Motion Sensors .....	53
• Doppler Effect-based sensing (radar or sonar)	
2.9 Vision-based sensors .....	55
• Visual ranging sensors • Stereo-vision • Visual Guidance System	
2.10 Map Based Positioning .....	57
2.11 Summary .....	60

---

One of the most important tasks of an autonomous system of any kind is to acquire knowledge about its environment. The problem of autonomous localization has received considerable attention over the past two decades and, as a result, a variety of paradigms exist for determining the position and orientation of a robot vehicle in relation to other objects in the environment. This is done by taking measurements using various sensors and extracting meaningful information from those measurements. This chapter examines the most common sensors and systems used in mobile robots and the techniques for extracting information from them.



## 2.1 Sensors for Mobile Robots

There are a wide variety of sensors used for the navigation and guidance of mobile robots. Some sensors are simple but some others are sophisticated and equipped with complex and costly processing electronics, which can be used to acquire information about the robot's environment or even to directly measure a robot's absolute position. As the mobile robot moves around, it will frequently encounter with unexpected environmental characteristics, and therefore such sensing is particularly critical. General classification of sensors used for localization of robots is listed in table 2.1. Examples of different types of sensors and the information they provide are also presented. Sensors are broadly collected under headings of proprioceptive (internal) sensing and exteroceptive (external) sensing [32].

	<b>General classification</b>	<b>Use</b>	<b>Examples</b>
1.	Tactile sensors	Detection of physical contact or closeness with external objects	Micro-switches, Optical barriers, Proximity sensors
2.	Odometric Sensors	Wheel/motor speed and position	Brush encoders Potentiometers Optical encoders Magnetic encoders Inductive encoders Capacitive encoders
3.	Heading sensors	Orientation of the robot with respect to a fixed reference frame	Compass Gyroscopes Inclinometers
4.	Beacons	Localization in a fixed reference frame	GPS Optical or RF beacons Ultrasonic beacons Reflective beacons Infrared beacons
5.	Active ranging	Distance and bearing measurements based on time-of-flight, and geometric triangulation technique	Reflectivity sensors Sonar Radar Laser rangefinder Structured light
6.	Motion sensors	Speed relative to fixed or moving objects	Doppler radar Doppler sonar
7.	Vision sensors	Ranging, image analysis, object recognition	CCD/CMOS camera(s)

*Table 2.1 General classification of sensors used for mobile robot localization*

### **2.1.1 Proprioceptive Sensors**

Proprioceptive sensors measure the “kinematic states” of a platform or vehicle; velocity, angular rates or acceleration. These are then integrated to provide the location and attitude of the vehicle. Proprioceptive sensors include accelerometers, gyroscopes, inclinometers and encoders (odometry), for example.

Proprioceptive sensors often provide motion rate information incrementally along a trajectory. Position information from proprioceptive sensors is normally obtained through time integration of measurement sequences. Measurement errors in such sensors are consequently integrated in providing position information. This causes the error in vehicle location estimates produced by such sensors to grow without bound (random walk). The error growth rates of these systems are usually unacceptable. Careful modeling of bias and other errors in these sensors is necessary to minimize this drift. Proprioceptive sensors are rarely used by themselves in a vehicle navigation system.

However, proprioceptive sensors also have many advantages. In particular, sensors such as accelerometers and gyroscopes are self contained, non-radiating devices which do not depend on the physics of the environment for its operation. Further such sensors are often capable of providing very high information rates. In practice, most navigation systems incorporate proprioceptive sensors of some form to provide high-bandwidth prediction information. This information is then fused with landmark or beacon data from lower bandwidth exteroceptive or external sensors.

### **2.1.2 Exteroceptive Sensors**

Exteroceptive sensors obtain measurements that depend on the external environment. This has the advantage of providing the vehicle with knowledge of its local environment and subsequently in using this knowledge to navigate. These

sensors may measure both incremental motions (Doppler velocity sensors for example) [33], and also absolute motion with respect to a number of fixed landmarks or beacons. A special case of exteroceptive sensing is when artificial landmarks or beacons in the environment emit signals, which is detected by receivers on the robot vehicle. Such is the case with GPS (on land) [23, 34] or long baseline sonar in subsea applications [35]. When the locations of the emitters are known, the absolute location of the robot vehicle can be determined with ease.

Exteroceptive sensors can be either active or passive. Active sensors radiate energy and detect the reflected energy from the environment. Time of flight, phase difference or amplitude information are measured and used to interpret physical properties of the objects in the environment. Various signal processing methods may then be applied to identify the objects of interest. Active sonar is a good example of this type of sensor. Magnetic compass, proximity switches and certain inclinometers come under passive sensors.

## **2.2 Tactile Sensors**

Tactile sensors are critical to virtually all mobile robots, and are well understood and easily implemented. In order to protect the robot from collisions, special bumpers with mechanical or electronic proximity sensors are integral part of any mobile robot. The implementation point of view it is very simple and the microcontroller based actuator controller can easily read the status with out any complexity or processing. Various types proximity sensors based on magnetic, optic and Hall effect techniques are widely utilized in industrial and robotic applications [32].

## **2.3 Odometric Sensors**

Odometry is the most widely used navigation method for mobile robot positioning; it provides good short-term accuracy, allows very high sampling rates and is inexpensive. However, the fundamental idea of odometry is the integration of incremental motion information over time, which leads, inevitably, to the unbounded accumulation of errors. Specifically, orientation errors will cause large lateral position errors, which increase proportionally with the distance traveled by the robot vehicle. Various methods for fusing odometric data with absolute position measurements to obtain more reliable position estimation are available [36,11].

Wheel/motor shaft encoder sensors are devices used to measure the internal state and dynamics of a mobile robot. These sensors have vast applications in industry and robotics and, as a result, mobile robotics has enjoyed the benefits of high-quality, low-cost wheel and motor sensors that offer excellent resolution. Most widely used one such sensor is the optical incremental encoder.

### **2.3.1 Optical Encoders**

Optical incremental encoders have become the most popular device for measuring angular speed and position and direction of rotation within a motor drive or at the shaft of a wheel or steering mechanism. In mobile robotics, encoders are used to control the position or speed of wheels and other motor-driven systems. Because these sensors are *proprioceptive*, their estimate of position is best in the reference frame of the robot and, when applied to the problem of robot *localization*, significant corrections are required.

An optical encoder is basically a mechanical light chopper that produces a certain number of wave pulses for each shaft revolution [32,37,38,39]. It consists of an illumination source, a fixed grating that masks the light, a rotor disc with a

fine optical grid that rotates with the shaft, and fixed optical detectors. As the rotor moves, the amount of light striking the optical detectors varies based on the alignment of the fixed and moving gratings. Resolution is measured in *pulses per revolution*. The minimum angular resolution can be readily computed from an encoder's *pulses per revolution* rating. Usually in mobile robotics the *quadrature encoder* is used. In this case, a second illumination and detector pair is placed in order to produce a 90 degrees shifted waveform with respect to the original. The resulting twin square waves, shown in figure 2.1, provide significantly more information. The ordering of which square wave produces a rising edge first identifies the direction of rotation. Furthermore, the four detectably different states improve the resolution by a factor of four with no change to the rotor disc. Commercial quadrature encoders integrated with a gear-motor assembly are available for industrial and mobile robot applications.

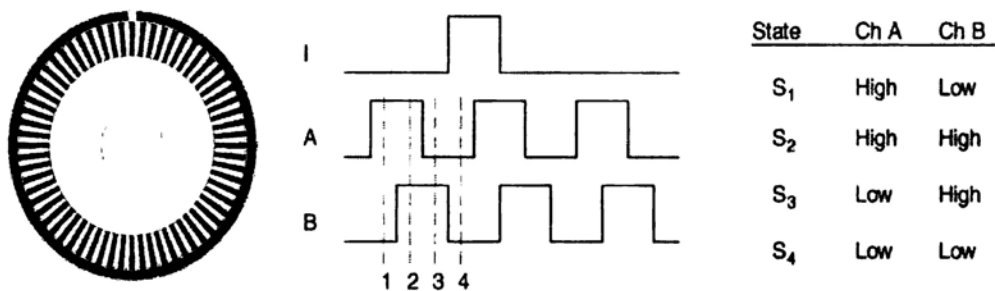


Figure 2.1 A quadrature encoder disc and the resulting channel A and B pulses.

## 2.4 Electronic Compasses

The two most common modern sensors for measuring the direction of a magnetic field are the Hall effect and flux gate compasses [32]. Each has its own advantages and disadvantages, as described below. The Hall effect describes the

behavior of electric potential in a semiconductor in the presence of a magnetic field. When a constant current is applied across the length of a semiconductor, there will be a voltage difference in a perpendicular direction, across the semiconductor's width, based on the relative orientation of the semiconductor to magnetic flux lines. In addition, the polarity of the potential identifies the direction of the magnetic field. Thus, a single semiconductor provides a measurement of flux and direction along one dimension. Hall effect digital compasses are inexpensive as well as compact and hence are popular in mobile robotics.

The flux gate compass operates on a different principle. Two small coils are wound on ferrite cores and are fixed perpendicular to one another. When alternating current is activated in both coils, the magnetic field causes shifts in the phase depending on its relative alignment with each coil. By measuring both the phase shifts, the direction of the magnetic field in two dimensions can be computed. The flux gate compass can accurately measure the strength of a magnetic field and has improved resolution and accuracy; however, it is bigger in size and more expensive than a Hall effect compass. Regardless of the type of compass used, a major drawback concerning the use of the Earth's magnetic field for mobile robot applications involves disturbance of that magnetic field by other magnetic objects and man-made structures, as well as the bandwidth limitations of electronic compasses and their susceptibility to vibration. Particularly in indoor environments, mobile robotics applications have often avoided the use of compasses, although a compass can conceivably provide useful *local* orientation information indoors, even in the presence of steel structures.

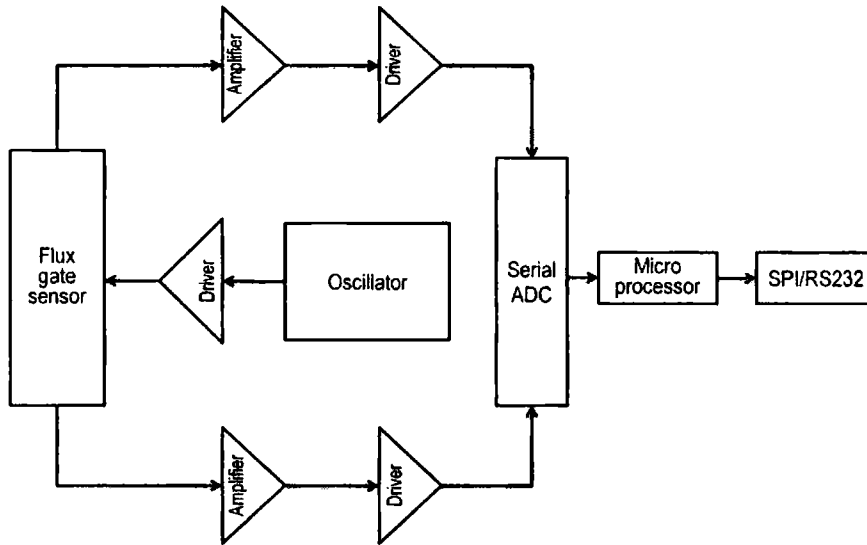


**Figure 2.2** Block diagram of a digital flux gate compass.

The system block diagram of a digital flux gate compass is shown in Figure 2.2. This unit contains an A/D converter to read the amplified outputs of the two sensor channels, and a microprocessor/microcontroller, which computes the direction of the magnetic field. The system also incorporates a serial interface to the navigational system. The update rate of these systems are normally less than 1 Hz [39, chap2].

Philips semiconductors manufactures compass sensors [40] based on the magnetoresistive effect and provide the required sensitivity and linearity to measure the weak magnetic field of the earth. The devices are equipped with integrated set/reset and compensation coils. These coils allow to apply the flipping technique for offset cancellation and the electro-magnetic feedback technique for elimination of the sensitivity drift with temperature. Besides the sensor elements, a signal conditioning unit and a direction determination unit are required to build up an electronic compass.

A typical low cost, low power, compact and robust electronic compass; Sparton SP3003D shown in figure 2.3 provides affordable superior performance [41]. The three-axis, tilt compensated digital compass provides three-dimensional absolute magnetic field measurement and full 360° tilt compensated bearing, pitch, and roll. This digital compass can be integrated to a computer/microcontroller through a UART/SPI built in interface.



Figure 2.3 A commercially available Electronic Compass SP3003D from Sparton Electronics (2008).

## 2.5 Inertial Navigation Sensors

Inertial sensors are used to determine the robot's incremental position and orientation. They allow together with appropriate velocity information, to integrate the movement to a position estimate. This procedure, which has its roots in vessel and ship navigation, is called *dead reckoning*.

Inertial navigation is the determination of the pose of a vehicle through the implementation of inertial sensors. It is based on the principle that an object will remain in uniform motion unless disturbed by an external force. This force in turn



generates acceleration on the object. If this acceleration can be measured and then mathematically integrated, then the change in velocity and position of the object with respect to an initial condition can be determined.

Inertial Navigation System (INS) [18, 34, 42, 43] is complex and expensive and requires more information processing for extracting the required position and attitude information. The localization based on INS uses accelerometers or gyros. The accelerometer data must be integrated twice to yield the position information, thereby making these sensors extremely sensitive to drift. A very small error in the rate information furnished by the INS can lead to unbounded growth in the position errors with time and distance. The gyros measure angular velocity, and if mathematically integrated provides the change in angle with respect to an initially known angle. The combination of accelerometers and gyros allows for the determination of the pose of the vehicle.

The principal advantage of using inertial units is that given the acceleration and angular rotation rate in three dimensions, the velocity and position of the vehicle can be evaluated in any navigation frame. For land vehicles, a further advantage is that unlike wheel encoders, an inertial unit is not affected by wheel slip.

### **2.5.1 Accelerometers**

The accelerometers measure the inertia force generated when a mass is affected by change in velocity. This force may change the tension of a string or cause a deflection of beam or may even change the vibrating frequency of a mass. The Accelerometers are composed of three main elements: a mass, a suspension mechanism that positions the mass and a sensing element that returns a observation proportional to the acceleration of the mass. Some devices include an additional servo loop that generates an opposite force to improve the linearity of the sensor. A

basic functional diagram of an accelerometer with one degree of freedom is shown in figure 2.4. Many of the accelerometers are based on the pendulum principle. They are built with a proof mass, a spring hinge and a sensing device [44].

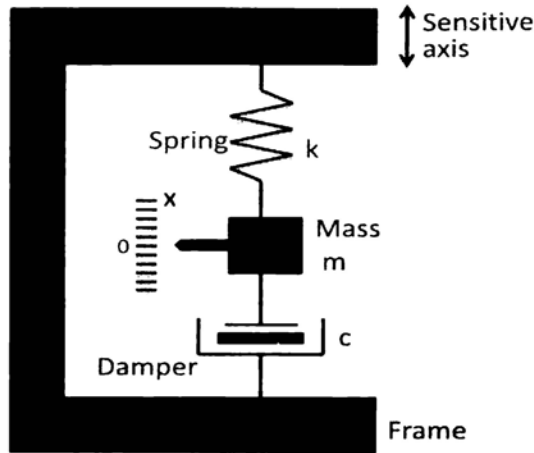


*Figure 2.4 Basic components of a one degree of freedom accelerometer.*

Test results from the use of accelerometers for mobile robot navigation have been generally poor. Accelerometers also suffer from extensive drift, and they are sensitive to uneven ground because any disturbance from a perfectly horizontal position will cause the sensor to detect a component of the gravitational acceleration  $g$ . One low-cost inertial navigation system aimed at overcoming the latter problem included a tilt sensor [18, 42]. The tilt information provided by the tilt sensor was supplied to the accelerometer to cancel the gravity component projecting on each axis of the accelerometer. Nonetheless, the results obtained from the tilt-compensated system indicate a position drift rate of 1 to 8 cm/s, depending on the frequency of acceleration changes. This is an unacceptable error rate for most mobile robot applications.

## 2.5.2 Gyroscopes

Gyroscopes are heading sensors, which preserve their orientation in relation to a fixed reference frame. Thus they provide an absolute measure for the heading of a mobile system. Gyroscopes (also known as “rate gyros” or just “gyros”) [32, 45] are of particular importance to mobile robot positioning because they can help to compensate for the foremost weakness of odometry: in an odometry-based positioning method, any small momentary orientation error will cause a constantly growing lateral position error. For this reason it would be of great benefit if orientation errors could be detected and corrected immediately. Highly accurate gyros were too expensive for mobile robot applications. However, very recently fiber-optic gyros (also called “laser gyros”), which are known to be very accurate, have fallen dramatically in price and have become a very attractive solution for mobile robot navigation. Gyroscopes can be classified into three categories; mechanical gyroscopes, optical gyroscopes and *micro electro-mechanical system* (MEMS) gyroscopes.

### 2.5.2.1 Mechanical Gyroscope

The concept of a mechanical gyroscope [34, 45, 46] relies on the inertial properties of a fast-spinning rotor. The property of interest is known as the gyroscopic precession. If you try to rotate a fast-spinning wheel around its vertical axis, you will feel a harsh reaction in the horizontal axis. This is due to the angular momentum associated with a spinning wheel and will keep the axis of the gyroscope inertially stable. The reactive torque and thus the tracking stability with the inertial frame are proportional to the spinning speed, the precession speed and the wheel’s inertia.

The fundamental equation describing the behavior of the gyroscope is:

$$\boldsymbol{\tau} = \frac{d\mathbf{L}}{dt} = \frac{d(I\boldsymbol{\omega})}{dt} = I\boldsymbol{\alpha} \quad (2.1)$$

Where the vectors  $\boldsymbol{\tau}$  and  $\mathbf{L}$  are, respectively, the torque on the gyroscope and its angular momentum, the scalar  $I$  is its moment of inertia, the  $\boldsymbol{\omega}$  vector is its angular velocity, and the vector  $\boldsymbol{\alpha}$  is its angular acceleration.

It follows from this that a torque  $\boldsymbol{\tau}$  applied perpendicular to the axis of rotation, and therefore perpendicular to  $\mathbf{L}$ , results in a rotation about an axis perpendicular to both  $\boldsymbol{\tau}$  and  $\mathbf{L}$ . This motion is called *precession*. The angular velocity of precession  $\boldsymbol{\Omega}_p$  is given by the cross product:

$$\boldsymbol{\tau} = \boldsymbol{\Omega}_p \times \mathbf{L} \quad (2.2)$$

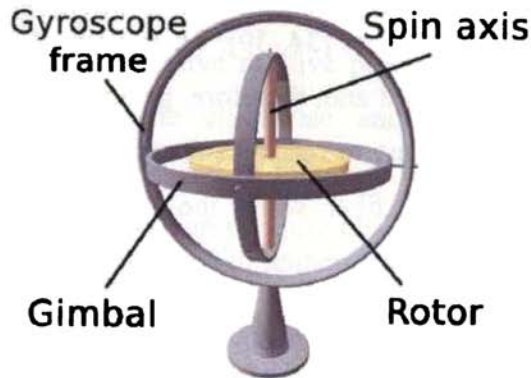


Figure 2.5 A mechanical gyroscope Model.

By arranging a spinning wheel, as seen in figure 2.5, no torque can be transmitted from the outer pivot to the wheel axis. The spinning axis will therefore be space-stable (i.e., fixed in an inertial reference frame). Nevertheless, the remaining friction in the bearings of the gyro axis introduces small torques, thus limiting the long-term space stability and introducing small errors over time. A

high quality mechanical gyroscope is costly and has an angular drift of about 0.1 degrees in 6 hours. For navigation, the spinning axis has to be initially selected. If the spinning axis is aligned with the north-south meridian, the earth's rotation has no effect on the gyro's horizontal axis. If it points east-west, the horizontal axis reads the earth rotation.

Rate gyros have the same basic arrangement as shown in figure 2.5 but with a slight modification. The gimbals are restrained by a torsional spring with additional viscous damping. This enables the sensor to measure angular speeds instead of absolute orientation.

### ***2.5.2.2 Optical Gyroscope***

The commercial use of optical gyroscopes began in the early 1980s when they were first installed in aircrafts. Optical gyroscopes are angular speed sensors that use two monochromatic light beams, or lasers, emitted from the same source, instead of moving, mechanical parts [34, 39]. They work on the principle that the speed of light remains unchanged and, therefore, geometric change can cause light to take a varying amount of time to reach its destination. One laser beam is sent traveling clockwise through a fiber while the other travels counterclockwise. Because the laser traveling in the direction of rotation has a slightly shorter path, it will have a higher frequency. The difference in frequency  $\Delta f$  of the two beams is proportional to the angular velocity  $\omega$  of the cylinder. New solid-state optical gyroscopes based on the same principle are built using micro-fabrication technology, thereby providing heading information with resolution and bandwidth far beyond the needs of mobile robotic applications. Bandwidth, for instance, can easily exceed 100 kHz while resolution can be smaller than 0.0001 degrees/hr.

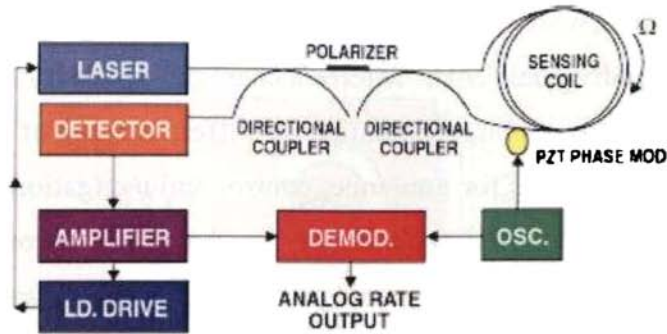


Figure 2.6. Basic components of a fiber optical gyroscope.

The principal optical components of a fiber optical gyroscope (FOG) are illustrated in figure 2.6, which shows a common laser source generating both clockwise and anticlockwise light waves traveling around a loop of optical fiber. Inertial rotation of this device in the plane of the page will change the effective path lengths of the clockwise and counter clockwise beams in the loop of fiber (Sagnac effect), causing an effective relative phase change at the detector. The interference phase between the clockwise and counterclockwise beams is measured at the output detector, but in this case the output phase difference is proportional to the rotation rate. Temperature changes and accelerations can alter the strain distribution in the optical fiber, which could cause output errors. Minimizing this effect is a major concern in the art of FOG design [34].

### 2.5.2.3 MEMS gyroscope

MEMS gyroscopes are a relatively new innovation. Fabrication technologies for microcomponents, microsensors, micromachines and microelectromechanical systems (MEMS) [47, 48] have rapidly developed, and represent a major research effort worldwide. There are many techniques currently being utilized in the production of different types of MEMS, including

inertial microsensors, which have made it possible to fabricate MEMS in high volumes at low individual cost. Micromechanical vibratory gyroscopes or angular rate sensors have a large potential for different types of applications as primary information sensors for guidance, control and navigation systems. They represent an important inertial technology because other gyroscopes such as solid-state gyroscopes, laser ring gyroscopes, and fiber optic gyroscopes, do not allow for significant miniaturization. MEMS sensors are commonly accepted as low performance and low cost sensors. These sensors have a large potential for different types of applications as primary information sensors for guidance, control and navigation systems.

In most micro-mechanical vibratory gyroscopes, the sensitive element can be represented as an inertia element and elastic suspension with two prevalent degrees of freedom (figure 2.7). Massive inertia element is often called proof mass. The sensitive element is driven to oscillate at one of its modes with prescribed amplitude. This mode usually is called primary mode. When the sensitive element rotates about a particular fixed-body axis, which is called sensitive axis, the resulting Coriolis force causes the proof mass to move in a different mode. Contrary to the classical angular rate sensors based on the electromechanical gyroscopes, information about external angular rate is contained in these different oscillations rather than nonharmonic linear or angular displacements. The excited oscillations are referred to as primary oscillations and oscillations caused by angular rate are referred to as secondary oscillations or secondary mode.

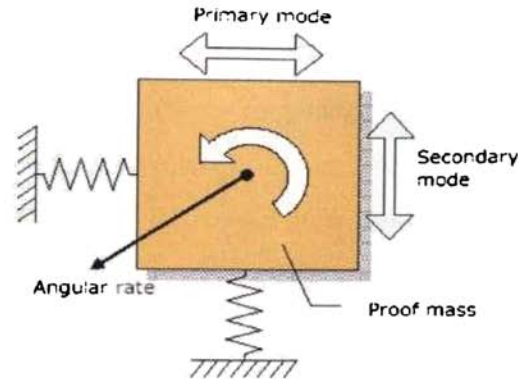


*Figure 2.7 Basic Structure of MEMS Gyro.*

It is possible to design gyroscopes with different types of primary and secondary oscillations. It is worth mentioning that the nature of the primary motion does not necessarily have to be oscillatory but could be rotary as well. Such gyroscopes are called rotary vibratory gyroscopes. However, it is typically more convenient for the vibratory gyroscopes to be implemented with the same type and nature of primary and secondary oscillations. The device's low power and small size will benefit the design of mobile robots, automotive and industrial products. The tremendous immunity to shock and vibration benefits automotive, robotics and other applications that are subject to harsh environmental conditions. Integrating both accelerometers and gyros on a single chip, results in an inertial measurement unit that would enable even tiny mobile robot vehicles to be navigated autonomously.

Analog devices ADIS16251 [49] is a complete angular rate gyroscope measurement system available in a single compact package. By enhancing Analog Devices MEMS sensor technology with an embedded signal processing solution, the ADIS16251 provides factory-calibrated and tunable digital sensor data in a convenient format that can be accessed using a simple SPI serial interface. The SPI interface provides access to measurements for the gyro data, temperature, power supply, and one auxiliary analog input. Easy access to calibrated digital sensor data provides



developers with a ready to use device, reducing development time, cost, and program risk. The device can be operated at 5V single ended supply voltage. The sensor bandwidth is 49Hz and has a form factor of around 11mm x 11mm. The device is available in 20pin terminal stacked Land Grid Array (LGA) package. The functional block diagram of the device is shown in figure 2.8. Figure 2.9 shows the bias and sensitivity characteristics of the device. We have studied a mobile vehicle position estimation system by incorporating this system with an optical encoder odometry. Photograph of a MEMS rate gyro chip is shown in Figure 2.10.

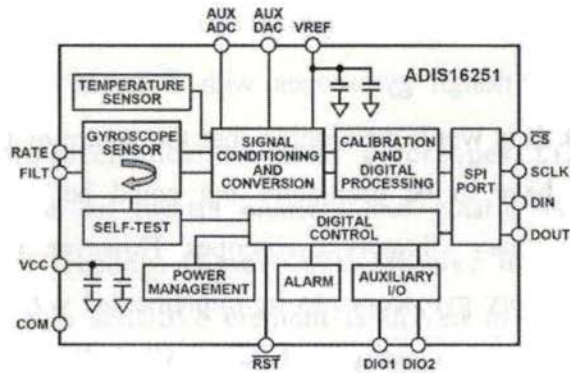


Figure 2.8 Functional block diagram of ADIS16251.

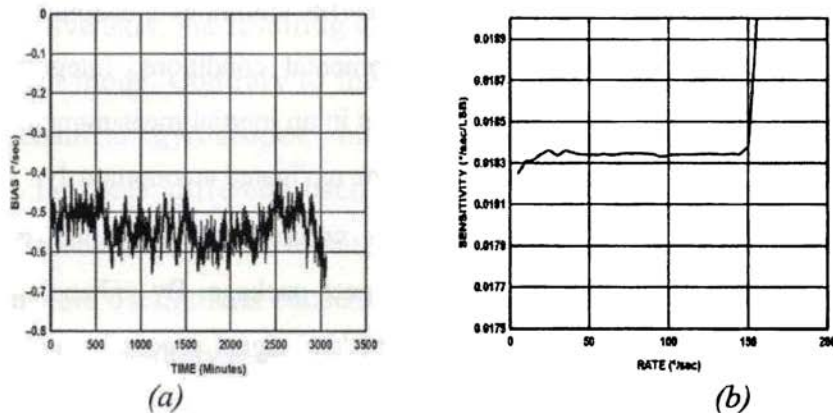
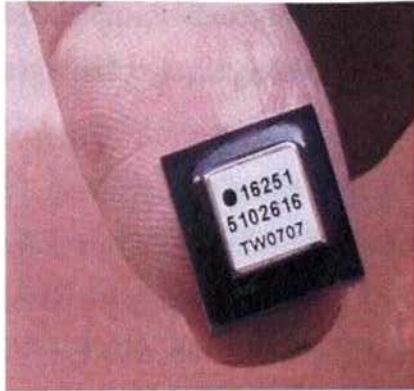


Figure 2.9 (a) The bias vs. time and (b) The sensitivity vs. angular rate at  $\pm 80$  degree per sec. range of ADIS16251.



*Figure 2.10 Photograph of an iMEMS gyro chip.*

## **2.6 Beacon based Localization**

Beacon navigation systems are the most common navigation aids on ships and aircrafts as well as on commercial mobile robot systems. Active beacons can be detected reliably and provide accurate positioning information with minimal processing. As a result, this approach allows high sampling rates and yields high reliability, but it does also incur high cost in installation and maintenance.

Most of the beacon based localization systems rely on a set of beacons placed at known positions in the environment. The mobile robot vehicle is equipped with a sensor(s) that can observe the beacons, and the navigational system uses these observations and knowledge of the beacon positions to locate the robot vehicle. Accurate mounting of beacons is required for accurate positioning. Unlike odometry and INS, the accuracy of the localization does not deteriorate with time in a beacon based system. This is due to the fact that the sensor on the robot vehicle provides observations of position, rather than observations of motion, and therefore is not subject to the accumulation of integration errors.

Beacon based localization systems can be categorized according to the type of signal used by the sensor, which relates to the beacon characteristics, and

according to the type of information processing employed by the system. The main types of signals used by beacon based localization systems are infrared, laser, ultrasound and millimeter wave radar.

In laser systems, the mobile robot vehicle is equipped with a rotating laser emitter/receiver, and the beacons are reflective strips placed at known positions in the environment. The angle of the sensor is registered when a laser reflection is observed, thus giving the bearing of the observation. Laser is by far the most widespread signal used in beacon based localization systems.

The second common signal type is ultrasound. This system usually relies on active (emitting) rather than passive (reflecting) beacons. Most objects in typical environments easily reflect ultrasound. Consequently, passive beacons would be difficult to identify using ultrasound. Another advantage of active beacons is that the transmitted signal may contain a specific code to identify the emitting beacon [50], or the beacons may identify themselves by transmitting in a particular sequence with the first beacon emitting a modified signal to the others [12].

The third type of signal used in beacon based localization systems is the millimeter wave radar (MMWR). The MMWR signal is reflected by metallic beacons placed at known locations in the environment, and the radar emitter/receiver provides both range and bearing to the beacons [51].

### **2.6.1 Localization Techniques**

Two main categories of beacon based localization systems can be identified according to the type of *information processing* employed by the system. These are triangulation or trilateration and estimation. Triangulation involves combining several bearing observations to deduce the position of the mobile robot vehicle, using the assumption that the position and attitude (pose) of the vehicle does not change between the observations. Trilateration uses the range measurements for the

computation of pose of the mobile vehicle. An alternative approach to triangulation is to form an estimate of the vehicle pose. Estimation relies on a model of the vehicle and the sensor. The estimate is updated each time a new observation is made, and the vehicle is localized from observation to observation using a prediction of the vehicle pose based on the vehicle control inputs, as shown in Figure 2.11. The Kalman filter [52, 53, 54] is widely used to form a probabilistic estimate of the vehicle pose, according to Bayesian Estimation Theory [55], in terms of a mean estimate and the covariance of the estimate.

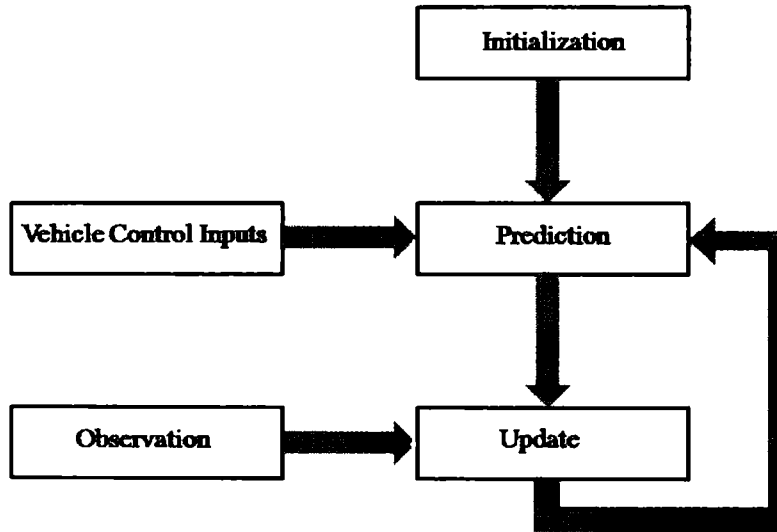


*Figure 2.11 The estimation process*

### **2.6.1.1 Trilateration**

Trilateration is a method to determine the position of an object based on simultaneous range measurements from three stations located at known sites [28]. In trilateration navigation systems, there are usually three or more transmitters mounted at known locations in the environment and one receiver on board the

robot. Conversely, there may be one transmitter on board and the receivers are mounted on the walls or rooftop. Using time-of-flight information, the system computes the distance between the stationary transmitters and the onboard receiver. This problem has been traditionally solved either by algebraic or numerical methods. It can be trivially expressed as the problem of finding the intersection of three spheres, that is, finding the solutions to the following system of quadratic equations:

$$\left. \begin{aligned} (x - x_1)^2 + (y - y_1)^2 + (z - z_1)^2 &= l_1^2 \\ (x - x_2)^2 + (y - y_2)^2 + (z - z_2)^2 &= l_2^2 \\ (x - x_3)^2 + (y - y_3)^2 + (z - z_3)^2 &= l_3^2 \end{aligned} \right\} (2.3)$$

where  $P_i = (x_i, y_i, z_i)$ ,  $i = 1, 2, 3$  are the coordinates of station, and  $l_i$  is the range measurement associated with it. In Figure 2.12, thick segments between stations define the *base plane*, and thin ones, those connecting the moving object and the stations correspond to the range measurements. Global Positioning System (GPS), discussed in Section 2.6.2, is an example of trilateration.

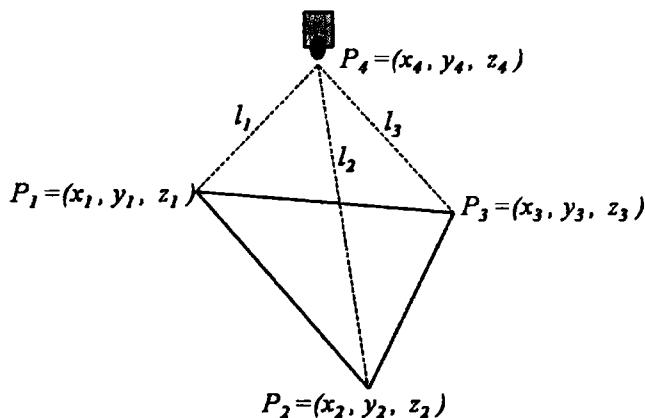


Figure 2.12 Trilateration method to obtain location of a mobile robot  $P_4$  from its distance from three stations located at  $P_1$ ,  $P_2$  and  $P_3$

### 2.6.1.2 Triangulation

Triangulation is the most widespread method used to localize a mobile robot vehicle [11]. In this configuration there are three or more active transmitters mounted at known locations, as shown in Figure 2. 13. A rotating sensor on board the robot registers the angles  $\theta_1$ ,  $\theta_2$  and  $\theta_3$  at which it “sees” the transmitter beacons relative to the vehicle's longitudinal axis. From these three measurements the unknown x and y coordinates and the unknown vehicle orientation can be computed. Some cases beacons are not visible in many areas, a problem that is particularly grave because at least three beacons must be visible for triangulation. Cohen and Koss [56] had performed a detailed analysis on three-point triangulation algorithms. The heading of at least two of the beacons was required to be greater than 90 degrees and the angular separation between any pair of beacons was required to be greater than 45 degrees for the efficient computation of the algorithms.

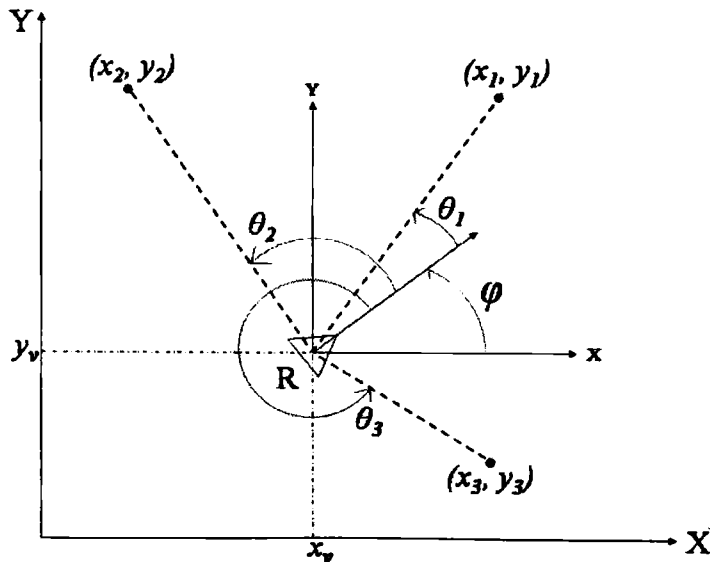


Figure 2.13 The basic triangulation problem on three observations  $\theta_1$ ,  $\theta_2$  and  $\theta_3$

Because of their technical maturity and commercial availability, optical triangulation systems are widely used in mobile robotics applications. Typically these systems involve some type of scanning mechanism operating in conjunction with fixed location references, strategically placed at predefined locations within the operating environment. A number of variations on this theme are seen in practice [43].

### **2.6.2 Global Positioning System**

The Global Positioning System (GPS) [34, 39, 57, 58] is a form of beacon based localization using active beacons. GPS based localization relies on the reception of signals emitted by several GPS satellites. The Navstar Global Positioning System (GPS) developed as a Joint Services Program by the Department of Defense uses a constellation of 24 satellites (including three spares) orbiting the earth every 12 hours at a height of about 10,900 nautical miles. Four satellites are located in each of six planes inclined 55 degrees with respect to the plane of the earth's equator [59]. The absolute three-dimensional location of any GPS receiver is determined through simple trilateration techniques based on time of flight for uniquely coded spread-spectrum radio signals transmitted by the satellites. Precisely measured signal propagation times are converted to *pseudoranges* representing the line-of-sight distances between the receiver and a number of reference satellites in known orbital positions. The measured distances have to be adjusted for receiver clock offset. Knowing the exact distance from the ground receiver to three satellites theoretically allows for calculation of receiver latitude, longitude, and altitude.

Although conceptually very simple [60], this design philosophy introduces at least four obvious technical challenges:

- Time synchronization between individual satellites and GPS receivers.
- Precise real-time location of satellite position.
- Accurate measurement of signal propagation time.
- Sufficient signal-to-noise ratio for reliable operation in the presence of interference and possible jamming.

The first of these problems is addressed through the use of atomic clocks (relying on the vibration period of the cesium atom as a time reference) on each of the satellites to generate time ticks at a frequency of 10.23 MHz. Each satellite transmits a periodic pseudo-random code on two different frequencies (designated L1 and L2) in the internationally assigned navigational frequency band. Multiplying the cesium-clock time ticks by 154 and 128, respectively, generates the L1 and L2 frequencies of 1575.42 and 1227.6 MHz. The individual satellite clocks are monitored by dedicated ground tracking stations operated by the Air Force, and continuously advised of their measured offsets from the ground master station clock. High precision in this regard is critical since electromagnetic radiation propagates at the speed of light, roughly 0.3 metres per nanosecond.

To establish the exact time required for signal propagation, an identical pseudocode sequence is generated in the GPS receiver on the ground and compared to the received code from the satellite. The locally generated code is shifted in time during this comparison process until maximum correlation is observed, at which point the induced delay represents the time of arrival as measured by the receiver's clock. The problem then becomes establishing the relationship between the atomic clock on the satellite and the inexpensive quartz-crystal clock employed in the GPS receiver. This is found by measuring the range to a fourth satellite, resulting in four independent trilateration equations with four unknowns.



In addition to its own timing offset and orbital information, each satellite transmits data on all other satellites in the constellation to enable any ground receiver to build up an almanac after a “cold start.” Diagnostic information with respect to the status of certain onboard systems and expected range-measurement accuracy is also included. This collective “housekeeping” message is superimposed on the pseudo-random code modulation at a very low (50 bits/s) data rate, and requires 12.5 minutes for complete downloading [61]. Timing offset and ephemeris information is repeated at 30 second intervals during this procedure to facilitate initial pseudorange measurements.

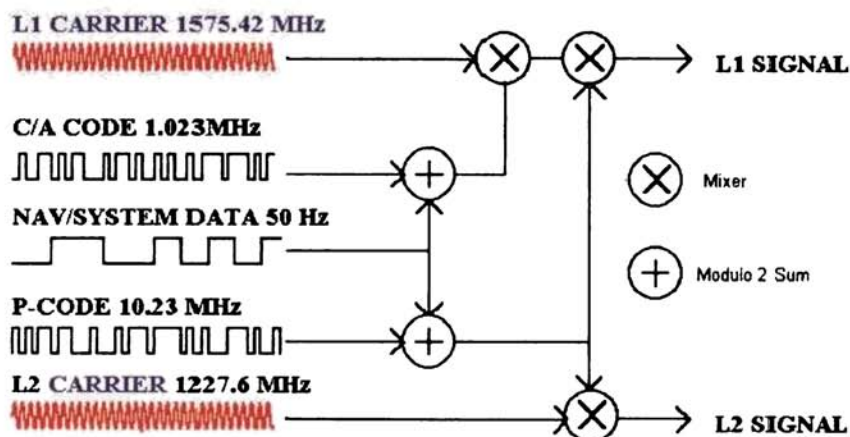


Figure 2.14 GPS Satellite signals.

To further complicate matters, the sheer length of the unique pseudocode segment assigned to each individual Navstar Satellite (i.e., around 6.2 trillion bits) for repetitive transmission can potentially cause initial synchronization by the ground receiver to take considerable time. For this and other reasons, each satellite broadcasts two different non-interfering pseudocodes. The first of these is called the *coarse acquisition*, or C/A code, and is transmitted on the L1 frequency to assist in acquisition. There are 1023 different C/A codes, each having 1023 chips

(code bits) repeated 1000 times a second [59] for an effective chip rate of 1.023 MHz (i.e., one-tenth the cesium clock rate). While the C/A code alone can be employed by civilian users to obtain a fix, the resultant positional accuracy is understandably somewhat degraded. The Y code (formerly the precision or P code prior to encryption on January 1st, 1994) is transmitted on both the L1 and L2 frequencies and scrambled for reception by authorized military users only with appropriate cryptographic keys and equipment. This encryption also ensures *bona fide* recipients cannot be “spoofed” (i.e., will not inadvertently track false GPS-like signals transmitted by unfriendly forces). Figure 2.14 shows various GPS Satellite signals.

Another major difference between the Y and C/A code is the length of the code segment. While the C/A code is 1023 bits long and repeats every millisecond, the Y code is  $2.35 \times 10^{14}$  bits long and requires 266 days to complete [61]. Each satellite uses a one-week segment of this total code sequence; there are thus 37 unique Y codes (for up to 37 satellites) each consisting of  $6.18 \times 10^{12}$  code bits set to repeat at midnight on Saturday of each week. The higher chip rate of 10.23 MHz (equal to the cesium clock rate) in the precision Y code results in a chip wavelength of 30 meters for the Y code as compared to 300 meters for the C/A code [61], and thus facilitates more precise time-of-arrival measurement for military purposes.

A number of factors affect the performance of a localization sensor that makes use of the GPS. First, it is important to understand that, because of the specific orbital paths of the GPS satellites, coverage is not geometrically identical in different portions of the Earth and therefore resolution is not uniform. Specifically, at the North and South Poles, the satellites are very close to the horizon and, thus, while resolution in the latitude and longitude directions is good, resolution of altitude is relatively poor as compared to more equatorial locations.

The second point is that GPS satellites are merely an information source. They can be employed with various strategies in order to achieve dramatically different levels of localization resolution. The basic strategy for GPS use, called *pseudo range* and described above, generally performs at a resolution of a few metres. An extension of this method is *differential GPS (DGPS)*, which makes use of a second receiver that is static and at a known exact position. A number of errors can be corrected using this reference, and so resolution improves to the order of 1 m or less. A disadvantage of this technique is that the stationary receiver must be installed, its location must be measured very carefully, and of course the moving robot must be within kilometers of this static unit in order to benefit from the DGPS technique.

The principle advantage of using GPS over land based beacons is that the GPS signal is readily available which reduces the deployment cost and time of the system. Further, a GPS system is less susceptible to damage since the satellites, the beacons of the GPS, are maintained by international reputed organizations. GPS is extremely effective for outdoor ground-based and flying robots.

A complete GPS receiver implemented on the HPM103H-6 GPS *Engine Module* [62, 63] is shown in figure 2.15. The engine module having a form factor of only 25.4x25.4mm uses GPS radio based on uN8021 RF chip, base-band processor based on uN8031 chip with integrated serial data communication and real time clock (RTC). The system needs only 3V regulated power supply and consumes nearly a power of 130mW in navigational mode. An external GPS antenna (50 ohm, active or passive) can be connected to this sub system using the RF-input line. For establishing communication with the module a baud rate of 4800, n, 8, 1 is used. This GPS module is compatible with NMEA2.1 protocol, so that by sending commands the control processor or GPS software (message strings)

can read the sentences for further applications. The National Marine Electronics Association (NMEA) defined a RS-232 communication standard for devices that include GPS receivers. The GPS receivers can output geo-spatial location, time, headings and navigation-relevant information in the form of ASCII command limited message strings. The photograph of the GPS sub system is shown in figure 2.16. We have realized a drivers safety system based on this module.

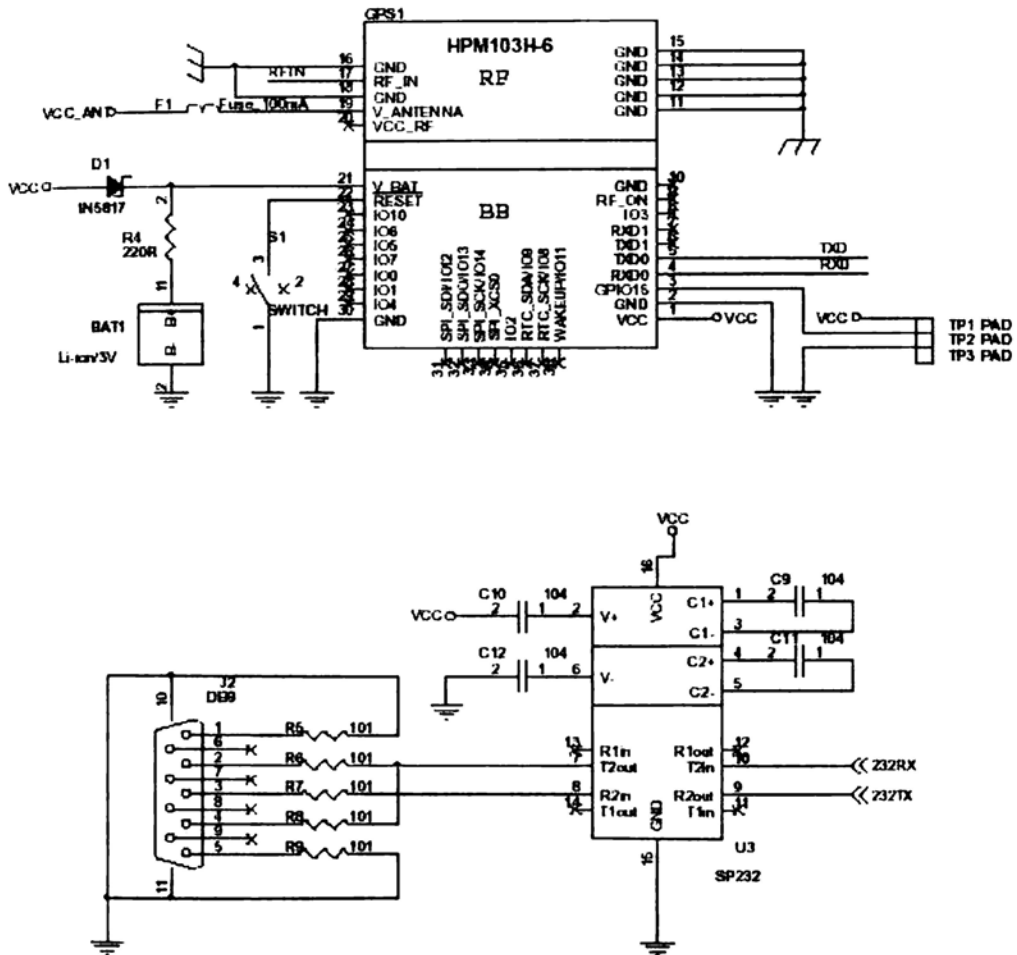


Figure 2.15 The schematic of the GPS sub system.

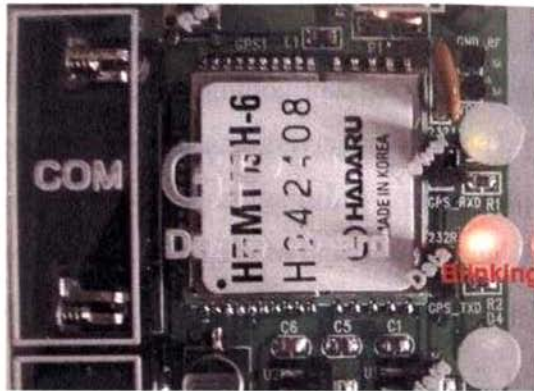


Figure 2.16 Photograph of the GPS sub system studied.

## 2.7 Active Ranging Systems

Active ranging sensors continue to be the most popular sensors in mobile robotics [32]. Many ranging sensors have a low price point, and, most importantly, all ranging sensors provide easily interpreted outputs: direct measurements of distance from the robot to objects in its vicinity. For obstacle detection and avoidance, most mobile robots rely heavily on active ranging sensors. But the local freespace information provided by ranging sensors can also be accumulated into representations beyond the robot's current local reference frame. Thus active ranging sensors are also commonly found as part of the localization and environmental modeling processes of mobile robots.

### 2.7.1 Time-of-Flight Active Ranging

Time-of-flight ranging makes use of the propagation speed of sound or an electromagnetic wave. It is important to point out that the propagation speed of sound is approximately 0.3 m/ms whereas the speed of electromagnetic signals is 0.3 m/ns, which is 1 million times faster. The time of flight for a typical distance, say 3 m, is 10 ms for an ultrasonic system but only 10 ns for a laser rangefinder. It is thus evident that measuring the time of flight with electromagnetic signals is

more technologically challenging. This explains why laser range sensors have only recently become affordable and robust for use on mobile robots.

The quality of time-of-flight range sensors depends mainly on:

- Uncertainties in determining the exact time of arrival of the reflected signal
- Inaccuracies in the time-of-flight measurement (with laser range sensors)
- The dispersal cone of the transmitted beam (mainly with ultrasonic range sensors)
- Interaction with the target (e.g., surface absorption, specular reflections)
- Variation of propagation speed
- The speed of the mobile robot and target (in the case of a dynamic target)

#### ***2.7.1.1 The Ultrasonic Rangefinder (Sonar)***

The basic principle of an ultrasonic sensor is to transmit a packet of (ultrasonic) pressure waves and to measure the time it takes for this wave packet to reflect and return to the receiver. The distance of the object causing the reflection can be calculated based on the propagation speed of sound and the time of flight.

A threshold value is set for triggering an incoming sound wave as a valid echo. This threshold is often decreasing in time, because the amplitude of the expected echo decreases over time based on dispersal as it travels longer. But during transmission of the initial sound pulses and just afterward, the threshold is set very high to suppress triggering the echo detector with the outgoing sound pulses. A transducer will continue to ring for up to several milliseconds after the initial transmission, and this governs the *blanking time* of the sensor. Note that if, during the blanking time, the transmitted sound were to reflect off of an extremely close object and return to the ultrasonic sensor, it may fail to be detected.

However, once the blanking interval has passed, the system will detect any above threshold reflected sound, triggering a digital signal and producing the distance measurement using the integrator value or timer count. The ultrasonic wave typically has a frequency between 40 and 180 kHz and is usually generated by a piezo or electrostatic transducer. Often the same unit is used to measure the reflected signal, although the required blanking interval can be reduced through the use of separate output and input devices. Frequency can be used to select a useful range when choosing the appropriate ultrasonic sensor for a mobile robot. Lower frequencies correspond to a longer range, but with the disadvantage of longer post-transmission ringing and, therefore, the need for longer blanking intervals. Most ultrasonic sensors used by mobile robots have an effective range of roughly 12cm to 5m. In mobile robot applications, specific implementations generally achieve a resolution of approximately 2 cm. In most cases a narrow opening angle for the sound beam is preferred in order to obtain precise directional information about objects that are encountered. This is a major limitation since sound propagates in a cone-like manner with opening angles around 20 to 40 degrees. Consequently, when using ultrasonic ranging one does not acquire depth data points but, rather, entire regions of constant depth. This means that the sensor tells us only that there is an object at a certain distance within the area of the measurement cone.

However, recent research developments show significant improvement of the measurement quality in using sophisticated echo processing [64]. Ultrasonic sensors suffer from several additional drawbacks, namely in the areas of error, bandwidth, and cross-sensitivity. The published accuracy values for ultrasonics are nominal values based on successful, perpendicular reflections of the sound wave off of an acoustically reflective material. This does not capture the effective error modality seen on a mobile robot moving through its environment. As the ultrasonic transducer's angle to the object being ranged varies away from perpendicular, the

chances become good that the sound waves will coherently reflect away from the sensor, just as light at a shallow angle reflects off of a smooth surface. Therefore, the true error behavior of ultrasonic sensors is compound, with a well-understood error distribution near the true value in the case of a successful retroreflection, and a more poorly understood set of range values that are grossly larger than the true value in the case of coherent reflection. Of course, the acoustic properties of the material being ranged have direct impact on the sensor's performance. For example, foam, fur, and cloth can, in various circumstances, acoustically absorb the sound waves.

A final limitation of ultrasonic ranging relates to bandwidth. Particularly in moderately open spaces, a single ultrasonic sensor has a relatively slow cycle time. For example, measuring the distance to an object that is 3 m away will take such a sensor 20 ms, limiting its operating speed to 50 Hz. But if the robot has a ring of twenty ultrasonic sensors, each firing sequentially and measuring to minimize interference between the sensors, then the ring's cycle time becomes 0.4 seconds and the overall update frequency of any one sensor is just 2.5 Hz. For a robot conducting moderate speed motion while avoiding obstacles using ultrasonics, this update rate can have a measurable impact on the maximum speed possible while still sensing and avoiding obstacles safely. Airborne sonar devices are popular in mobile robotics, although they are typically limited to ranges of up to 10m [65]. These typically operate around 45KHz (wavelength about 7mm). Disadvantages of the sonar reside in its poor angular resolution (wide beam) and ambiguous returns from specular target surfaces.

### ***2.7.1.2 Laser Rangefinder (Lidar)***

The laser rangefinder is a time-of-flight sensor [39] that achieves significant improvements over the ultrasonic range sensor owing to the use of laser light



instead of sound. This type of sensor consists of a transmitter, which illuminates a target with a collimated beam (e.g., laser), and a receiver capable of detecting the component of light, which is essentially coaxial with the transmitted beam. Often referred to as optical radar or *Lidar* (light detection and ranging), these devices produce a range estimate based on the time needed for the light to reach the target and return. A mechanism with a mirror sweeps the light beam to cover the required scene in a plane or even in three dimensions, using a rotating, nodding mirror. One way to measure the time of flight for the light beam is to use a pulsed laser and then measure the elapsed time directly, just as in the ultrasonic solution described earlier. Electronics capable of resolving picoseconds are required in such devices and they are therefore very expensive. A second method is to measure the beat frequency between a frequency modulated continuous wave (FMCW) and its received reflection. Another, even easier method is to measure the phase shift of the reflected light.

The main advantages of most laser based range measuring sensors are as follows:

- Narrow beam footprint
- Small beam divergence
- Long Range
- High accuracy
- High bandwidth

The main shortcoming of laser based range sensors is their limited visibility under adverse atmospheric effects. Small particles, such as water molecules and dust can distort and attenuate laser light, resulting in limited range measurements. Target reflectivity is another topic of concern when considering lasers. The ability to reflect light in a given range of frequencies will depend highly on target properties and the angle of incident light. Dark objects tend to absorb most light whilst lighter objects tend to reflect most of it. The micro-topology of a targets surface will affect the amount of light returned. Specular reflection occurs mostly with

smooth surfaces, where light is reflected in a well-defined direction. In this case, it is quite possible that no energy is returned to the detector (assuming the receiver lies on the same plane as the transmitter). An optically rough surface is defined as a surface with a micro-topology variability in the order of the light beam wavelength. Most natural features fall under this definition, and diffuse light in many directions, consequently reducing the amount of light returned in the direction of the laser receiver.

Due to the narrow beam footprint of typical laser systems many measurements are required to construct a qualitative representation of the structure of complex and large objects. Therefore, laser systems are usually mounted on a scanning device, or contain a built-in scanning device. The high bandwidth of laser sensors do allow for fast data acquisition, however most laser measuring systems are limited by the speed of the mechanical scanning device employed (e.g. motor-driven mirrors, pan-tilt units).

As expected, the angular resolution of laser rangefinders far exceeds that of ultrasonic sensors. The Hokuyo UBG-05LN laser scanner [66] shown in Figure 2.17 achieves an angular resolution of 0.36 degrees, measurement accuracy of 2% and has a wide detecting area (5mx4m). This device operates at 24V DC and consumes a current of 150mA or less.



*Figure 2.17 UBG-05LN laser scanner from Hokuyo Automatic Company.*

As with ultrasonic ranging sensors, an important error mode involves coherent reflection of the energy. With light, this will only occur when striking a highly polished surface. Practically, a mobile robot may encounter such surfaces in the form of a polished desktop, file cabinet or, of course, a mirror. Unlike ultrasonic sensors, laser rangefinders cannot detect the presence of optically transparent materials such as glass, and this can be a significant obstacle in environments, for example, museums, where glass is commonly used.

### *2.7.1.3 Radar Devices*

By detecting a reflection of radiated electromagnetic energy, radar devices are able to determine range of objects. No other sensor can measure range to the accuracy possible with radar, at long ranges, and under adverse weather conditions [67]. Radars can provide diverse information about an object, such as, velocity, angular direction, size and shape, in addition to range. The intensity of returned echo is also an important source of information. Returned intensity information can be used to determine changes in the radar cross-section of a target, due to changes in the target's radial surface projection. Intensity information can also be used for measuring induced modulation due to rotation and vibration of target components [67].

The size of the radar antenna mostly depends on the frequency used. The higher the frequency, the smaller the antenna can be, although physical and electronic constraints restrict the achievable frequencies. The typical waveforms that range measuring radars employ are the short pulse or modulated continuous waves (frequency or phase modulated). Millimetre wave (mmWave) radars operate in the electromagnetic frequency range of about 30 to 300GHz (wavelength 1mm to 1cm) [65,68]. Low atmospheric attenuation occurs at 35GHz and 94GHz. Consequently, many mmWave radars are designed for operating around 94GHz and possibly 77GHz [69].

Figure 2.18 shows a schematic block diagram of an FMCW RADAR transceiver [71]. The input voltage to the voltage controlled oscillator (VCO) is a ramp signal. The VCO generates a signal of linearly increasing frequency  $\delta f$  in the frequency sweep period  $T_d$ . This linearly increasing chirp signal is transmitted via the antenna. A frequency modulated continuous wave (FMCW) RADAR measures the distance to an object by mixing the received signal with a portion of the transmitted signal [70].

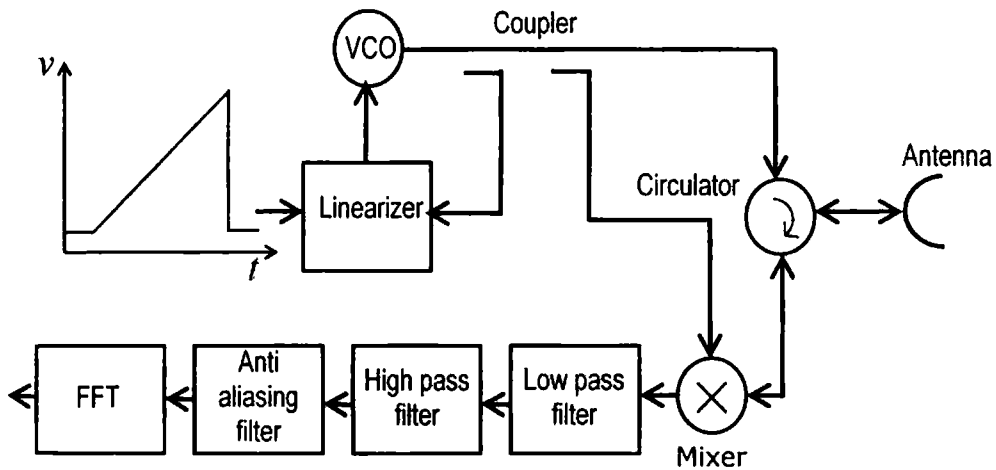


Figure 2.18 Block diagram of a MMW RADAR transceiver.

Let the transmitted signal  $v_T(t)$  as a function of time,  $t$ , be represented as

$$\begin{aligned} v_T(t) &= [A_T + a_T(t)] \cos\left[\omega_c t + A_b \int_a^t t dt + \varphi(t)\right] \\ &= [A_T + a_T(t)] \cos\left[\omega_c t + \frac{A_b}{2} t^2 + \varphi(t)\right] \end{aligned} \quad (2.4)$$

where  $A_T$  is the amplitude of the carrier signal,  $A_b$  is the amplitude of the modulating signal,  $\omega_c$  is the carrier frequency (i.e.,  $2\pi \times 77$  GHz),  $a_T(t)$  is the amplitude noise, and  $\varphi(t)$  is the phase noise present in the signal which occurs inside the transmitting electronic sections.

At any instant of time, the received echo signal,  $v_R$  is shifted in time from the transmitted signal by a round trip time,  $\tau$ . The received signal is

$$v_R(t - \tau) = [A_R + a_R(t - \tau)] \cos[\omega_c(t - \tau) + \frac{A_b}{2}(t - \tau)^2 + \varphi(t - \tau)] \quad (2.5)$$

Where  $A_R$  is the received signal amplitude,  $a_R(t - \tau)$  is the amplitude noise, and  $\varphi(t - \tau)$  is the phase noise. The sources of noise affecting the signal's amplitude consist of external interference to the RADAR system (e.g., atmospheric noise, man-made interference signals) and internally produced noise at the receiver antenna and amplifiers in the system.

In the mixer, the received signal is mixed with a portion of the transmitted signal with an analog multiplier.

$$\begin{aligned} v_T(t)v_R(t - \tau) &= [A_T + a_T(t)] [A_R + a_R(t - \tau)] \\ &\times \left\{ \cos \left[ \omega_c t + \frac{A_b}{2} t^2 + \varphi(t) \right] \right\} \\ &\times \left\{ \cos \left[ \omega_c(t - \tau) + \frac{A_b}{2}(t - \tau)^2 + \varphi(t - \tau) \right] \right\} \end{aligned} \quad (2.6)$$

The output of the mixer,  $v_{out}(t)$  is (using the trigonometric identity for the product of two sine waves)  $\cos A \cos B = 0.5[\cos(A + B) + \cos(A - B)]$

$$v_{out}(t - \tau) = \frac{[A_T + a_T(t)] [A_R + a_R(t - \tau)]}{2} [B_1 + B_2] \quad (2.7)$$

where

$$B_1 = \cos \left[ (2t - \tau) \left( \omega_c - \frac{A_b}{2} \tau \right) + A_b t^2 + \varphi(t) + \varphi(t - \tau) \right] \quad \text{and}$$

$$B_2 = \cos \left[ \left( \omega_c - A_b \left( \frac{\tau}{2} - t \right) \right) \tau + \varphi(t) - \varphi(t - \tau) \right]$$

The second cosine term,  $B_2$ , is the signal containing the beat frequency. The output of the low pass filter consists of the beat frequency component,  $B_2$  and noise components with similar frequencies to the beat frequency, while other components are filtered out. The beat frequency,  $f_b$ , is directly proportional to the delay time,  $\tau$  which is directly proportional to the round trip propagation time to the target. The relationship between beat frequency and target distance is

$$R = \frac{cT_s}{2} \frac{1}{f_s} f_b \quad (2.8)$$

where  $R$  is the range of the object,  $c$  is the velocity of the electromagnetic wave,  $T_s$  is the frequency sweep period, and  $f_s$  is the swept frequency bandwidth [71].

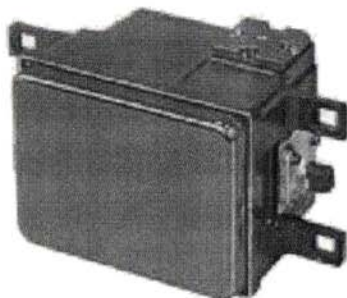


*Figure 2.19. 76GHz Millimeter Wave Automobile Radar using Single Chip MMIC.*

Modern automobile vehicles equipped with Adaptive Cruise Control (ACC) and Collision Mitigation Systems use Millimeter Wave radar [72]. As an approach to price reduction aimed at expanding the use of Millimeter Wave radar, *Fujitsu Ten Limited* developed a single chip for Monolithic Microwave Integrated Circuit (MMIC) modules in Millimeter wave transceivers and also developed radar that

utilizes that technology (figure. 2.19). The same can be adopted in autonomous mobile robot vehicle applications.

Millimetre wave radars have been shown to suffer from attenuation of around seven orders of magnitude lower than lasers under the same environmental conditions [65, 69].

A few advantages of using radar devices as a range measuring device is as follows:

- Adverse weather functionality
- Independent of ambient radiation
- Long Range
- Medium-High accuracy
- High bandwidth

Disadvantages of such radar systems lie mostly in their higher cost and typically larger size. The cost of radar also makes its use somewhat prohibitive, although recent developments in microwave integrated circuitry have brought the cost of system down.

### **2.7.2 Structured Light Sensor**

Sheet of light or structured lighting is another method for range determination. A specific, regular light pattern is projected onto the area of interest. A typical setup is shown in Figure 2.20. The emitter must project a known pattern (structured light) onto the environment. Many systems exist which either project light textures or emit collimated light (possibly laser) by means of a rotating mirror. Yet another popular alternative is to project a laser stripe by turning a laser beam into a plane using a prism. Regardless of how it is created, the projected light has a known structure, and therefore the image taken by the CCD or CMOS

receiver can be filtered to identify the pattern's reflection. The distortion in the light pattern is used to calculate range and depth information [73, 74]. Lighting patterns can consist of single dots and lines or a regular grid depending on the application. Note that the problem of recovering depth is in this case far simpler than the problem of passive image analysis. Various light sources may be used to create the structured pattern depending on the desired accuracy and lighting conditions present. Furthermore, the structured light sensor is an active device so it will continue to work in dark environments as well as environments in which the objects are featureless. (e.g., uniformly colored and edgeless). In contrast, stereovision would fail in such texture free circumstances.

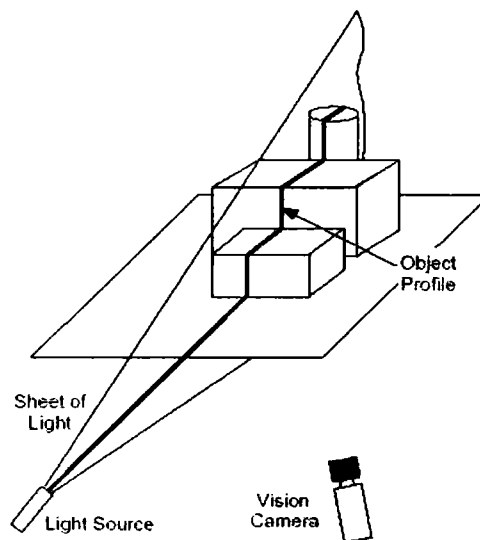


*Figure 2.20 Basic Structured Light Setup.*

## **2.8 Motion Sensors**

Some sensors measure directly the relative motion between the robot and its environment [32]. Since such motion sensors detect relative motion, so long as an object is moving relative to the robot's reference frame, it will be detected and its



speed can be estimated. There are a number of sensors that inherently measure some aspect of motion or change. For example, a pyroelectric sensor detects change in heat. When a human walks across the sensor's field of view, his or her motion triggers a change in heat in the sensor's reference frame.

### 2.8.1 Doppler Effect-based Sensing (Radar or Sonar)

The Doppler effect is a frequency shift that results from relative motion between a frequency source and a listener. The doppler shift is directly proportional to speed between source and listener, frequency of the source, and the speed with which the wave travels. The measured frequency at the receiver is a function of the relative speed between transmitter and receiver. This change in frequency is known as the *Doppler shift*. The Doppler effect applies to sound and electromagnetic waves. It has a wide spectrum of applications [32, 45]:

- *Sound waves*: industrial process control, security, fish finding, speed measurement.
- *Electromagnetic waves*: vibration measurement, radar systems, object tracking.

Doppler systems can be used to determine a moving object's speed by measuring the frequency shift of the acoustic/electromagnetic wave returned from a fixed reflector. Assuming the reflector to be directly ahead and the same plane as the transmitting/receiving transducer, the frequency shift is given by:

$$f_d = \frac{2Vf_o}{c} \quad (2.9)$$

Where  $f_d = f_o - f_r$

$f_o$  - transmitted frequency

$f_r$  - received frequency

$V$ - Velocity of object and

$C$ - Propagation velocity of acoustic/electromagnetic wave.

The frequency deviation  $f_d$  caused by the movement of the object can be used for the computation of velocity of the object. Existing systems can provide information on multiple targets at approximately 2 Hz.

A *Doppler radar* uses the Doppler effect of the returned echoes from targets to measure their radial velocity. Doppler radars are used in air defense, air traffic control, sounding satellites, police speed guns and radiology. The Doppler sonar has tremendous applications in marine systems. The availability of a reflecting stationary or moving object with a known velocity limits their applications in robotics.

## **2.9 Vision-based Sensors**

Vision is our most powerful sense. It provides us with an enormous amount of information about the environment and enables rich, intelligent interaction in dynamic environments. It is therefore not surprising that a great deal of effort has been devoted to providing machines with sensors that mimic the capabilities of the human vision system. The first step in this process is the creation of sensing devices that capture the same raw information that the human vision system uses.

### **2.9.1 Visual Ranging Sensors**

Range sensing is extremely important in mobile robotics, as it is a basic input for successful obstacle avoidance [32]. A number of sensors such as ultrasonic, laser rangefinder, optical rangefinder, and so on are popular in robotics explicitly for their ability to recover depth estimates. It is natural to attempt to implement ranging functionality using vision chips as well. However, a fundamental problem with visual images makes range finding relatively difficult. Any vision chip collapses the 3D world into a 2D image plane, thereby losing depth information. If one can make strong assumptions regarding the size of

objects in the world, or their particular color and reflectance, then one can directly interpret the appearance of the 2D image to recover depth. But such assumptions are rarely possible in real-world mobile robot applications. Without such assumptions, a single picture does not provide enough information to recover spatial information. The general solution is to recover depth by looking at *several* images of the scene to gain more information, hopefully enough to at least partially recover depth. The images used must be different, so that taken together they provide additional information. They could differ in viewpoint, yielding *stereo* or *motion* algorithms. An alternative is to create different images, not by changing the viewpoint, but by changing the camera geometry, such as the focus position or lens iris. This is the fundamental idea behind depth from focus and depth from defocus techniques.

### 2.9.2 Stereo-Vision

Stereo-vision systems [75, 76] rely on images from single or multiple cameras in order to obtain depth information. Hager and Atiya [77] developed a method that uses a stereo pair of cameras to determine correspondence between observed landmarks and a pre-loaded map, and to estimate the two dimensional location of the sensor from the correspondence. Landmarks are derived from vertical edges. By using two cameras for stereo range imaging the algorithm can determine the two dimensional locations of observed points in contrast to the ray angles used by single-camera approaches [32].

The basic stereo techniques for creating depth maps rely on patch or feature correlation within various images and performing triangulation. Unfortunately, the quality of stereo-vision range data is typically very poor, relying highly on camera calibration, lighting conditions, patch/feature associations, and the baseline between cameras or images. Different filtering techniques can be used to reduce the

amount of spurious data, but this usually results in a significant loss of good data. At the other extreme, visual interpretation by means of one or more CCD/CMOS cameras provides a broad array of potential functionalities, from obstacle avoidance and localization to human face recognition. However, commercially available sensor units that provide visual functionalities are only now beginning to emerge.

### **2.9.3 Visual Guidance System**

The role of visual guidance system (VGS) in the autonomous vehicle system is to capture raw sensory data and convert it into model representations of the environment and the vehicle's state relative to it. The sensory processing system that populates the world model fuses inputs from multiple sensors and extracts feature information, such as terrain elevation, road edges, and obstacles. As the vehicle moves, new sensed data inputs can either replace the historical ones, or a map-updating algorithm can be activated. The image processing capability of recent computer systems makes VGS a popular navigational tool for mobile robot vehicles [71]. Figure 2.21 shows the architecture of a visual guidance system.

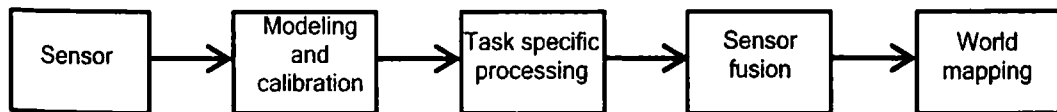


*Figure. 2. 21 Architecture of a visual guidance system.*

### **2.10 Map Based Positioning**

Map-based positioning, also known as “map matching,” is a technique in which the robot uses its sensors to create a map of its local environment. This local map is then compared with a global map previously stored in memory. If a match is found, then the robot can compute its actual position and orientation in

the environment. The prestored map can be a CAD model of the environment, or it can be constructed from prior sensor data [39].

The main advantage of map-based positioning is that this method uses the naturally occurring structure of typical indoor environments to derive position information without modifying the environment. It can be used to generate an updated map of the environment, which allows a robot to learn a new environment and to improve positioning accuracy through exploration.

The position estimation strategies that use map-based positioning rely on the robot's ability to sense the environment and to build a representation of it, and to use this representation effectively and efficiently. The sensing modalities used significantly affect the map making strategy. Error and uncertainty analyses play an important role in accurate position estimation and map building. Modeling the errors by probability distributions and using Kalman filtering techniques are good ways to deal with these errors [78].

The various steps for map building process involve feature extraction from raw sensor data, fusion of data, matching and determining the correspondence between the most recent sensor models [81, 82] and updation of an environment model with different degrees of abstraction. [79, 80]

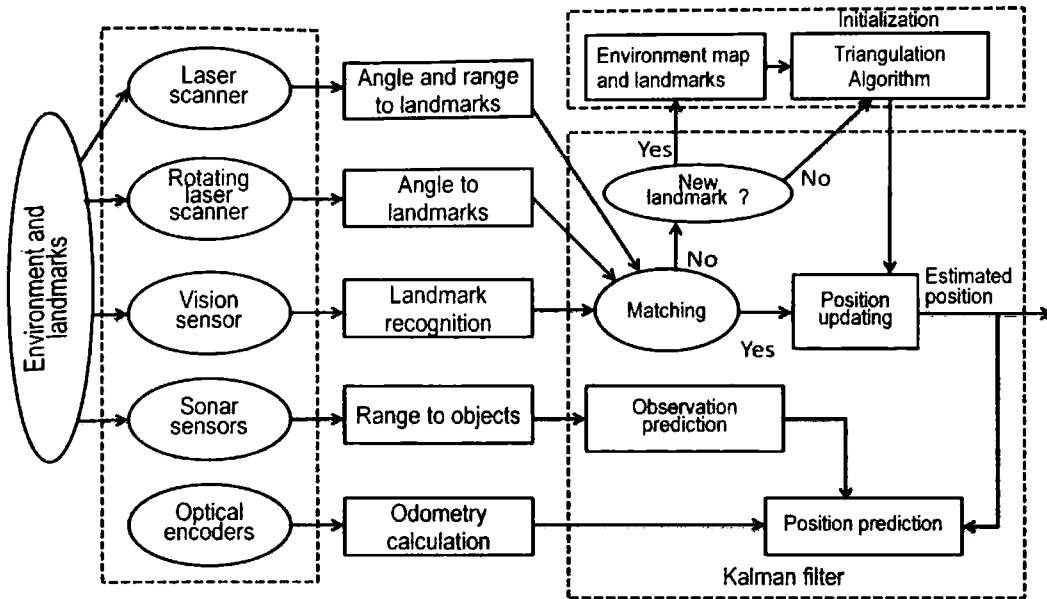


Figure 2.22 Block diagram of the concurrent map-based localization.

Since 1990s, the problem of map building has been dominated by probabilistic techniques. Since then, the conjunction of the localization and mapping problems has commonly been referred to as simultaneous localization and map building (SLAM) [13, 14]. The SLAM problem asks if it is possible for an autonomous vehicle to start in an unknown location in an unknown environment and then to incrementally build a map of this environment while simultaneously using this map to compute absolute vehicle location [83, 84, 85, 86, 87, 88].

Figure 2.22 shows the block diagram of a SLAM system that is able to implement concurrent localization and map building automatically. It is a closed-loop navigation process for position initialization, position updating, and map building [71]. The ability to place an autonomous vehicle at an unknown location in an unknown environment and then have it build a map, using only relative observations of the

environment, and then to use this map simultaneously to navigate would indeed make such a robot “autonomous”. Thus the main advantage of SLAM is that it eliminates the need for artificial infrastructures or *a priori* topological knowledge of the environment.

Disadvantage of map-based positioning is the specific requirements of enough stationary, easily distinguishable features that can be used for matching. The sensor map should be accurate enough (depending on the tasks) and a significant amount of sensing and processing power should be available.

## 2.11 Summary

This chapter presents the necessary background to this thesis by discussing common localization methods available for the estimation of position and attitude of mobile robot vehicles. The robotic systems utilize various sensing techniques and processing algorithms for the extraction of information. The wide variety of sensing techniques reported for mobile robot localization have been briefly surveyed in this chapter.

Some sensors are simple but some others are robust and equipped with complex and costly processing electronics, which can be used to acquire information about the robot’s environment or even to directly measure a robot’s absolute position. As the mobile robot moves around, it will frequently encounter with unpredictable environmental conditions, and therefore such sensing is particularly critical. The general classification of sensors used for localization of robots and their features are also discussed alongwith the typical sensors. Odometric sensors, INS and active ranging sensors are thoroughly discussed. Complex systems like vision based localization and SLAM are also briefly explained. The merits and demerits of various beacon based systems for the localization of autonomous mobile robots are examined.

## METHODOLOGY

### Chapter 3

---

3.1 Mounting Assembly .....	62
3.2 The Development Support Systems .....	62
3.3 Beacon Transmitter .....	64
3.4 Beacon Receiver .....	64
3.5 DISLiB System .....	65
3.6 Beacon Networking .....	65
3.7 Error Reduction .....	66
3.8 Traffic Control .....	66
3.9 Visually Impaired Support .....	66
3.10 Summary .....	67

---

The methodology adopted for the design, construction and experimental details of a beacon system developed for the localization of autonomous robot vehicle is briefly discussed in this chapter. A mounting assembly in conjunction with an encoded digital infrared sheet of light beacon (DISLiB) transmitter designed around a microcontroller has been utilized for the localization study. A battery operated handy beacon receiver unit has been designed and developed for investigating its characteristics. A networking scheme for the beacon based indoor mobile robot vehicle has also been proposed. A three wheeled vehicle model has been considered for the implementation and pose update. A PC based monitoring and control of the mobile robot vehicle and its traffic management is also proposed.



An odometric error reduction technique has been developed by utilizing the redundant encoder information that is implemented in FPGA with an SPI interface to the robot vehicle controller. Using the DISLiB developed and the existing GSM network, the feasibility of a roadway traffic control system has been studied in detail. A differently able assistance for the visually impaired has also been developed based on the DISLiB technology, which supports a microcontroller selectable voice message play back in natural language.

### **3.1 Mounting Assembly**

An innovative assembly has been developed for mounting the encoded digital infrared beacon transmitter to produce a sheet of light for localization applications. The infrared beam is guided through the space between two identical sand blasted parallel metal plates. These metal plates will be acting as Lambertian scattering surfaces (diffuse reflectors) and their dimensions have effects on the sheet thickness as well as infrared light intensity. A single infrared LED mounted at the centre of the LED housing is seen to have a beam angle of around 45 degrees, which can be increased by mounting multiple LEDs.

### **3.2 The Development Support Systems**

For carrying out the proposed work, the different application modules have been developed around various PIC microcontrollers. For the characterization of the beacon system an 8-pin flash based 8-bit CMOS microcontroller, the PIC12F675 has been utilized. An operating speed upto 20 MHz (200nsec/instruction), flash program memory of 1Kx14 words, six I/O pins with individual direction control, 64 bytes of general purpose RAM, programmable code protection, power saving sleep mode are some of its features. The PIC16F676, a 14-pin microcontroller has been used for the beacon with RS485 network. The vehicle

control and the localization system has been realized using the PIC18F4550 microcontroller having inbuilt USB support, PWM modules and hardware multiplier.

A development system having an inbuilt 20x4 LCD module, USB, RS-232, RS-485 ports, inbuilt push button key switches and I/O termination in header pins has been designed and constructed and used throughout the work for prototyping. The photograph of the development board is shown in figure 3.1.

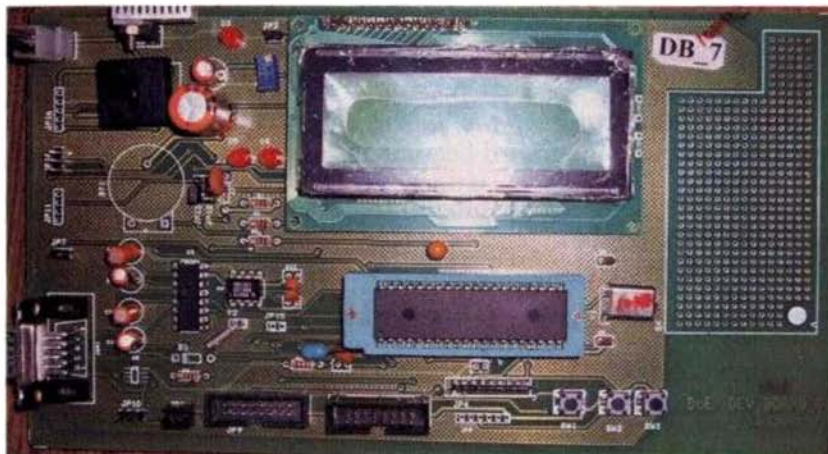


*Figure 3.1 Photograph of the PIC Microcontroller Development Board*

PIC18F2550, a compatible version of 4550, with less number of I/O pins has been utilized for the design and development of USB - RS485 bridge. The *Hi-Tech C* and *MPLab* tools have been utilized for the software development for microcontroller systems. The *Matlab* was utilized for the study of the characteristics and generating the various plots. A three wheeled prototype vehicle has also been fabricated for the studies and is shown in figure 3.2.



*Figure 3.2 Photograph of the fabricated three wheeled prototype vehicle*

### **3.3 Beacon Transmitter**

In order to study the characteristics of the beacon transmitter and its assembly a system has been designed using a PIC12F675 microcontroller [94]. The system transmits an encoded bit stream, which incorporates a location and traffic information. The RS 485 networked beacons and a host computer can modify the position information, in case of restructuring of the environment as well as online traffic signaling commands. The variation of the infrared effective light sheet thickness (ELST) against the height of the mounting structure has been studied and the results illustrate a linear increase in light sheet thickness for mounting heights from two to six metres for a particular assembly.

### **3.4 Beacon Receiver**

For the study of the beacon transmitter performance a handy receiver unit has been developed around a PIC12F675, 8-pin microcontroller and an infrared remote control receiver module. For the localization of the robot vehicle a

receiver/controller unit has been realized using microchip PIC18F4550 microcontroller [99]. The odometric sensors in the vehicle provide the position information to the microcontroller, which manages the drive and control systems.

### **3.5 DISLiB System**

The Digital Infrared Sheet of Light Beacons (**DISLiB**) developed using the above assembly are location encoded and are designed around a microcontroller. The system transmits a carrier frequency of 40kHz, which is pulse width modulated with 12 bit Beacon Identification Number (**BIN**), one parity bit and appropriate start pulse. The BIN is assigned to each beacon installed in the workspace. During path execution, the position information gathered by the infrared remote control receiver modules from the beacon is processed by the microcontroller system of the vehicle that manages its navigation and guidance. As the vehicle crosses the infrared light sheet, the microcontroller based navigation system directly captures the location encoded information (**BIN**) and the position is updated after retrieving the corresponding absolute position from the database and the attitude is computed using baseline technique and is also updated. A resolution enhancement algorithm is developed utilizing the odometric sensor information.

### **3.6 Beacon Networking**

An RS 485 network among the beacons and a host computer has been established for interconnecting the beacons. The RS 485 interface is designed using a transceiver [98] chip and the RS 485–USB bridge is designed around a PIC microcontroller [99] with inbuilt USB support. A wireless link is established to monitor and assist the navigational guidance system of the robot vehicle, which utilizes an RF Programmable System on Chip (PSoC) module [100]. The module can have a range of about 200 metres and operates at 2.4GHz ISM band. It has

inbuilt Direct Sequence Spread Spectrum (DSSS) communication [101] facility with a 64 bit PN code for spreading and despreading of data. The on chip serial peripheral interface (SPI) of the microcontroller can be utilized for configuring and establishing communication with the module.

### **3.7 Error Reduction**

An odometric localization error reduction system has been developed to improve the performance of the wheeled mobile robot vehicles. The odometric localization errors caused by over count readings of an optical encoder based odometric system in a mobile robot due to wheel-slippage and terrain irregularities are studied. Redundant odometric sensors are considered in this technique. In addition to this an adaptive speed and position measurement to reduce the error has been developed. The system has been realized using an FPGA.

### **3.8 Traffic Control**

The application of encoded Digital Infrared Sheet of Light Beacon (DISLiB) system can be extended to intelligent control of the public transportation system. The system is capable of receiving traffic status input through a GSM (Global System Mobile) modem. The vehicles have infrared receivers and processors capable of decoding the information, which generate the audio and video messages to assist the driver.

### **3.9 Visually Impaired Support**

The DISLiB technique is extended to assist the movement of differently-able (blind) persons in indoor or outdoor premises of his residence. The Digital Infrared Sheet of Light Beacons (DISLiB) transmit the encoded location information and an infrared receiver module decodes this data and the message is retrieved from the corresponding location in a voice recorder/playback chip. The

orientation/location of the person can as well be informed through natural language. This system is simple, cost effective and provides less body gear without much computational burden or significant processing. Therefore, the navigation and guidance of a visually impaired can be achieved with a reduced body gear, which verbally guides the personnel. The user can use this system in conjunction with the conventional electronic cane or a guide dog too.

### **3.10 Summary**

The present work utilizes an assembly of infrared LEDs that restricts the spreading of the light intensity distribution and confines it to a sheet of light and is encoded with localization and traffic information. A standard infrared receiver module and a microcontroller based system is utilized for the pose updating in mobile robot vehicle applications. An odometric error reduction scheme has been addressed. The use of the system is extended to intelligent traffic and transport control and differently able assistance. The tools and support systems used in this work are briefly introduced in this chapter.

## DIGITAL INFRARED SHEET OF LIGHT BEACON SYSTEM




---

4.1 Brief History of Indoor Localization.....	71
4.2 Sheet of Light Beacon .....	73
• Principle of operation • The Beacon Transmitter	
4.3 Vehicle Localization .....	81
• Method of Installation • The Beacon Receiver and Controller	
• The Beacon Performance and Evaluation	
4.4 Resolution Enhancement .....	89
4.5 Position and Attitude update.....	91
4.6 Summary .....	96

---

Sensing of vehicle position and attitude is still a very challenging problem in many mobile robot applications. For indoor applications where a stable and accurate localization system is necessary, the ultrasonic, infrared, radio frequency and laser techniques are commonly used. The existing indoor beacon systems have been generally less successful for a number of reasons. The expense of environmental modification in an indoor setting is not amortized over an extremely large useful area, as it is, for example, in the case of the GPS. Furthermore, indoor environments offer significant challenges not seen outdoors, including multipath and environmental dynamics. A laser-based indoor beacon system, for example, must disambiguate the one true laser signal from possibly tens of other powerful

signals that have reflected off walls, smooth floors, and doors. Confounding this, humans and other obstacles may be constantly changing the environment, perhaps occluding the one true path from the beacon to the robot. In commercial applications, such as manufacturing plants, the environment can be carefully controlled to ensure success. In less structured indoor settings, beacons have nonetheless been used, and the problems are mitigated by careful beacon placement and the use of passive sensing modalities.

A new absolute localization approach developed to increase the navigational capabilities and object manipulation of autonomous mobile robots, based on an encoded digital infrared sheet of light beacon system, which provides position errors smaller than 0.02m is described in this chapter. To achieve this minimal position error, a resolution enhancement technique has been developed by utilising an inbuilt odometric/optical flow sensor information. An innovative assembly developed for mounting the encoded digital infrared transmitter can transmit the beacon identification number, so that the location coordinates can be inferred utilizing a database stored in the receiver unit. Hence the location identification is so direct that no triangulation or trilateration is needed. A single beacon reading specifies the location information. The possible reflected signals have no role, as the signal strength will be insufficient for proper decoding. Hence the ambiguity in receiving the signals other than the direct signal is eliminated.

For better guidance of mobile robot vehicles, an online traffic signaling capability is also incorporated. Other added features are its less processing time, networking support, ease of restructuring the environment and online localization capability and all these without any estimation uncertainty. This provides a cost effective position and attitude sensing system designed specifically to face the challenges in a realistic, cluttered indoor environment, such as that of an office



building or warehouse. In the proposed approach, a number of beacon transmitters are installed in the well defined and structured workspace as required and all the transmitters provide the estimates in a common reference frame or even universal frame, which make it especially suited as a practical indoor positioning system. Two sensor units on the mobile robot read the beacon and process the measurements to determine its position, attitude and traffic signaling information. The real-time identification and correction methods mitigate the impact of localization errors caused by the robot vehicles and the environment. A novel resolution enhancement algorithm suggested in this thesis satisfies the requirements for a high resolution localization system. The constructional details, experimental results and computational methodologies of the system are also described.

#### **4.1 Brief History of Indoor Localization**

The origin of mobile robot localization extends back to the 1950s with the installation of wire-guided tractors in industrial factories [89]. By the 1970s the *path following* concept had been developed to the point where *autonomous guided vehicles* (AGVs) navigated by following lines on the ground—either buried wires (via magnetic inductance) or painted stripes [90] came into existence. Buried wires were reliable and permanent but suffered from substantial installation effort and subsequent inflexibility. Painted lines enabled more rapid path generation and alteration but required continued maintenance to ensure reliability (against wear and fading). The basic limitation of path following is that it restricts navigation to fixed trajectories and, therefore, limits AGV application to simple repetitive tasks. Thus, the path following method, while not actually localization in the pose estimation sense, was a precursor to autonomous localization in establishing the problem of autonomous navigation and precipitating the need for more flexible navigation strategies.

Increased flexibility via pose estimation was introduced through the use of artificial beacons. These were either active beacons such as infrared [91] or ultrasonic [12] transducers, or passive beacons such as retro-reflective markers [92] or radar trihedrals [93], and they enabled mobile robots to localize relative to the known beacon locations. This meant that the prescribed navigation paths could easily be redefined in software without any change to the physical environment and the robot could generate adaptive trajectories to bypass obstacles. Nevertheless, this method still requires the introduction of specialized infrastructure (the beacons themselves) that need to be carefully surveyed so as to provide accurate landmark locations.

The use of the natural environment structure to provide landmarks was the next step in the development of autonomous localization, removing the need for specialized infrastructure. By providing the robot with accurate metric maps of the environment [23] the sensed environment could be registered with the map to determine its location. The use of natural landmarks introduced the problem of data association: the process of finding a correspondence between elements of two data sets. In the case of mobile robot localization, data association concerns assigning sensed features to appropriate map landmarks. All the above localization schemes require complex processing and large amount of memory, which results in more cost, size and computational delay.

The functional block diagram of a mobile robot vehicle control system is shown in figure 4.1. The information provided by the sensors is processed in the localization unit. The cognition (planning) module derives the desired paths for goal reaching. The motion control unit generates the required control sequences for the actuators. The localization unit is very crucial in goal reaching as well as path planning and obstacle avoidance. Sensors attached to the actuators also have

significant role in localization; the best example is the incremental optical encoder based odometry. Other sensors like inertial navigation systems (INS), range finders, vision systems etc. support to reduce the localization uncertainty but an absolute localization system that updates the position is of great importance in highly precise applications.

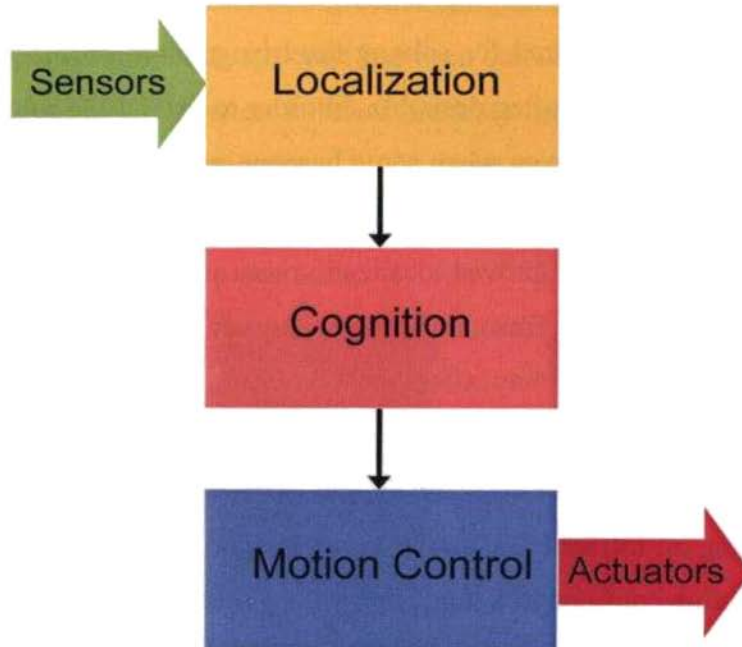


*Figure 4.1 Functional block diagram of a mobile robot vehicle control system.*

## **4.2 Sheet of Light Beacon**

The localization systems based on computer vision, range finders or other sensors that do not require a special arrangement of the environment are computationally expensive and not so robust. So they are not common in industrial or service applications. Localization through marks or beacons is usually preferred for these applications [12, 13]. A number of variants are used in practice [11] like

scanning detectors with fixed active beacon emitters, scanning emitters/detectors with passive retro-reflective targets, scanning emitter/detectors with active transponder targets, and rotating emitters with fixed detector targets. The general principle is always the same i.e. some marks or beacons are placed at known positions in the environment and are detected by appropriate sensors. Thus the robot position is then obtained through a triangulation or trilateration algorithm. At least three beacons are required for solving the triangulation problem. However, more than three beacons are often desirable, in order to extend the robot operation area and to locate the robot even when some beacons are occluded by obstacles in the environment (e.g., structures, moving personals). Furthermore, the use of more than three beacons leads to improved localization rate and precision. In addition to this, most of the infrared, ultrasonic or radio frequency beacons have inherent emission characteristics that may affect the resolution of the measuring system. Hence it is essential to consider a robust, low-cost system for the absolute positioning of mobile robots or other moving objects. This work describes a beacon assembly utilizing an infrared LED source that restricts the spreading of the light intensity distribution confined to a sheet of light.

#### **4.2.1 Principle of Operation**

Sheet of light techniques were utilized in robotics and industrial applications for sensing objects, its shape and size [73, 74]. Here a new approach to produce the sheet of light and an encoding scheme for localization application has been described. In order to produce a sheet of light for localization applications, an innovative assembly as shown in figure 4.2 has been developed. The infrared beam is guided through the space between two identical sand blasted parallel metal plates of dimensions 100 mm x 100 mm, kept 2.5 mm apart. These metal plates will be acting as Lambertian scattering surfaces (diffuse reflectors) and their dimensions

have effects on the sheet thickness as well as infrared light intensity. A single infrared LED mounted at the centre of the LED housing, as shown, is seen to have a beam angle of around 45 degrees, which can be increased by mounting multiple LEDs. *The width of the region of the infrared light sheet where the receiving system can properly read the encoded information is the Effective Light Sheet Thickness (ELST).* The variation of effective infrared light sheet thickness against the height ( $h$ ) of the mounting structure has been studied and the results are shown in figure 4.3, which illustrates a linear increase in light sheet thickness for mounting heights above two metres.

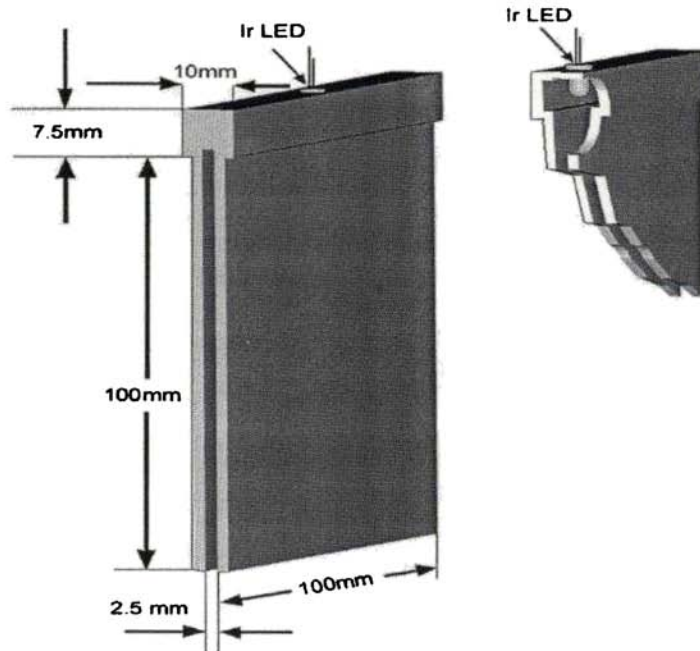


*Figure 4.2 The infrared LED of the beacon transmitter mounted on the structural assembly made up of sand blasted metal plates, which act as Lambertian scattering surfaces providing a sheet of light.*

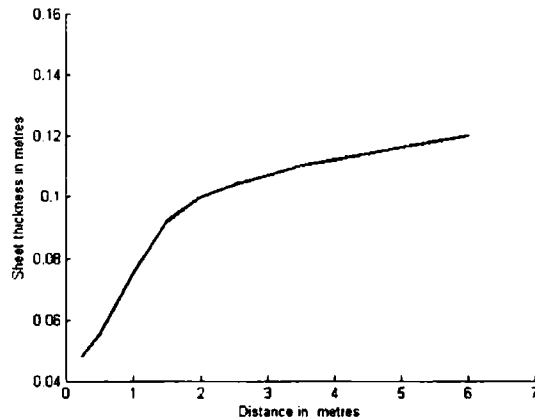


*Figure 4.3 Variation of effective light sheet thickness against the mounting height of the beacon ( $h$ ). The sheet thickness varies nearly linear above a height of two metres.*

In order to study the characteristics of the beacon transmitter and its assembly a system has been designed using PIC12F675 microcontroller [94] as shown in figure 4.4. The system transmits an encoded bit stream, where the pattern of the bit stream is selected according to the status of the micro switch inputs (SW1-SW3). For generating a stable 40kHz carrier a 20MHz crystal oscillator is utilized even though the microcontroller has inbuilt RC clock oscillator. A switching transistor 2N3904 is used to drive the infrared emitter. The photograph of the prototype beacon transmitter is shown in figure 4.5.

The schematic diagram of the beacon receiver constructed for studying the performance of the transmitter and assembly is shown in figure 4.6. A battery operated small handy unit has been constructed around PIC12F675 microcontroller and an infrared remote control receiver module has been used to read the beacon. The LED indicator D2 blinks if the IR detector receives the beacon signals and the LED glows stable when the system receives the encoded bit stream properly. The transmitter is fixed at a location and the detector unit is moved to find the *ELST* at

various distances from the transmitter, which corresponds to the mounting heights (h) and the results are studied. The IR remote control photo modules TSOP1740 [95] and GP1U58Y [96] from Vishay Telefunken and Sharp Corporation respectively are used in this study and their characteristics are found to be very similar. From the observations it is clear that for a defined transmitting power, assembly and detector type, the *ELST* varies with the beacon height. In the range of mounting height two to six metres the *ELST* variation is found to be linear for this assembly dimensions. This mounting height of two to six metres is reasonable for most of the indoor robot localization applications.

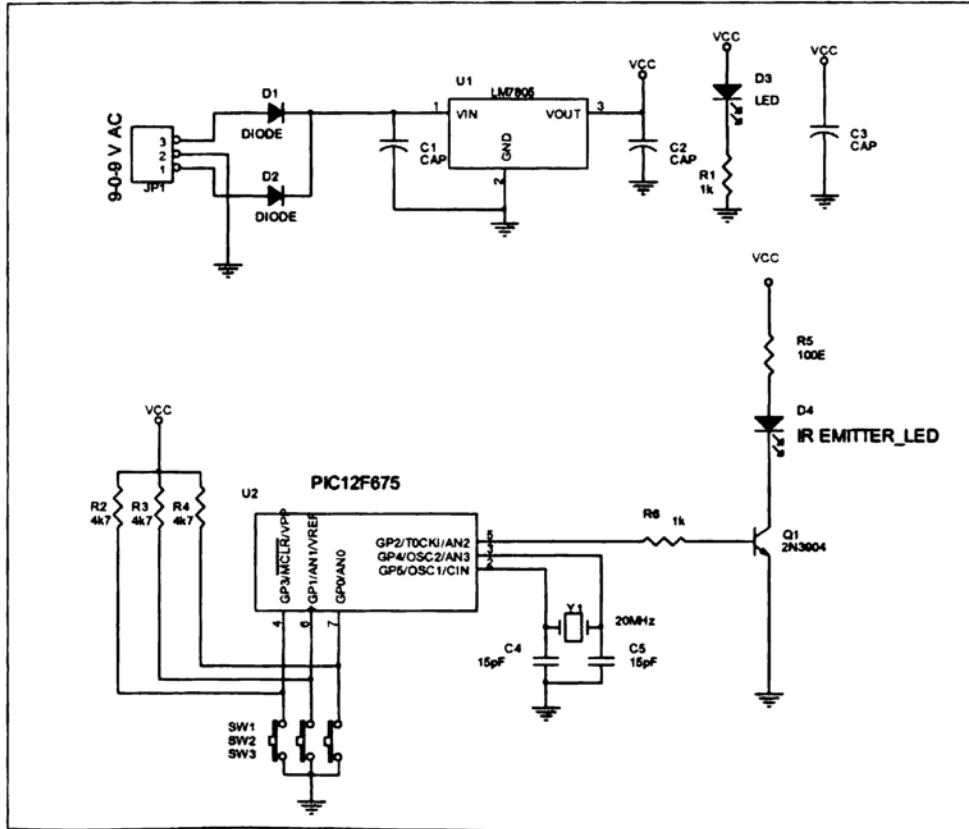


Figure 4.4 The schematic diagram of the beacon transmitter for the characterization of the assembly and the transmitter.

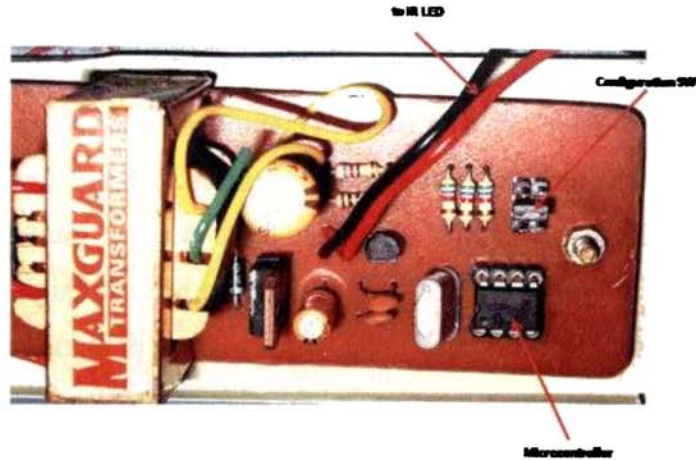


Figure 4.5 Photograph of the prototype of the beacon (DISLiB) implemented using PIC 12F675 microcontroller with three micro switch inputs for configuration.

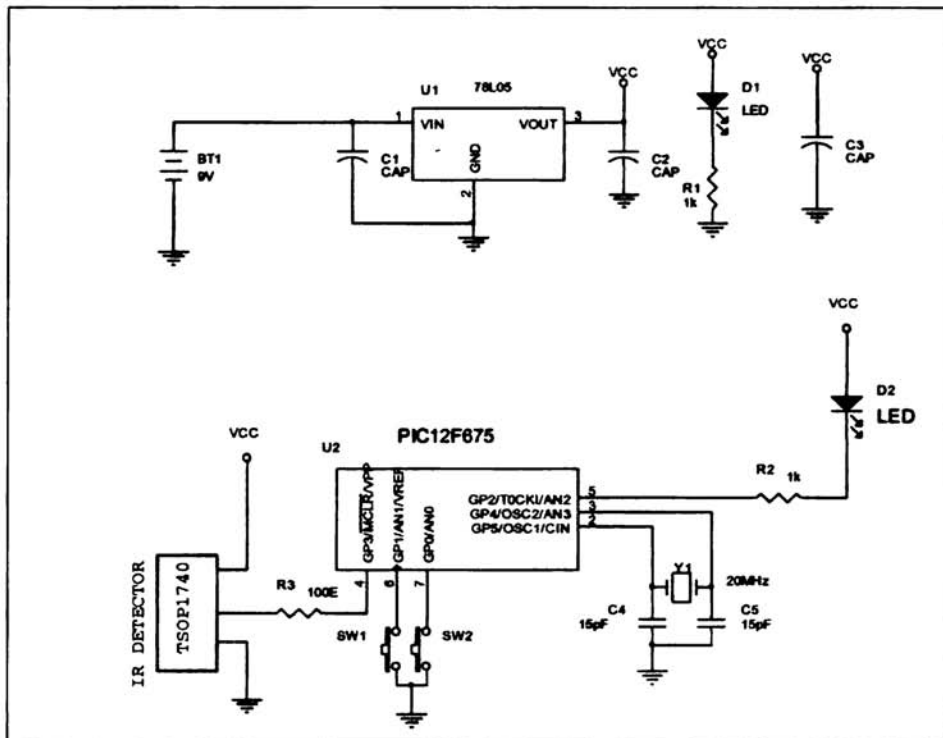
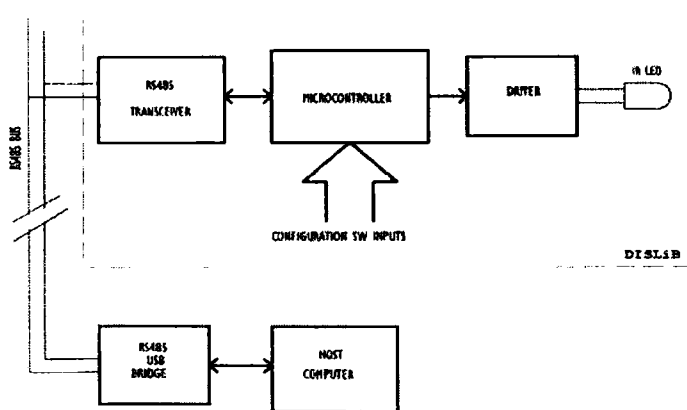


Figure 4.6 The schematic diagram of the portable beacon receiver for the characterization of the assembly and the transmitter.



## 4.2.2 The Beacon Transmitter

The Digital Infrared Sheet of Light Beacons (**DISLiB**) constructed using the above assembly are location encoded and are designed around a PIC16F676 [97] microcontroller as shown in figure 4.7. The system transmits a carrier frequency of 40kHz, which is pulse width modulated with 12 bit Beacon Identification Number (**BIN**), one parity bit and appropriate start pulse. The BIN is assigned to each beacon installed in the workspace. The system employs a scaled version of Sony Infrared Remote Control (**SIRC**) protocol to transmit the data and the protocol details are shown in figure 4.8. The time taken to transmit a location information is around 6ms, which may vary slightly as the protocol uses different burst lengths for '1's and '0's. Besides continuously transmitting the encoded position information the microcontroller in the beacon transmitter drives the infrared LED(s) by switching a transistor in series with a current limiting resistor as shown in figure 4.4.



*Figure 4.7 Functional block diagram of the beacon transmitter consisting of a microcontroller, which generates the encoded signal for driving the infrared LED mounted inside the special assembly and an RS485 network for establishing communication with a host computer.*

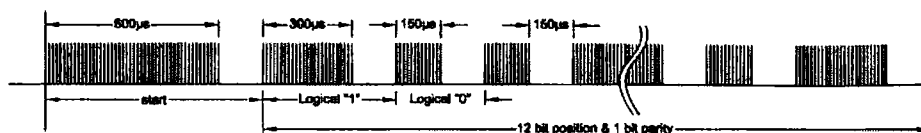


*Figure 4.8 The scheme of the scaled version of SIRC communication protocol format which uses 12-bits for location encoding, one parity bit for error detection and appropriate start pulse.*

By interfacing micro-switch inputs to the microcontroller for the configuration of a particular Beacon Identification Number (**BIN**), one can easily encode different location information to the beacons without modifying the firmware in each unit. Traffic signaling information like speed limits, sharp turnings etc., can be communicated by sending a few more bits and properly encoding the beacon. A number of beacon transmitters are mounted at various locations to define the environmental structure. Each beacon will send fixed BIN plus traffic signaling bits to the receiver. By establishing an RS 485 network among the beacons and a host computer, the position information in case of restructuring, as well as traffic signaling commands can be modified online. The RS 485 interface is designed using MAX485 [98] transceiver chip and the RS 485–USB bridge is designed around a 18F2550 PIC microcontroller [99, 102, 103] with inbuilt USB support. Thus the system can be made user friendly by incorporating the RS 485 network with the host computer. Figure 4.9 shows the schematic diagram of the USB to RS485 bridge and the photograph of the module is presented as figure 4.10.

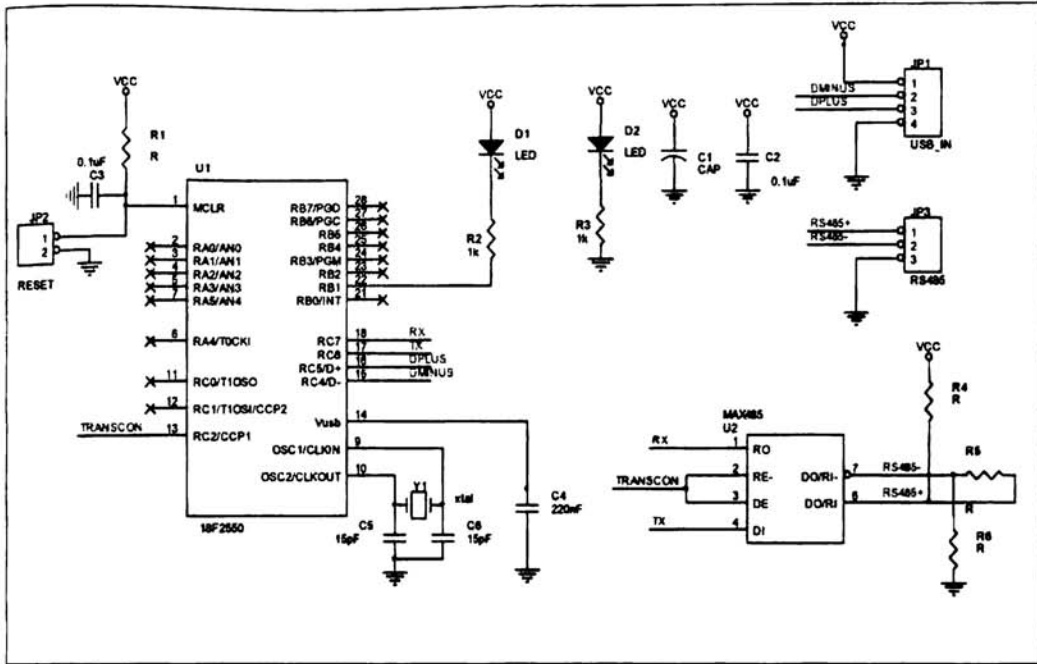


Figure 4.9 Schematic diagram of the USB to RS485 Bridge.

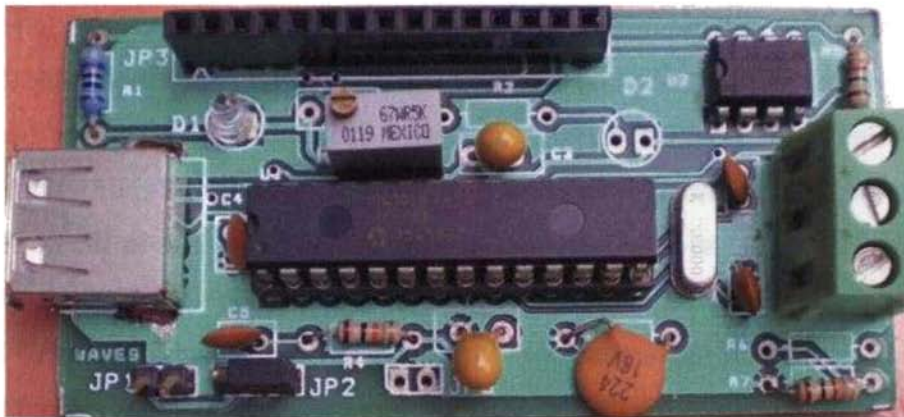


Figure 4.10 Photograph of the USB to RS485 bridge module.

### 4.3 Vehicle localization

Most of the absolute localization methods using ultrasonic, infrared, radio frequency or laser require multiple known beacons or encoded strips in the vicinity

of the robot vehicle as well as rotating/scanning, control and computational units to estimate the position of the system. If multiple localization systems are installed, a sensor fusion algorithm must be used to obtain a better estimate [23]. A prerequisite for a successful map matching or landmark based technique of localization, is an acceptable accuracy in the relative position estimation. By eliminating all the inherent problems and complexities of these existing systems a high resolution absolute localization is possible with the use of Digital Infrared Sheet of Light Beacons (**DISLiB**).

### 4.3.1 Method of Installation

By properly installing the Digital Infrared Sheet of Light Beacons (**DISLiB**) at known locations (**B**) vertically above the track as shown in figure 4.11, an accurate and robust representation of the workspace can be achieved for path planning and object identification of the mobile robot. In a typical indoor structure, the beacons should be mounted at a height (**h**) of about three metres for covering the entire width of the track and for greater track widths either multiple infrared LEDs or increased mounting heights within the reading threshold of the beacons are preferred. For a systematic implementation of the system, the entire workspace can be divided into various zones and tracks, where each track in the zones are properly labeled for effective functioning. The beacon distributions can be identified based on the systematic errors resulting from the kinematic imperfections of the vehicle and non-systematic errors due to the environment and depending on the resolution requirements.

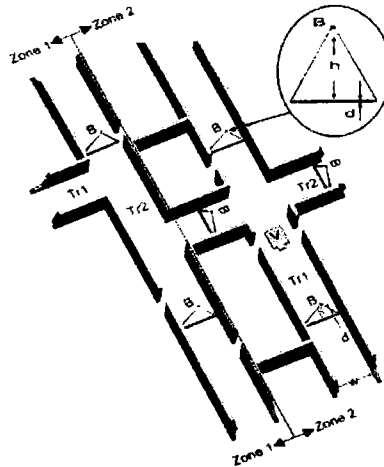


*Figure 4.11 A typical workspace showing the beacon positions (B) and mounting of the same vertically above the tracks Tr1,Tr2 etc. at a height of  $h$  metres.*

### 4.3.2 The Beacon Receiver and Controller

The receiver/controller unit is realized using microchip PIC18F4550 40-pin microcontroller [99] with inbuilt SPI support. The functional block diagram of a typical beacon receiver is shown in figure 4.12. The odometric sensors provide the position information to the microcontroller, which manages the drive and control systems. A wireless link is established to monitor and assist the navigational guidance system of the robot vehicle, which utilizes the CYWM6935 PAEC, the RF Programmable System on Chip (PSoC) module [100] from Cypress Semiconductor Corporation. The module can have a range of about 200 metres and operates at 2.4GHz ISM band. It has inbuilt Direct Sequence Spread Spectrum (DSSS) communication [101] facility with a 64 bit PN code for spreading and despreading of data. The on chip serial peripheral interface (SPI) can be utilized for configuration and establishing communication with the module. This RF transceiver module is ideal for short range indoor applications. The system

performance can further be improved by using multiple microcontroller based designs.

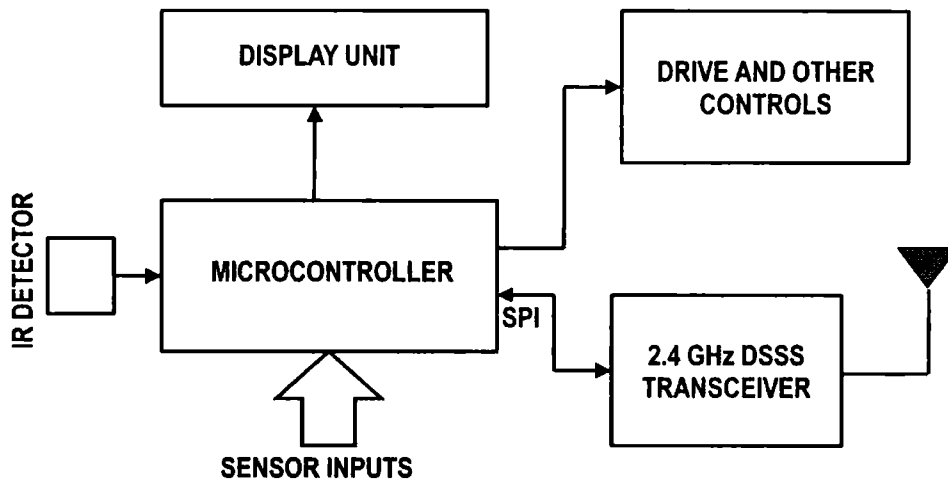


*Figure 4.12 Block diagram of the beacon receiver and controller consisting of PIC 18F4550 microcontroller, which manages motor control, RF link with host using CYWM6935 wireless module operating at 2.4GHz ISM band, 20X4 LCD display, optical incremental encoders attached to the wheels and the beacon receiver interface.*

The H-bridge driver chips (LMD18200) from National Instruments [104] interfaced to the microcontroller is utilized for driving the permanent magnet dc motors attached to the front steering driving wheel. The use of these driver ICs simplify the implementation of speed, direction and brake controls. This is also capable of monitoring the overload and stall conditions, by measuring the current drawn by the motors. A typical schematic diagram showing the driver IC and its associated components are shown in figure 4.13.

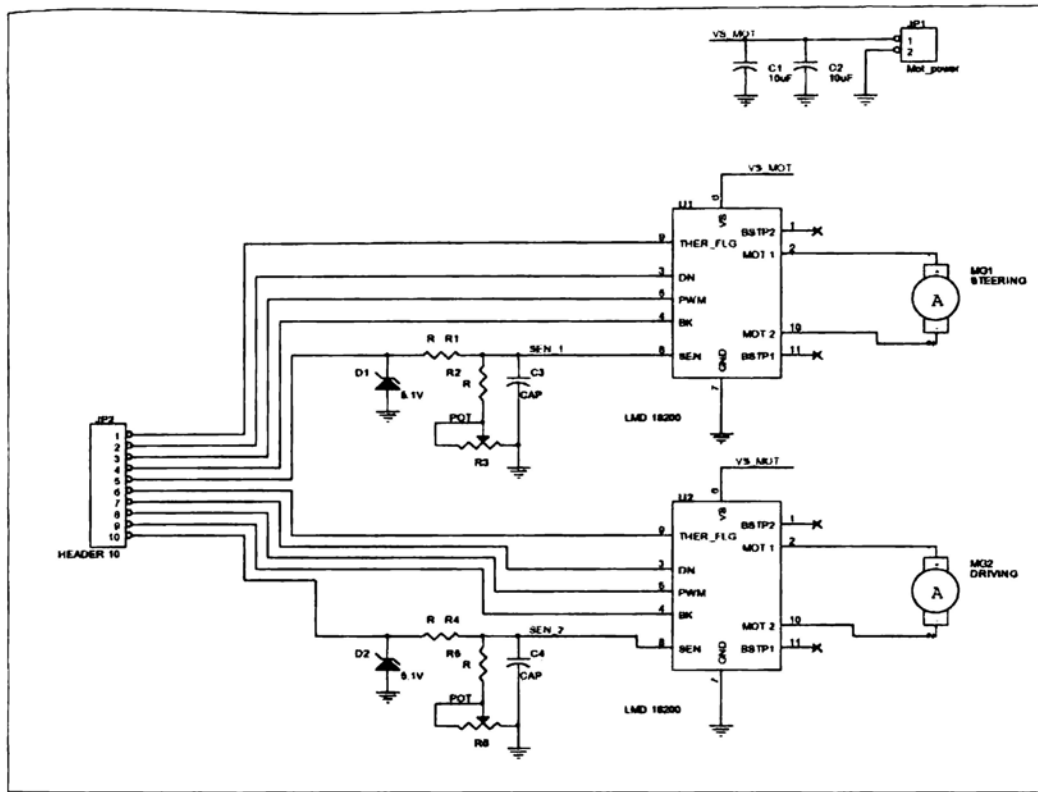
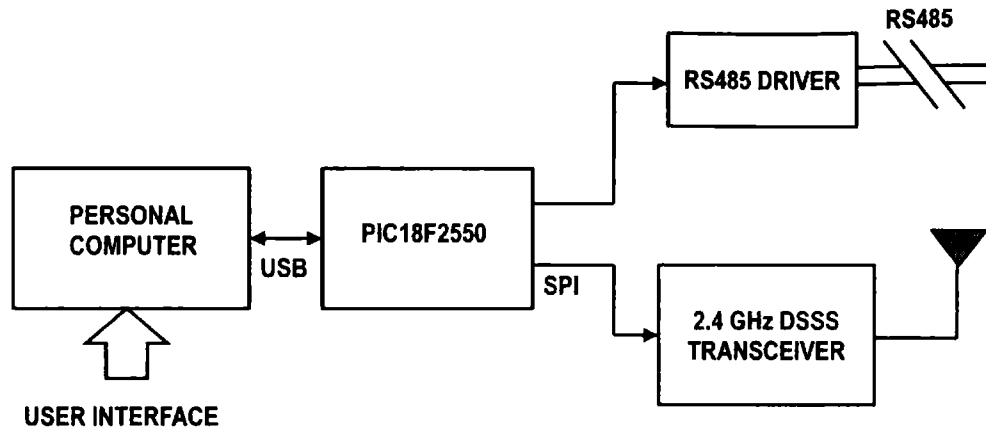


Figure 4.13 Schematic diagram of the motor drive using LMD18200 H-bridge

A vehicle traffic control and monitoring station can be setup for managing the path execution and service of the mobile robot vehicle. The functional block diagram of the PC based central monitoring and control station is shown in figure 4.14. The wireless module establishes a communication link with the robot vehicle and through this the system is capable of sending mission commands as well as monitoring the position, orientation, direction of motion and other vehicle status. The PIC18F2550 microcontroller is used to implement the USB to RS485 bridge and wireless link [102,103].



*Figure 4.14 Functional block diagram of the monitoring and control station*

During path execution, the position information gathered by the infrared remote control receiver module from the beacon is processed by the microcontroller system of the vehicle that manages its navigation and guidance. As the vehicle crosses the infrared light sheet of thickness  $d$ , the microcontroller based navigation system directly captures the location encoded information (**BIN**) and the position is updated after retrieving the corresponding absolute position from the database. By specifying certain scaling factors and the encoded value, it is possible to reduce the memory requirements of the system. The receiver takes 6ms for position decoding and hence at least 12 ms is required for a guaranteed position update while crossing a DISLiB. For a mounting height of about three metres the effective light sheet thickness ( $d$ ) is around 0.12m (figure 4.3), and hence the maximum speed of the vehicle has to be limited to a value less than 10m/s. As the speed of practical indoor vehicles is less than this, it does not cause any problem in field applications. Up to this speed, the resolution of the system remains as the effective light sheet thickness. The photograph of the prototype of the beacon receiver and controller is shown in figure 4.15.



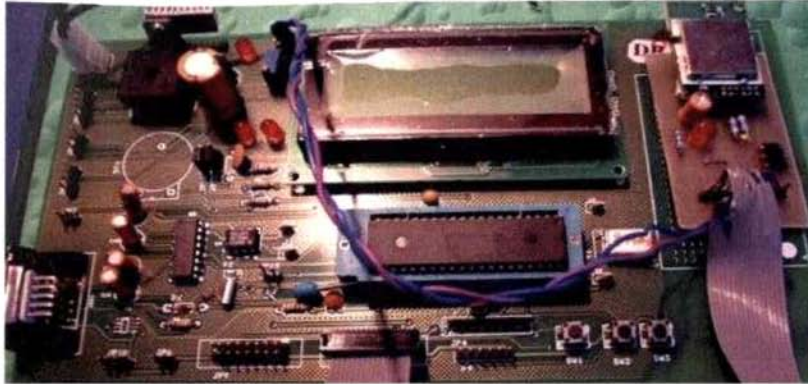
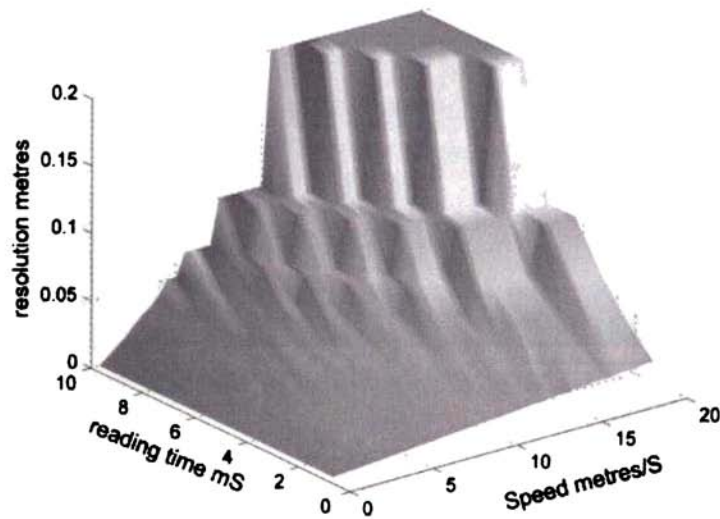


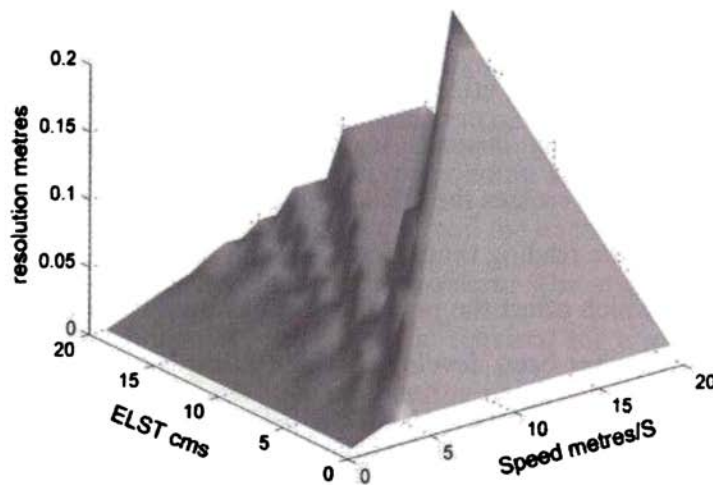
*Figure 4.15 Photograph of the prototype of the beacon receiver and controller*

### **4.3.3 The Beacon Performance and Evaluation**

This is an absolute localization system for correcting the errors caused by the inbuilt sensory system of the mobile robot vehicle. In situations where frequent correction is required, more number of beacons are to be installed. The beacon (DISLiB) performance is associated with various parameters like the speed of the vehicle (during beacon crossing), effective light sheet thickness (*ELST*) of the system and the reading time, which depends upon the coding scheme of the beacon transmitter. As the vehicle crosses the **DISLiB**, the system takes a certain number of readings depending on the reading time, *ELST* and the speed of the vehicle. The role of these parameters, which affect the performance, has been studied and a resolution enhancement algorithm has been developed which is explained in section 4.4. The characteristics are plotted in figure 4.16. These 3-D surface plots show the role of vehicle speed, beacon's reading time and Effective Light Sheet Thickness (*ELST*) on the resolution of the system. Figure 4.16(a) indicates the plot of speed and reading time against the resolution with an effective sheet width of 0.12 metres. The discrete variation of the resolution depends on the number of beacon readings, which is a function of speed and reading time. Figure 4.16(b) shows the effect of *ELST* on the resolution and vehicle speed.



(a)



(b)

**Figure 4.16.** 3-D surface plots showing the role of vehicle speed, beacon receiver's reading time and Effective Light Sheet Thickness (ELST) against the resolution of the system. (a) indicates the variation of resolution with respect to speed and reading time (b) the variation of resolution with respect to speed and ELST.

### 4.4 Resolution Enhancement

During path execution, as the vehicle crosses the **DISLiB**, the system takes  $n$  number of readings depending on the ELST and the speed of the vehicle. For vehicles moving at a speed less than the maximum speed allowed by the system, the resolution can be increased by making use of a resolution enhancement algorithm. Fast moving vehicles have to be slowed down during the localization process for achieving acceptable resolution enhancement. The system generates a lookup table with the count ( $n$ ), beacon reading (**BIN**) and the odometric position information ( $P_n$ ), as shown in table 4.1. Under a particular **DISLiB** the beacon identification number is the same for all the observations. The beacon identification number points to a memory location in the database from where the position information can be retrieved. The

	<b>BIN</b>	
1	<b>BIN</b>	$P_1$
2	<b>BIN</b>	$P_2$
3	<b>BIN</b>	$P_3$
.	<b>BIN</b>	.
.	<b>BIN</b>	.
.	<b>BIN</b>	.
$n$	<b>BIN</b>	$P_n$

Table 4.1 Lookup table formulated for the execution of the resolution enhancement algorithm

position information furnished by the proprioceptive sensors corresponding to  $n/2^{th}$  or  $(n+1)/2^{th}$  position respectively for even or odd values of  $n$  can be updated. For an even value of  $n$ ,  $P_{n/2}$  can be replaced with an absolute position value from the database pointed by **BIN** and hence the resolution of the system is enhanced from effective width of light sheet  $d$  to  $d/n$ . In fact the algorithm replaces the  $P_{n/2}^{th}$  position value with  $[BIN] + (P_{n/2}$

-  $P_{n2}$ ). The flowchart shown in figure 4.17 describes the resolution enhancement algorithm. The vehicles fitted with two sensors create separate tables and finally updates with the average value.

The resolution is effectively improved in the present set up as it is the product of the speed of the vehicle and reading time, as illustrated below. The enhanced resolution  $r$ , which is the ratio of the effective light sheet thickness to the number of readings, can be deduced to:

$$r = \frac{d}{n} = \frac{s_v t_b}{INT(t_b / t_r)} \approx (s_v t_r) \quad (4.1)$$

where

$s_v$  - speed of the vehicle

$t_b$  - time taken by the vehicle to cross the light sheet (ELST)

$t_r$  - time required for one successful beacon reading

$INT(t_b/t_r)$  - integer value of the ratio  $(t_b/t_r)$ .

Equation (4.1) gives the inference that a reduced vehicle speed improves the resolution. Either we can feed the information to the receiver regarding the locations at which the beacons are placed or the system can keep a rough estimate about the locations at which the beacons are available. For high resolution applications the vehicle can reduce its speed while approaching the beacons if desired. When  $t_r = t_b$ , the resolution enhancement algorithm will fail since  $n=1$ , and the resolution remains as  $d$ . For a vehicle crossing the **DISLiB** at a speed of around 3 m/sec. with a reading time of 6ms equation (4.1) computes the resolution to be approximately 0.02m. A further improvement in resolution can be obtained by reducing the beacon reading time which in turn is achieved by decreasing the infrared burst lengths. Only micro robot vehicles engaged in very precise work need such resolution. Usually the reading time is constant for a set up so that the resolution of the system varies with the speed of the vehicle.

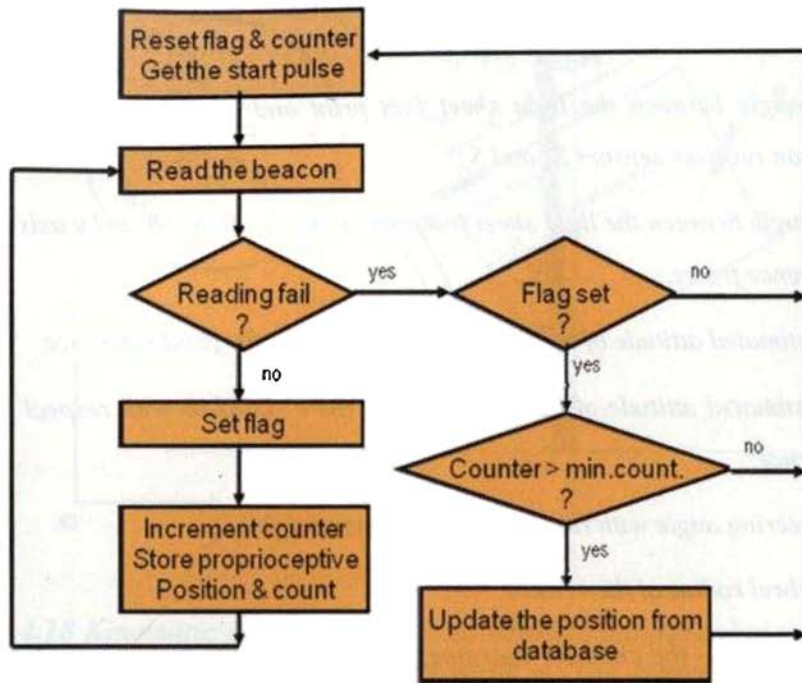


Figure 4.17 Flowchart showing the implementation details of the resolution enhancement algorithm

## 4.5 Position and attitude update

The kinematics and navigation equations for a three-wheeled mobile vehicle with one driving-steering wheel and two fixed rear wheels in-axis is considered for this study. The odometric navigational systems are implemented using four optical incremental encoders. The driving steering wheel (front) is attached with geared permanent magnet DC motors with inbuilt encoder, which measures the angular increments for the measurement of the steering angle  $\phi$  and the distance moved by the vehicle. The rear wheels are also attached with encoders to estimate the position and attitude of the vehicle. The **DISLiB** beacon receivers are utilized to update the position and heading of the vehicle by utilizing the update equations for this vehicle geometry.

The symbols used in the update equations are defined below:

$X_k(x, y, \theta)$  - position and attitude vector

$\alpha$  - the angle between the light sheet foot print and the line joining between the beacon receiver sensors  $S_1$  and  $S_2$ .

$\beta_i$  - the angle between the light sheet footprint of the  $i^{\text{th}}$  **DISLiB** and y axis of the fixed reference frame.

$\theta$  - the estimated attitude of the vehicle with respect to the fixed reference

$\theta_i$  - the estimated attitude of the vehicle using the  $i^{\text{th}}$  **DISLiB** with respect to the fixed reference

$\phi$  - the steering angle with respect to axis of symmetry

$R$  - the wheel radius of the vehicle

$n_L$ -  $n_R$  -  $n_F$  -  $n_S$  - the encoder incremental pulse counts from the left, right, front and steering - wheel encoders respectively.

$N$  - the number of pulses per revolution of the encoder.

$L$  - the distance between the rotation axis of the front (driver) wheel and the axis of the back wheel.

$D$  - the distance between rear wheels

$t_b$  - the time required to cross the beacon light sheet

$t_d$  - the time delay between two sensor outputs

$a$  - half the distance between two beacon sensors

$(x, y)$  - the position estimated by sensors with respect to the fixed reference frame of the point 'P' on the vehicle.

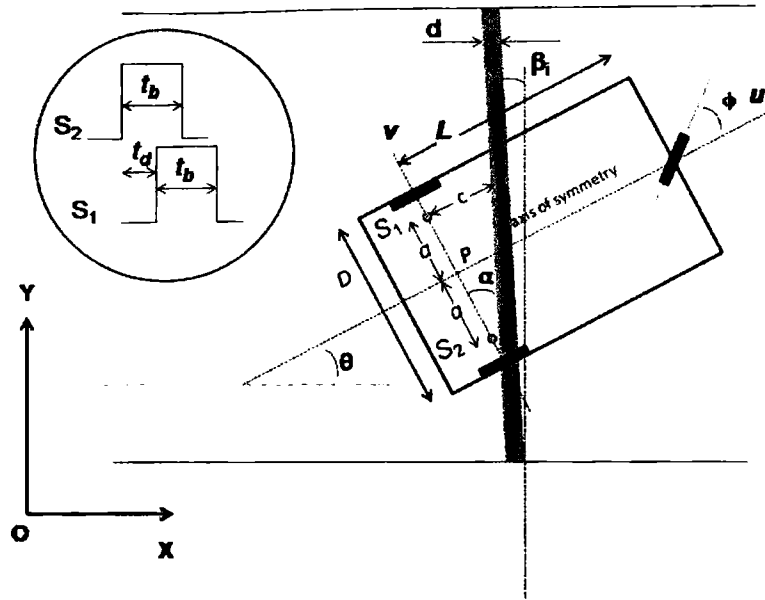


**Figure 4.18** Kinematic scheme of the three wheeled mobile robot vehicle and the footprint of the effective light sheet width  $d$ . The attitude  $\theta$  is the angle between the absolute reference frame  $OXY$  and the mobile reference frame  $PUV$ . The origin  $P$  is attached to the mid point of the axes joining the rear wheels and the sensors  $S_1$  and  $S_2$ . The time delay  $t_d$  between the encoded signals reaching the sensors is also shown.

Figure 4.18 shows a typical posture of the mobile vehicle with an orientation “ $\theta$ ” and steering angle “ $\phi$ ”. Two identical DISLiB sensors  $S_1$  and  $S_2$  are mounted at the top of the rear wheel axis of the vehicle at a distance of  $2a$ . If the vehicle’s axis of symmetry is normal to the sheet of light both the sensors receive the signal simultaneously. From the BIN received, the mounting angle of the corresponding beacon transmitter,  $\beta_i$  can be retrieved from the database. If the vehicle crosses the beacon with a heading angle “ $\theta$ ” (not equal to  $\beta_i$ ) there will be a lag or lead between the received signals, which is a measure of the attitude of the vehicle. The signal waveforms derived from the start pulse is shown in figure 4.18 (inside the circle), in which the time duration  $t_b$  is the time required to cross the

beacon and the lag or lead time  $t_d$  is the time required to cover the distance “ $c$ ” by the vehicle. The lead or lag time  $t_d$  is a measure of the attitude of the vehicle. The attitude  $\theta_i$  computed by the receiver unit in the vehicle is given by the following expression:

$$\theta_i = \tan^{-1} \left( \frac{c}{2a} \right) + \beta_i = \tan^{-1} \left( \frac{t_d s_v}{2a} \right) + \beta_i \quad (4.2)$$

The better a vehicle’s odometry, the better will be its ability to navigate and lesser will be the requirement for frequent position updates with respect to external sensors. For the computation of the position and attitude let us consider the pulse counts from the two independent optical encoders attached to the rear non-driven idler wheels of the vehicle which have less coupling with the steering and driving system and very less slippage between point of contact and the floor. The update equations for this model are as follows [105]:

$$x(k+1) = x(k) + \frac{\pi R}{N} (n_R(k) + n_L(k)) \cos \theta(k) \quad (4.3)$$

$$y(k+1) = y(k) + \frac{\pi R}{N} (n_R(k) + n_L(k)) \sin \theta(k) \quad (4.4)$$

$$\theta(k+1) = \theta(k) + \frac{2\pi R}{N} \frac{(n_R(k) - n_L(k))}{D} \quad (4.5)$$

The distance moved by the wheel’s point of contact can be derived by considering the vehicle’s front driving steering wheel’s incremental pulse count data and steering angle. The steering rotation is limited to  $\pm 40^\circ$  about the axis of symmetry of the vehicle. The steering angle can be computed by counting the pulses ( $n_s$ ) from encoder attached to the steering wheel as follows.

$$\phi = \frac{\pi n_s}{2NG}$$



Where  $G$  is the gear ratio between the encoder shaft and robot steering coupling.

The update equations for this model are described as follows [105]:

$$x(k+1) = x(k) + \left( \frac{2\pi R}{N} \right) n_F(k) \cos \theta(k) \cos \phi(k) \quad (4.6)$$

$$y(k+1) = y(k) + \left( \frac{2\pi R}{N} \right) n_F(k) \cos \theta(k) \sin \phi(k) \quad (4.7)$$

$$\theta(k+1) = \theta(k) + \left( \frac{2\pi R}{N} \right) n_F(k) \frac{\sin \phi(k)}{L} \quad (4.8)$$

Equations (4.3, 4.4 & 4.5) utilize the rear wheel encoder data for the computation of position and attitude where as equations (4.6, 4.7 & 4.8) utilize front wheel encoder data and steering angle for the same. The  $x(k)$  and  $y(k)$  values in these equations are updated from the system database after executing the resolution enhancement algorithm described in section 4.4.

The computed value of  $\theta$ , which is  $\theta(k)$  in equations (4.5) and (4.8) is updated with  $\theta_i$  obtained from equation (4.2). Farther apart the sensors  $S_1$  and  $S_2$  are kept (*i.e.*, the greater the *baseline* between them), the greater the orientation accuracy. Thus these systems fundamentally require a certain vehicle size for attitude measurements, no matter how small the electronics can be made.

In a practical environment the pulse count received from certain encoders may indicate an over count due to workspace and operating conditions. So the least value of  $x(k+1)$ ,  $y(k+1)$  and  $\theta(k+1)$  estimated from the equations (4.3) to (4.8) can be used for computing the pose of the vehicle. A detailed description of the same is presented in chapter 5. Maximum resolution of the DISLiB system is limited to the resolution of the odometry.

## **4.6 Summary**

The development of a cost effective, accurate and reliable system, utilising an infrared sheet of light, which minimizes position errors during the path execution is presented in this chapter. The constructional details of the encoded digital sheet of light beacon, method of installation and its implementation using a microcontroller are explained. The results of the characteristics study of the beacon transmitter are also presented. A resolution enhancement algorithm has been developed and the variations of resolution with the environmental parameters are presented. The position and attitude updating for a three wheeled mobile vehicle with one driving-steering wheel and two fixed rear wheels in-axis is also discussed.

# ODOMETRIC ERROR REDUCTION SYSTEM




---

5.1 The Odometric System.....	99
• Position Measurement • Speed/Velocity Estimation	
5.2 Position and Attitude Estimation.....	103
• Position Updates from Encoder Data	
• The Error Reduction Technique	
5.3 Implementation.....	106
• The Sine/Cosine Module	
• The Realization Details	
5.4 Summary.....	113

---

A variety of techniques have been developed and used successfully to provide the position and attitude information of autonomous mobile robot vehicles operating in industries and other environments. However, many of these existing positioning systems have inherent limitations of their own in the workspace when they are guided through terrain irregularities like humps, cracks or other disturbances. In mobile robot applications, two basic position estimation methods are employed concurrently, viz., the *absolute* and *relative* positioning [11]. Relative position estimation is based on proprioceptive sensing systems like odometry [17], Inertial Navigation System (INS) [18] or optical flow techniques [19], where the error growth rate of these systems are usually unacceptable. For implementing a navigational system most of the mobile robots use position

odometric system together with traditional inertial navigation systems employing gyros or accelerometers or both. The odometric system provides accurate and precise intermediate estimation of position during the path execution.

Though the odometric system is simple, inexpensive and accurate over short distances, it is prone to several sources of errors due to wheel slippage, variations in wheel radius, body deflections, surface roughness and undulations. Odometric system is reliable and reasonably accurate, on smooth flat terrain, and in the absence of wheel slippage, since a wheel revolution corresponds to linear travel distance. On paths having terrain irregularities the odometric systems are not considered to be useful, because the measured rotations of the wheels do not accurately reflect the distance traveled due to wheel slippage and motion over humps and cracks. Such odometric errors need to be corrected in practical mobile robotic applications.

This chapter presents the realization of a new, simple and efficient system to reduce the errors caused by terrain irregularities like humps, cracks or other disturbances, which contribute to errors in an odometric system in a mobile robot vehicle. The detection and correction is based on redundant encoder measurements. In addition to this we present an adaptive speed measurement and standard quadrature technique to improve the position and speed resolution. The CORDIC algorithm has been used for the computation of sine and cosine terms in order to solve the update equations. The system has been realized in an FPGA and the results are discussed. By using this system one can reduce the odometric error so as to increase the travel distance between absolute position updates, thereby lowering the installation and operating costs of the system.

## **5.1 The Odometric System**

In this work a three-wheeled mobile robot vehicle with one driving-steering wheel and two fixed rear wheels in-axis, fitted with incremental optical encoders is considered. The incremental encoders are the most frequently adopted position transducers for the mobile robotic applications. The low level information furnished by the encoder in the form of two pulse trains namely Ch\_A and Ch\_B are  $90^\circ$  out of phase (quadrature) and depending on the direction of rotation, one of these pulses will lead or lag the other. The optical incremental encoders are described in detail in section 2.3 of chapter 2. The low level signals are passed to the control system, which computes the actual position, speed and acceleration information needed for the controller. Incremental encoders, which have been used for this purpose, are characterized by high accuracy, high resolution, high noise immunity, low maintenance and low cost and hence are generally preferred.

### **5.1.1 Position Measurement**

The position measurement involves counting the encoder pulses with the help of a quadrature decoder circuit and the direction of movement of the wheel can also be decoded from the encoder pulses. The count is incremented or decremented depending on which pulse leads the other.

The simplified block diagram of the Encoder Pulse Processing Module (EPPM) is shown in figure 5.1. The encoder pulses Ch\_A and Ch\_B are fed to the quadrature decoder circuit, which decodes the direction indicator bit and generates pulses during the rise and fall fronts of both channels. A 20-bit up/down counter is implemented and the direction bit would set the counter as up or down depending upon the direction of movement of the wheel. The computational unit resets the

counter after reading the position or position increment. The present position  $P$  (or position increment) and the position error noise  $\delta P$  due to quantization are given by

$$P = \frac{\pi QR}{2NG} ; \quad \delta P = \frac{\pi R}{2NG}$$

Where  $Q$  is the counter value,  $R$  is the radius of the wheel in metres,  $N$  is the number of pulses per revolution of the encoder and  $G$  is the gear ratio between the encoder shaft and robot wheel coupling.

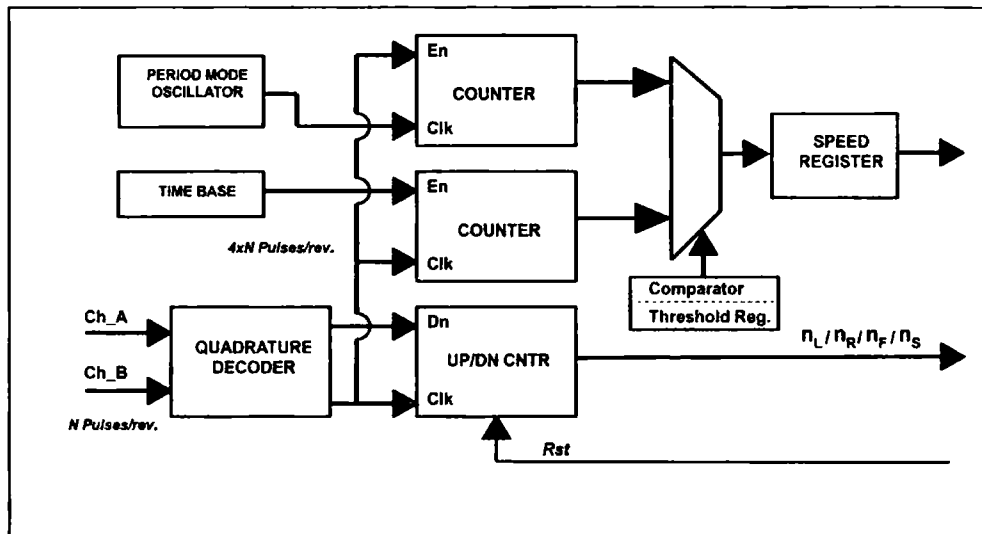


Figure 5.1 Functional block diagram of the optical incremental Encoder Pulse Processing Module (EPPM), which computes the velocity information in period mode and pulse mode depending upon the current speed of the vehicle. It also provides the incremental position (distance) update of the wheel.

### 5.1.2 Speed/Velocity Estimation

Two major techniques for extracting the speed data from an incremental encoder are *pulse counting* and *period measurement* [106, 107, 108] of the pulses. In pulse counting mode the number of pulses  $Q$  in an observation time window  $T$  is counted and the speed is approximated to the discrete incremental ratio as:

$$S = \frac{\pi QR}{2NTG}$$

The speed error due to one bit quantization  $\delta S = \frac{\pi R}{2NTG}$

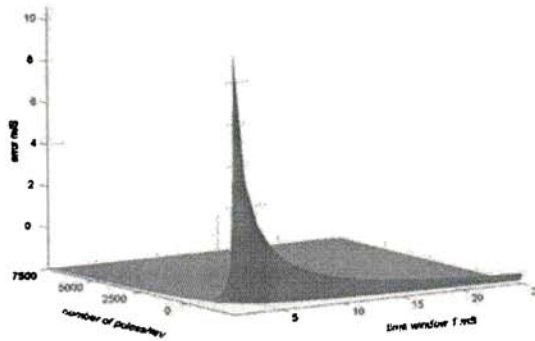
The other method for obtaining the speed is to measure the time between two successive pulses from the encoder. In this method a stable high frequency clock ( $f$ ) and gating circuit is normally used at the front end of the counter. The gating circuit is controlled by the encoder pulses, so the count value depends on the number of encoder pulses per revolution and the clock frequency. For a given system, the clock frequency and the number of encoder pulses per revolution are constant and hence the count value is inversely proportional to the speed of the vehicle and the relationship is given by

$$S = \frac{\pi f}{2NQG}$$

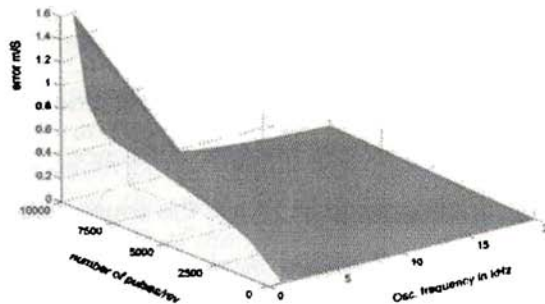
The upper part of the encoder pulse processing module in figure 5.1 shows the velocity measurement sections. In pulse counting scheme the pulses from the quadrature decoder ( $\times 4$ ) circuit is gated with the time base and fed to the counter and the final count value is latched. Instead of the direct pulses from the encoder, the quadrature decoded pulses are used as the pulse rate is four times higher. This reduces the switching between *period measurement* and *pulse counting* schemes.

The implementation of the period measurement scheme is very similar to pulse counting except that the counting clock is from the reference clock generator and the gating pulse is from the quadrature decoder. Hence the count value is a measure of the velocity as it counts the number of *period mode* clocks between successive pulse intervals. The system can switch between these two velocity measuring modes by monitoring the count register value because period counting is more accurate at low speeds and pulse counting is more accurate at high speeds. The 3D plot in figure 5. 2(a) shows the variation of error with respect to the time window  $T$  and encoder pulse per revolution  $N$  and in figure 5. 2(b) shows the error variation with respect to encoder pulse per revolution and the period mode oscillator frequency. From these plots it is

very evident that the proper switching between these two modes facilitates the accurate measurement of velocity information. If the pulse count value in the *pulse mode* counter is less than a reference value then the velocity measuring scheme switches to the period measuring mode and vice versa. The speed register value along with the mode bit (period/pulse) can be read to get the velocity information.



(a)



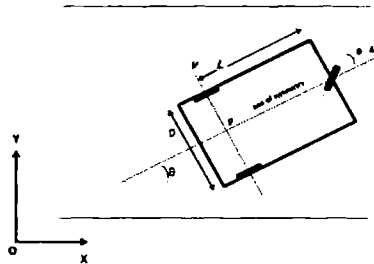
(b)

Figure 5.2 3-D surface plot showing the role of (a) quantization error plotted against encoder pulse per revolution and observation time window in pulse counting mode and (b) relative error plotted against encoder pulse per revolution and oscillator clock frequency in period counting mode.



## 5.2 Position and Attitude Estimation

The kinematics and navigation equations for a three-wheeled mobile vehicle with one driving-steering wheel and two fixed rear wheels in-axis is considered in this study. The odometric navigational system is implemented using four optical incremental encoders. The driving steering wheel (front) is attached with geared permanent magnet DC motors with inbuilt encoder, which measures the angular increments for the measurement of the steering angle and the distance moved by the vehicle. The rear wheels are also attached with encoders to estimate the position and attitude of the vehicle. A typical pose of the mobile robot vehicle with a steering angle  $\phi$  and an orientation  $\theta$  with respect to the absolute reference frame OXY is shown in figure 5.3.



*Figure 5.3 The Kinematic scheme of the three wheeled mobile robot vehicle having attitude  $\theta$ , which is the angle between the absolute reference frame OXY and the mobile reference frame PUV. The origin P is attached to the midpoint of the axes joining the rear wheels and the axis of symmetry of the vehicle.  $\phi$  is the steering angle.*

### 5.2.1 Position Updates from Encoder Data

The same three wheeled mobile robot vehicle used for the position and attitude update in chapter 4 is considered here. The update equations for this model using the rear wheel as well as the front wheel are given by equations (4.3) to (4.8) in section 4.5 of chapter 4. The pulse count received from certain encoders may indicate an over

count due to terrain irregularities and operating conditions. So the least value of  $x(k+1)$ ,  $y(k+1)$  and  $\theta(k+1)$  estimated from the equations (4.3) to (4.8) can be used for computing the pose of the vehicle. The necessary hardware is designed and developed for the independent computation and comparison of the position and attitude values from the rear wheel and front wheel encoder data. The digital comparators manage the switching of multiplexers that selects the least values among the computed values.

### **5.2.2 The Error Reduction Technique**

Conventional systems use data from a set of encoders to compute the posture of the vehicle. By utilizing the equations (4.3) to (4.5) and reading encoder pulse counts of the rear wheels one can compute the position and attitude of the robot vehicle. Using equations (3.6) to (3.8), the posture of the vehicle can be computed by utilizing the encoder data available from the front wheel.

The technique presented here utilises both the sets of encoder values and computes the position and orientation of the vehicle. Thus the redundant information for the computation of the posture of the vehicle is available. The wheel slippage, motion over humps, cracks or any other terrain disturbances cause more pulses than what corresponds to the actual distance travelled [109]. This may lead to over incremental update values of position and orientation. Independently computing the position increments and angular increments of the system and dropping the higher values eliminate this error. The new position and orientation are updated with the minimum (lower) values.

Figure 5.4 shows three typical postures of the vehicle over a hump. The figure 5.4(a) corresponds to an error condition of over counts from rear wheel encoders that records more distance than the actual. The front wheel encoders produce the data corresponding to the actual distance moved by the vehicle. Figure 5.4(b) represent a situation where the rear wheel encoders produce over counts and over attitude errors

while figure 5.4(c) shows the front wheel encoder pose over a hump that may cause over count from this encoder.

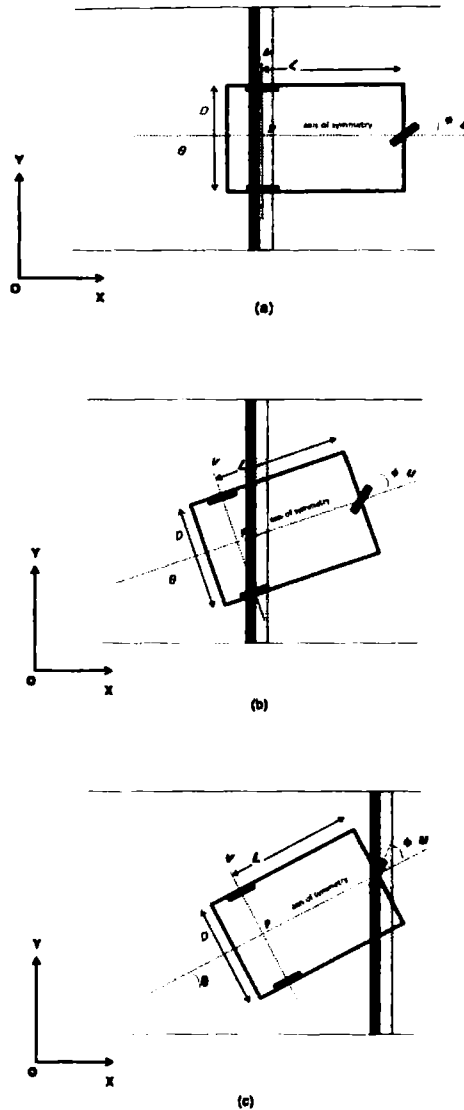


*Figure 5.4 Plan view of three typical postures of a vehicle over a hump show an error condition of over counts when (a) both the rear wheels are over the hump, (b) when one of the rear wheels and (c) the front wheel is over the hump.*

The simplified functional block diagram of the error reduction system is shown in figure 5.5 which has two computation units and two switching units. The two computation units independently calculate the position and orientation incremental values by reading the corresponding encoder pulse counters from the encoder pulse processing modules. The switching units compare the incremental values and the least value will be selected for updating.

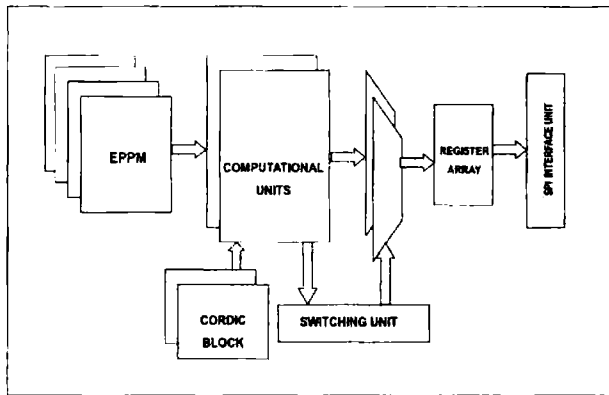


*Figure 5.5 The simplified functional diagram of the FPGA sub system which computes two sets of position increments and two attitude values. The switching, control and communication blocks are also shown.*

### 5.3 Implementation

The system implementation is achieved by using an Altera development board consisting of Cyclone-II EP2C70F672-C6 FPGA and associated components. The user interface termination provided on header connectors is used for realizing the system. The system is implemented with the help of the Quartus-II FPGA/CPLD design package and modelsim simulation tools [110]. In figure 5.5 the two encoder pulse processing modules (EPPM) used to process the pulses from the rear wheel encoders place the velocity and position information in the appropriate registers. The other two encoders' pulses from the front driving steering wheel are not utilized for velocity calculations. The average velocity

values measured from the rear wheels are available through the SPI interface of the system.

The computation unit utilizes the equations (4.3)-(4.8) for the calculation of position and attitude incremental update values. The sine and cosine calculation modules are necessary to speed up the process. So the outputs from the computation units are two sets of X axis and Y axis increments and two attitude values ( $\theta$ ). These values are stored in the corresponding registers and the switching module selects the least value set of position and attitude increments. All these values can be read through the SPI interface module.

### **5.3.1 The Sine/Cosine Module**

For the computation of sine and cosine terms, the famous CORDIC (COordinate Rotational DIgital Computer) algorithm is used. The CORDIC algorithm is an iterative technique based on the rotation of a vector which allows many transcendental and trigonometric functions to be computed [113, 116, 117, 120]. The highlight of this method is that it is achieved using only shifts, additions/subtractions and table look-ups, which map well with hardware and are ideal for FPGA implementation [114, 115, 118, 119]. The original work on CORDIC was carried out by Jack Volder [111] in 1959 for computing the trigonometric functions as a part of developing a digital solution to real time navigation problems. Since then, much research has been carried out on this algorithm. A thorough survey of this work with respect to FPGAs has been published by Andraka [112].

All the trigonometric functions can be computed or derived from functions using vector rotations. The CORDIC algorithm is derived from the Givens rotation transforms:

$$x_{i+1} = x_i \cos\theta(i) - y_i \sin\theta(i)$$

$$y_{i+1} = y_i \cos\theta(i) + x_i \sin\theta(i)$$

which rotates a vector  $(x_i, y_i)$  in Cartesian plane by an angle  $\theta(i)$ . These can be rearranged so that:

$$x_{i+1} = \cos\theta(i) [x_i - y_i \tan\theta(i)]$$

$$y_{i+1} = \cos\theta(i) [y_i + x_i \tan\theta(i)]$$

The process of rotating a unit vector  $(1,0)$ , until the angle is  $\theta$  is depicted in figure 5.6

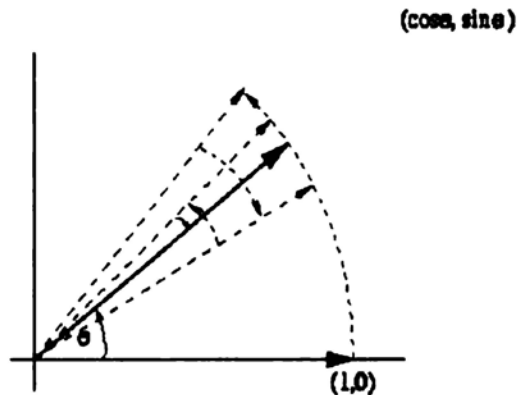


Figure 5.6 A unit vector rotated to angle  $\theta$  using iteration.

However if the rotation angles  $\theta(i)$  are restricted to  $\tan\theta(i) = \pm 2^{-i}$ , then the multiplication by the tangent term is reduced to simple shift operation. Arbitrary angles of rotation are obtainable by performing a series of successive smaller elementary rotations. The iterative rotation can now be expressed as:

$$x_{i+1} = K_i [x_i - y_i \cdot d_i \cdot 2^{-i}]$$

$$y_{i+1} = K_i [y_i + x_i \cdot d_i \cdot 2^{-i}]$$

where:

$$K_i = \cos(\tan^{-1} 2^{-i}) = \frac{1}{\sqrt{1+2^{-2i}}}$$

$$d_i = \pm 1$$

Removing the scaling factor  $K_i$  from the iterative equations yields a shift-add algorithm for vector rotation. The product of  $K_i$ 's can be applied elsewhere in the system. The product approaches a constant value as the number of iterations becomes infinity. The exact gain of the system depends on the number of iterations and is:

$$A_n = \prod_n \sqrt{1 + 2^{-2i}}$$

The set of all possible decision vectors in an angular measurement system is based on binary arctangents. Conversions between this angular system and the other can be accomplished with the help of a look-up table which can be easily implemented in an FPGA. The angle accumulator adds a third difference equation to the CORDIC algorithm:

$$z_{i+1} = z_i - d_i \cdot \tan^{-1} (2^{-i})$$

The CORDIC rotator is normally operated in one of the two modes. The first, called *rotation mode*, rotates the input vector by a specified angle and the second mode called *vectoring mode* rotates the input vector to the X axis while recording the angle required to make that rotation.

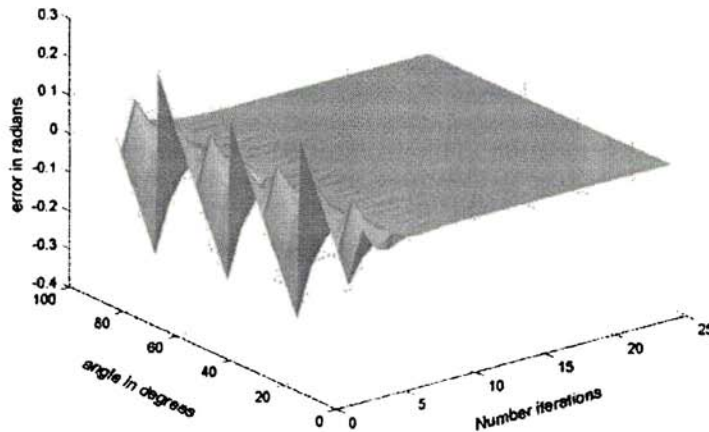


*Figure 5.7 The 3-D plot showing the variations in residual angle which is a measure of computational error against input angle and the number of iterations.*

In this system the rotation mode is used to compute the sine and cosine values to solve the position and attitude update equations. In this mode the angle accumulator is initialized with the desired rotation angle. The rotation decision at each iteration is made to diminish the magnitude of the residual angle in the angle accumulator. The decision at each iteration is therefore based on the sign of the residual angle after each step. For rotation mode the CORDIC equations are:

$$x_{i+1} = x_i - y_i \cdot d_i \cdot 2^{-i}$$

$$y_{i+1} = y_i + x_i \cdot d_i \cdot 2^{-i}$$

$$z_{i+1} = z_i - d_i \cdot \tan^{-1}(2^{-i})$$

where

$$d_i = -1 \text{ if } z_i < 0, +1 \text{ otherwise}$$

Which provides the following results:

$$x_n = A_n [x_0 \cos z_0 - y_0 \sin z_0]$$

$$y_n = A_n [y_0 \cos z_0 + x_0 \sin z_0]$$



$$z_n = 0$$

$$A_n = \prod_n \sqrt{1 + 2^{-2i}}$$

The rotation mode CORDIC operation can simultaneously compute the sine and cosine of the input angle. By setting  $x_0=1$  ;  $y_0=0$ ;  $z_0 = \text{the input angle}$ ; and multiplying the result with  $(1/A_n)$  the sine and cosine values can be computed. Figure 5.7 shows the angle error plot against the variations in residual angle with respect to the number of iterations. The value of  $1/A_n$  for 16 iterations is around 0.60725293510314. More than ten iterations give a satisfactory resolution and  $1/A_n$  is nearly a constant.

### 5.3.2 The Realization Details

The entire sub system has been designed and implemented in Altera Cyclone-II EP2C70F672-C6 FPGA. The main task is the implementation of the computational unit consisting of the CORDIC processors for the sine and cosine computation [121]. The design has been divided into various blocks [122, 123] like the Encoder Pulse Processing Module (EPPM), computational unit for evaluating the update equations incorporating the CORDIC processor, switching module for selecting the least values and SPI communication interface for establishing the link with the control processor. There are various read/write registers involved in the design for scaling, initialization and data storing.

The entire design entry process is carried out with the help of VHDL and the design is synthesized [124, 125, 126] with the above mentioned target device in Quartus II software. The CORDIC algorithm is implemented in sequential manner and the number of iterations required is seen to be 16. The sequential CORDIC design performs one iteration per clock cycle. With a system clock frequency of 50MHz, the total time taken by this module is less than 400ns, which is a very

small value, as most of the vehicle control system require only one sample per  $100\mu\text{s}$  or even less. Hence the results are ready with the sub system after initialization of the system registers and the role of the controller is to read the update values and velocity information through the SPI.

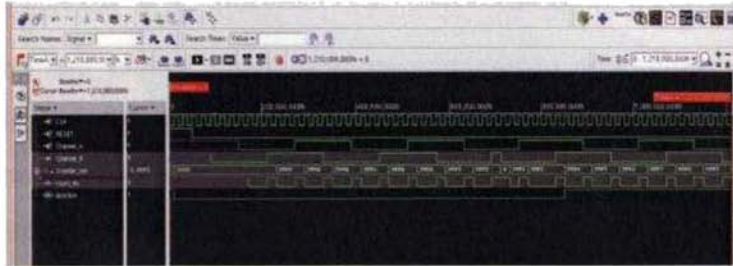


*Figure 5.8* Screen shot showing the various wave forms with the system clock of 50MHz of encoder pulse processing module.

The figure 5.8 shows the screen shot during simulation of the Encoder pulse processing module, while figure 5.9 shows the various waveforms during the computation of sine and cosine values for 30 degrees, 45 degrees and 60 degrees. The inputs to the CORDIC module `ANGLEin` and `LOAD` signals are pulsed and `RESULT_READY` indicates the availability of the results in the 16-bit registers after sixteen clock pulses. The photograph of the sub system is shown in figure 5.10.



*Figure 5.9* Screen shot showing the various results of computation along with the control and status signal associated with the sequential CORDIC module.

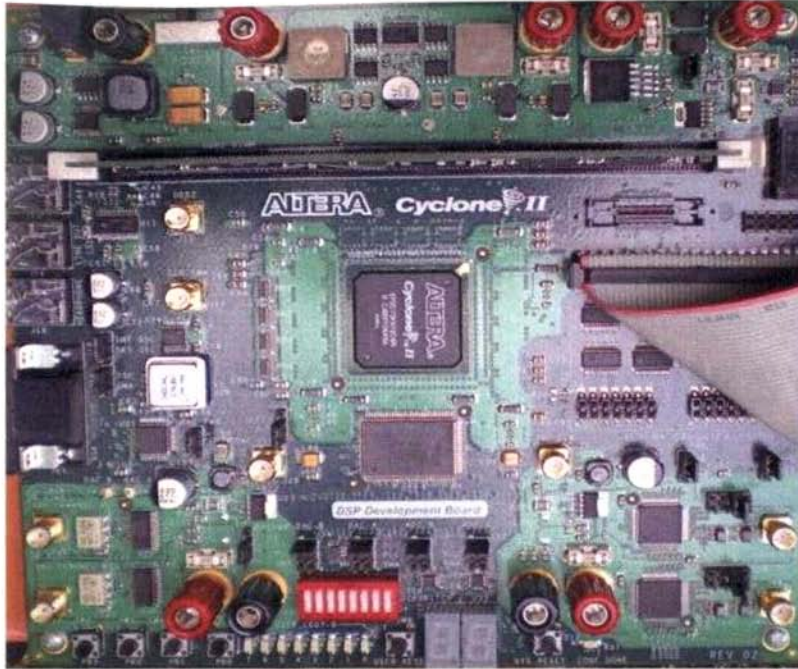


*Figure 5.10 Photograph of the sub system implemented in Altera Cyclone-II EP2C70F672-C6 FPGA development board.*

## **5.4 Summary**

A simple and efficient method and its implementation in an FPGA for reducing the odometric localization errors caused by over count readings of an optical encoder based odometric system in a mobile robot due to wheel-slippage and terrain irregularities is discussed in this chapter. The detection and correction is based on redundant encoder measurements. The method suggested relies on the fact that the wheel slippage or terrain irregularities cause more count readings from the encoder than what corresponds to the actual distance traveled by the vehicle. The standard quadrature technique is used to obtain four counts in each encoder period. The CORDIC algorithm has been used for the computation of sine and cosine terms in the update equations. The results presented demonstrate the effectiveness of the technique.

# 6

## APPLICATIONS OF DISLiB SYSTEM



---

6A Traffic and Transport Control.....	116
• Introduction	
• Outline of Traffic Control System	
• Infrared Sheet of Light Beacon	
• The Beacon Receiver and Vehicle Unit	
• Installation and Working	
6B Differently-able Assistance.....	126
• Introduction	
• Localization of the visually impaired	
• The Beacon Receiver	
• Position and heading	
6C. Summary.....	133

---

The application of Digital Infrared Sheet of Light Beacons (**DISLiB**) developed for the localization of autonomous mobile robot vehicles can be extended to other diverse fields. The suitability of DISLiB system to applications where the localization and guidance are of great importance, like intelligent control of the public transportation system as well as guidance of differently-able personnel are envisaged. An adaptive traffic control system should ensure safe and smooth traffic flow and inform the drivers about the traffic status. Guidance and obstacle avoidance systems for visually impaired personnel should provide less body gear and adequate information about the environment.

## **6A Traffic and Transport Control**

This section describes the design, characterization and implementation details of a encoded digital infrared sheet of light based beacon system for intelligent control of the public transportation system. The system consists of an encoded infrared sheet of light beacon, which can convey the current location and traffic information to the vehicles. The system is capable of receiving traffic status input through a GSM (Global System Mobile) modem. The vehicles have an infrared receiver and a processor capable of decoding the information, and generating the audio and video messages to the driver.

### **6A.1 Introduction**

Congestion and delay on roadways continue to increase everywhere. As congestion increases, heavier traffic loads are placed on streets. New construction to satisfy this ever-growing demand is not only costly but also raises environmental, social, and political issues. “Building our way out of congestion” is no longer a feasible approach. As a result, a great deal of emphasis is being placed upon programs to manage traffic and efficient use of available roadway capacity. This has led to the development of various types of intelligent traffic management systems.

The modernization of public transportation system is of great importance, to increase the performance, which may result in fuel saving, reduction of time loss in traffic congestion and even to overcome the constraints on building new roads and transit systems. The increasing motorization demands better operation and control of road traffic. Increased traffic congestions faced by the drivers day-by-day, lead to reduced safety, increased energy consumption, environmental pollution and even missed traffic signs or important information.

The application of advanced technologies in electronics and communications to transportation systems results in the design of intelligent and friendly traffic management and control systems [127, 128, 129]. The various systems used in some developed countries include traffic flow maps, frequently updated websites, changeable message signs, advisory radio, electronic traveller information displays, etc. The use of an intelligent system for solving the traffic and transport problems improves the utilization of existing infrastructure, reduces demand for new roads, makes traffic better, saves cost significantly, increases safety, improves mobility and livability for the region.

People use traveller information to assess traffic congestion in their route, judge the effects of incidents on their trip, decide among alternate routes and estimate their trip time to reach the destination [135]. For providing this information the traffic management centers/systems collect and coordinate traffic flow data using various sensors and technologies. Real-time data coordination allows traffic flows to be adjusted in response to changing conditions. This results in safer and more efficient traffic flow. Information regarding the conditions of the road gives carriers the best routing options, which may reduce delay, making them reach destinations early. The use of electronic clearance systems at the inspection points of the border crossing reduces delays and truck stops.

The purpose of a traffic control system is to ensure safe and smooth traffic flow, and it has functions for controlling traffic signals by traffic data acquired by various sensors and informing the drivers about the traffic status [130]. Today, each and every country requires an upgradation of their traffic control system in order to solve traffic problems such as increased traffic accidents, aggravated traffic congestions etc. It involves heavy detectorization of the streets and highways

where traffic data can be transmitted to the traffic control center [131, 132], and appropriate traffic management can be implemented

The concept calls for monitoring traffic flow conditions on all roadways by the help of various detectors like camera and providing that information in a variety of ways to vehicles travelling within the city or streets. The motorists can then make timely decisions about the route he has to take, and a more balanced use of road facilities will result. A high degree of coordination is jurisdictional entities in the operation of traffic management and control system for roadways [133, 134].

This work proposes a simple, efficient and economic system to control the road traffic. The system consists of an encoded infrared sheet of light beacon, which can convey the current location and traffic information to the vehicles. The system is capable of receiving traffic status input through a GSM (Global System Mobile) modem from the traffic management center and traffic personnel, which eliminates the need for a dedicated channel and the associated instruments. The vehicles have an infrared receiver and a processor unit capable of decoding the information, and generating the audio and video messages to the driver. The receiver in the vehicle can refer to an inbuilt database and get the above information with negligible computational overhead. The vehicle unit can be manufactured based on the sophistication demanded by the user. The immediate alterations or changes required in traffic, perhaps due to an emergency or a VIP being on the road can be communicated instantly to the driver. Even activating speed limit to conventional vehicles and restricting to sidetracks can help the easy passage of ambulance and VIP vehicles.

## **6A.2 Outline of Traffic Control System**

Beacon based traffic and transport control as well as driver safety support systems are used in some developed countries to improve their transportation

systems [136, 137]. Most of them use infrared, ultrasonic or radio frequency beacons for implementing the same. These have inherent emission characteristics that may affect the performance of the system. Most of the existing traffic control systems are complex, expensive and error prone. Hence it is essential to consider a robust, cost effective and easy to implement system for the assistance of the driver and improved quality of the existing traffic.

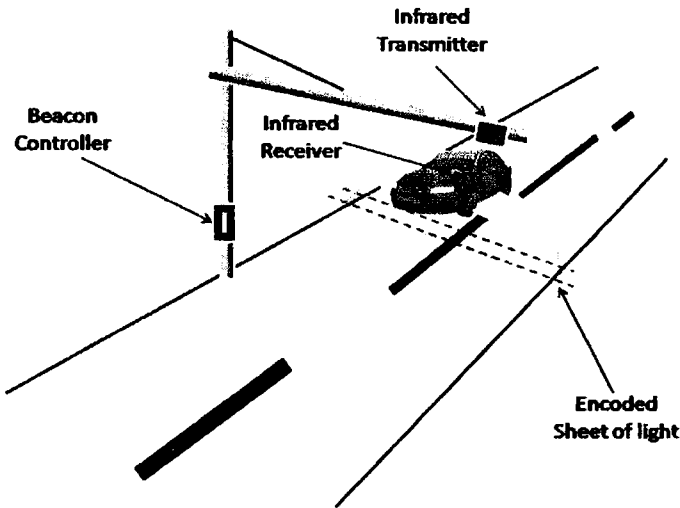


*Figure 6.1 A traffic signaling installation using an encoded infrared sheet of light beacon.*

This work describes a beacon assembly utilizing infrared LED source that confines the distribution of the light intensity to a sheet of light. A microcontroller derives the appropriate digitally encoded information and the infrared beacon transmits the same. The system is also capable of exchanging information through a GSM modem to the central or distributed traffic control stations. The traffic control center has a computer with GSM communication facility and is capable of receiving current traffic status through various means. The receiver at the vehicle



capable of decoding the signals displays the various traffic status and signs with audio indication.

The functional diagram of the system is shown in figure 6.1. An infrared light sheet assembly consisting of three infrared LEDs is mounted on an arm attached to the top of a mast as shown. The beacon controller is fixed to the bottom portion of the mast for convenient access. The power supply requirements can be met with the help of a solar panel or conventional electric supply. For tackling an emergency situation, portable units with the beacon assembly mounted on a stand in a side looking way can be used if needed.

### **6A.3 Infrared Sheet of Light Beacon**

The DISLiB scheme similar to the one described in chapter 4 is considered here. A beacon transmitter assembly of different dimensions as shown in figure 6.2 has been developed. The infrared beam is guided through the space between two identical sand blasted parallel metal plates of dimensions 0.15m x 0.15m, kept 15 mm apart. These metal plates are acting as Lambertian scattering surfaces (diffuse reflectors) and their dimensions have effects on the sheet thickness as well as infrared light intensity. Three infrared LEDs are mounted on the housing, 0.05m apart as shown in figure 6.2. The variation of effective infrared light sheet thickness (ELST) against the mounting height of this assembly has been studied and the results are shown in figure 6.3. Above a height of three metres the light sheet thickness is seen to be around one metre and the beacon receiver can read the encoded data within this distance with vanishingly small errors.

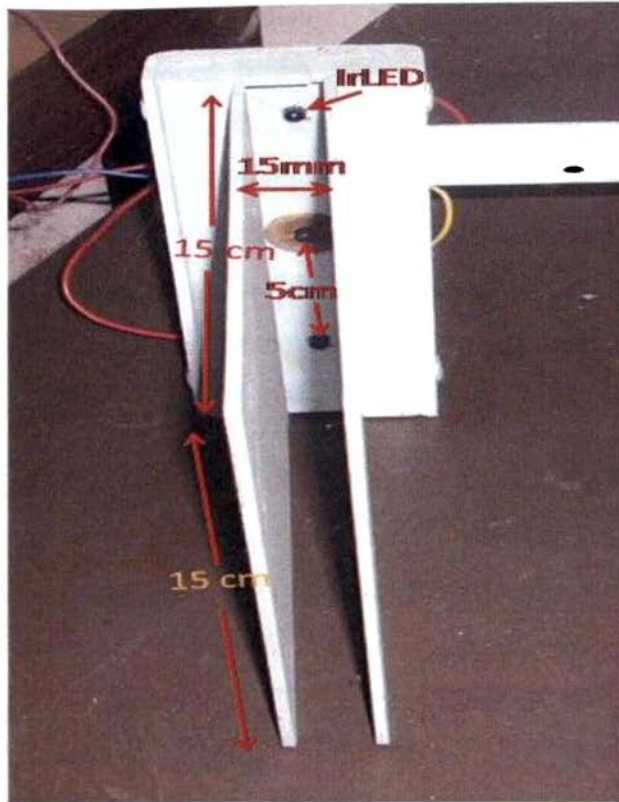


**Figure 6.2** The infrared LEDs of the beacon transmitter mounted on a structural assembly made up of sand blasted metal plates, which act as Lambertian scattering surfaces providing a sheet of light.

The Digital Infrared Sheet of Light Beacons (**DISLiB**) constructed using the above assembly are location as well as traffic data encoded and are designed around a 18F452 PIC microcontroller. The functional block diagram is shown in figure 6.4. The same carrier frequency of 40kHz with the Sony Infrared Remote Control (**SIRC**) protocol is used to transmit the position and traffic information. Besides continuously transmitting the encoded position and traffic information, the microcontroller in the beacon transmitter drives the three infrared LEDs by switching a transistor in series with a current limiting resistor.

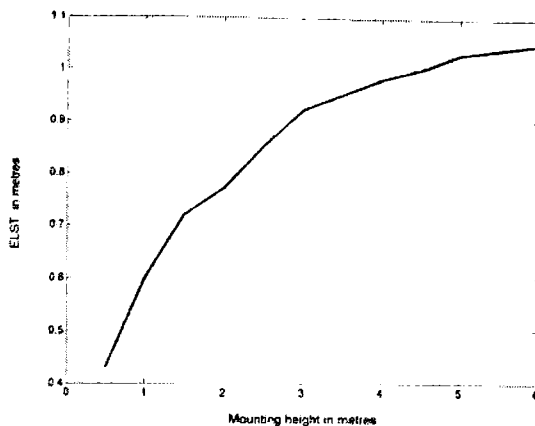


Figure 6.3 Variation of effective light sheet thickness against the mounting height of the beacon ( $h$ ).

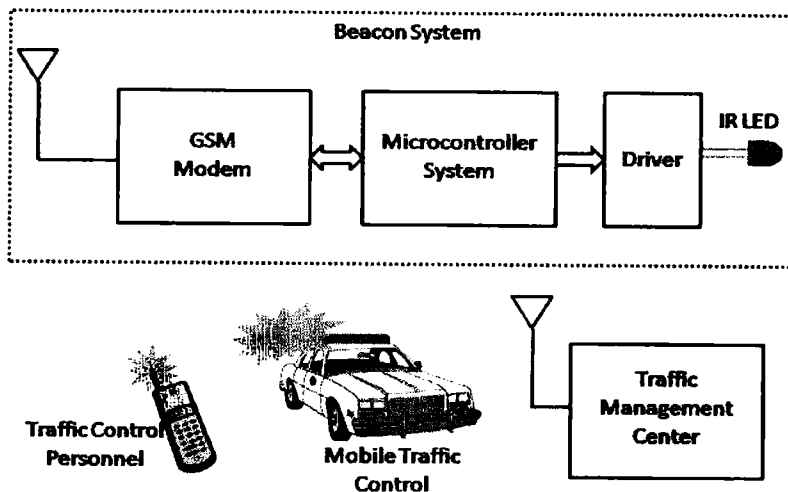


Figure 6.4 Functional block diagram of the beacon transmitter consisting of a microcontroller, which generates the encoded signal for driving the Infrared LEDs mounted inside the special assembly and a GSM Modem for establishing the communication with a traffic management center.

A beacon Identification Number (BIN) and the mobile number of the GSM service provider are assigned to every beacon transmitter for identifying the

location of installation and the establishing communication. The required traffic signaling information like speed limits, sharp turnings, warnings, etc. can be encoded and transmitted through the beacon. A traffic management center or a mobile traffic control unit can communicate through the GSM link incorporated in the system, so that the traffic signaling commands can be modified online, thereby updating the encoded information in the beacon. Even from the mobile phone of the traffic control personnel the beacons can be programmed for managing the traffic.

#### **6A.4 The Beacon Receiver and Vehicle Unit**

The functional block diagram of a beacon receiver used in vehicles is shown in figure 6.5. While crossing the sheet of light, the information gathered from the beacon by the infrared receiver module is processed by the microcontroller system on the vehicle that manages the traffic signal and guidance. With an effective light sheet thickness of around 1m (figure 6.3), there is no limit on the maximum speed of the vehicle because even at a speed of 200km/hr the receiver can take multiple readings.

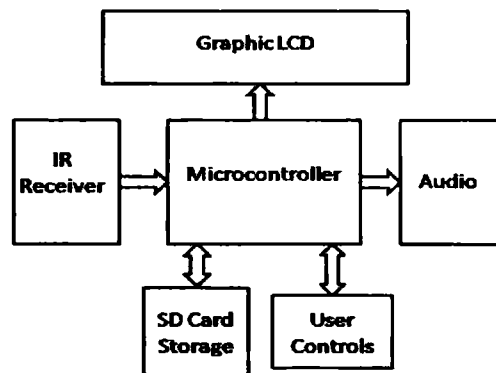


*Figure 6.5 Block diagram of the vehicle unit consisting of the infrared receiver module, a microcontroller and its associated components.*

The graphics LCD panel interfaced to the microcontroller is capable of visualizing the traffic signs and location information and the audio system provides appropriate sound to attract the driver. An SD card interfaced [149] to the system stores the database for traffic signals and location. This SD card can be easily updated by means of a website or fuel filling stations or other public places where this can be made available to the users. Territory/state wise detailed database can be created and easily updated. During long journey the vehicles may pass through various territories, but replacing the appropriate SD card can solve the information update process. The on-chip SPI interface in the microcontroller is utilized for interconnecting the SD card module.

The traffic authorities can classify the vehicles under different categories and assign different privilege levels for smooth movement of ambulances and official vehicles. The system generates the traffic sign and warnings by considering its category as well as the privilege level assigned to the vehicles.

### **6A.5 Installation and Working**

Most of the intelligent traffic and transport control systems require the installation of multiple beacons at known locations. By properly installing the Digital Infrared Sheet of Light Beacons (**DISLiB**) at known locations vertically above the road as shown in figure 6.1, the vehicle unit can receive the beacon while passing through the encoded infrared light sheet and identify the beacon (location) and receive the encoded traffic status and sign information. In a typical structure (figure 6.1), the beacons should be mounted at a height of about three metres for the **ELST** to cover the entire width of the road without any disturbance to the traffic flow. For greater road widths either more infrared LEDs or increased mounting heights within the reading threshold of the beacon is preferred. Even

multiple infrared assemblies with the same controller unit are recommended for wide highways.

The vehicle unit firmware and database play a very important role in guiding and supporting the driver by displaying the optimized and time dependant traffic signs and warnings. The database stores all the traffic sign, symbol data and location information corresponding to the beacons. The vehicle unit receives the encoded information for the traffic signs and locations, which may vary from time to time for smooth traffic flow. The system decodes the same and displays the graphical sign with audio message to support the driver. The various time dependant traffic signs are speed limit, one ways during peak time, no left/right turns, no entry for certain category of vehicles etc.

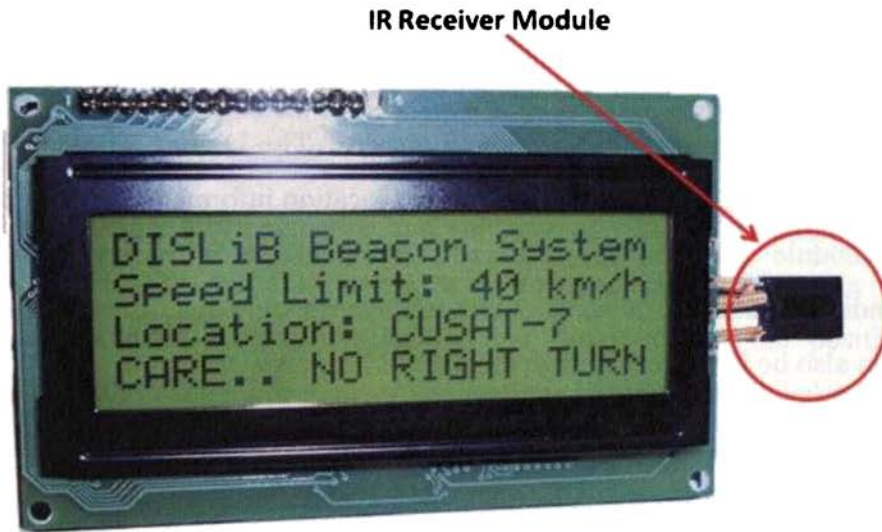


*Figure 6.6 Photograph of the prototype of the Vehicle Unit*

The vehicle unit can display the location name and distances from various reference points (main cities/streets). The unit can even calibrate the odometer by passing through a number of beacons. A route map can be built for frequently used

destinations to assist the driver. The parking places and parking restrictions can also be communicated to vehicles a few metres ahead of those locations/area. The driver must feed direction information (bit) to the system for identifying up and down journeys for interpreting certain functions. A pre recorded voice chip can be activated upon receiving the beacon and appropriate voice messages can be played back in driver's own language. The driver can enable or disable these features as required. The photograph of the prototype of the Vehicle Unit is shown in figure 6.6.

## **6B Differently-able Assistance**

A guidance system for assisting the visually impaired in structured indoor and partially outdoor environments is described in this section. The system consists of a number of encoded infrared sheet of light beacons installed at appropriate locations and a small receiver module attached to the shoulder of the visually impaired person. The system is intended for use in indoor environments, such as home, office buildings, supermarkets and airports. The Digital Infrared Sheet of Light Beacons (**DISLiB**) transmit the encoded location information and an infrared receiver module decodes this data and the message is retrieved from the corresponding location in a voice recorder/playback chip. The orientation of the person can also be informed through the natural language.

### **6B.1 Introduction**

Considerable effort has been made over the past few decades for developing navigation and guidance devices for the visually impaired. Electronic Cane using optical triangulation technique with laser diodes and Photo-detectors have been developed since 1973[138]. Thereafter various ultrasonic systems [139,140] have been reported for obstacle avoidance and navigation in different forms. Radio Frequency Identification (RFID) based canes and robot guides have been

developed for assisting the visually impaired in a structured environment [6, 141, 142]. The motorized wheelchair [150] equipped with modern sensors like vision system, sonars, differential GPS etc.[143] are very helpful in assisting the differently-able persons but the need for a powerful computational unit and reduced portability affects the use of these systems.

Accurate sensing of the position and attitude of visually impaired personnel is of great importance in designing navigation and guidance system for them. Most of the localization techniques used in mobile robots can be easily adopted for the use of visually impaired personnel, if the physical size and shape of the system is wearable. In order to navigate and guide to their destinations, the personnel must have some means of estimating his position and direction. A variety of technologies [144,145,146] have been developed and used successfully to provide position and attitude information. However, many of these existing systems have inherent limitations in practical environment such as large computational overhead and body gear, poor performance and reliability.

For the successful navigation and guidance of visually impaired persons, a well-defined and structured environment is required [147]. This can provide position and attitude information for reliable estimation of the position and navigational path [151]. For outdoor applications Differential Global Positioning System (DGPS) based localization techniques provide adequate resolution, whereas for indoor use, this resolution is insufficient and moreover the satellite signals may be obstructed, which further aggravate the situation. These localization systems, which utilize triangulation or trilateration techniques [28], have high uncertainty in position estimations and incur extra computational overheads as well as results in increased body gear.



The above examples brief the diverse ways of position estimation and support systems for differently-able people that are already in use. Their limitations open the scope for further research opportunities for improvement and innovations. The technique presented in this section is based on encoded infrared sheet of light beacons and receiver, which require only low power miniaturized hardware that reduces the body gear carried by the user. Therefore, the navigation and guidance of a visually impaired can be achieved with a reduced physical load, which verbally guides the personnel. The user can use this system in conjunction with the conventional navigation aids or a guide dog too.

### **6B.2 Localization of the Visually Impaired**

DISLiB transmitter and its assembly developed for guiding the visually impaired personnel has the same characteristics, dimensions, encoding scheme and features has that of the one developed for localization of the mobile robot vehicle. Each beacon transmitter transmits the assigned BIN and the coded navigation information regarding the environment. So beacon to beacon there may be a change in the transmitting information. This change in information normally needs a change in the firmware of the beacon transmitter. A generalized firmware can be configured by the microcontroller by reading the changes in the status of the micro-switch inputs interconnected to it. By establishing an RS 485 network among the beacons and a host computer, the position information as well as other navigational commands can be modified online. The system can be made user friendly by incorporating an RS485 network with the host computer.

By properly installing the Digital Infrared Sheet of Light Beacons (**DISLiB**) at known locations vertically above the passage, an accurate and robust representation of the environment can be achieved for better assistance. The beacon distributions can be identified based on the structure of the environment.

### **6B.3 The Beacon Receiver**

The functional block diagram of a typical beacon receiver (shoulder unit) is shown in figure 6.7. Two infrared receiver modules are employed in this design for estimating the position and orientation of the visually impaired personnel. A user interface for the control and configuration is inbuilt with the system. A ChipCorder (voice record and playback integrated circuit from Windbond Electronics Corporation, USA) [148] has been used to store the natural language commands and description of the environment. With the help of the microcontroller the appropriate voice message can be retrieved from the ChipCorder and the message is made available to the visually impaired personnel through an earphone. For the prototype design, ISD4004-08MP ChipCorder has been used. This ChipCorder provides high quality, fully integrated, single-chip Record/Playback solutions for eight minutes messaging applications that are ideal for use in navigation systems and other portable products. Various commands for address and control are accomplished through a Serial Peripheral Interface (SPI) port of the microcontroller. The chip is integrated with sampling clock, anti-aliasing and smoothing filters along with the nonvolatile multi-level voice storage array, providing zero-power message storage. The message and guidance information are stored directly into solid-state memory in their natural, uncompressed form, providing superior quality voice reproduction. The standby current for the device is less than  $1\mu\text{A}$ , which is ideal for battery operation.

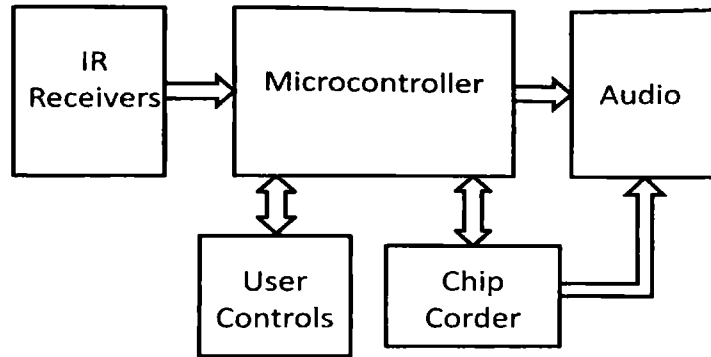


*Figure 6.7 Block diagram of the beacon receiver consisting of PIC18F2550 microcontroller, which manages the audio record playback ChipCorder*

During path execution, the position information gathered by the infrared receiver modules from the beacon is processed by the microcontroller system attached to the shoulder of the visually impaired personnel that supports the navigation and guidance. As the person crosses the infrared light sheet of thickness *ELST* (**d**), the microcontroller based support system directly captures the location encoded information (**BIN**) and updates the corresponding absolute position from the database. By specifying certain scaling factors and the encoded value, it is possible to reduce the memory requirements of the system. The receiver takes 6ms for position decoding and hence at least 12 ms is required for a guaranteed position update while crossing a DISLiB.

### **6B.4 Position and Heading**

Two infrared sensor modules arranged inline are utilized to receive the beacon and these information playbacks the position and heading of the visually impaired personnel who is wearing the module on his shoulder. The sensor can read the beacon data, which corresponds to a particular position as well as other signalling information regarding the environment for the visually impaired personnel. The visually impaired personnel wear the shoulder unit in which two

identical sensors  $S_1$  and  $S_2$  are mounted at a distance of  $2a$ . If the axis of symmetry is normal to the sheet of light both the sensors receive the signal simultaneously and the personnel is assumed to be moving normal to the sheet of light. If the person crosses the beacon with a heading angle " $\alpha$ " (not equal to zero) there will be a lag or lead between the received signals, which is a measure of the heading angle of the personnel. The signal waveforms derived from the start pulse is shown in Figure 6.8 (inside the circle), in which the time duration  $t_b$  is the time required to cross the beacon and the lag or lead time  $t_d$  is the time required to cover the distance " $c$ " by the person. The lead or lag time  $t_d$  is a measure of the orientation of the person wearing the shoulder unit.

For a person crossing the light sheet with a velocity  $P_v$ , the heading angle can be estimated as follows.

$$\alpha = \tan^{-1} \left( \frac{c}{2a} \right) = \tan^{-1} \left( \frac{t_d P_v}{2a} \right) = \tan^{-1} \left( \frac{t_d d}{t_b 2a} \right) \quad (6.1)$$

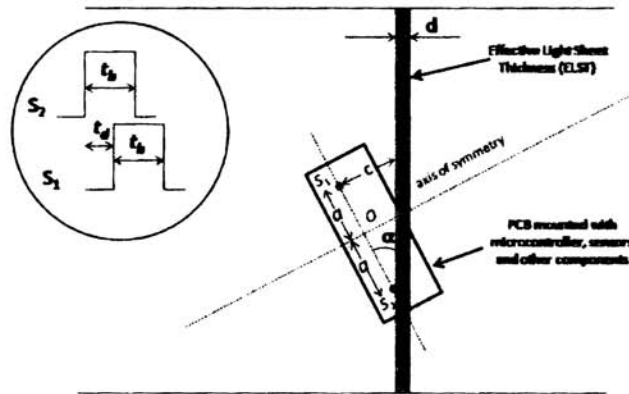
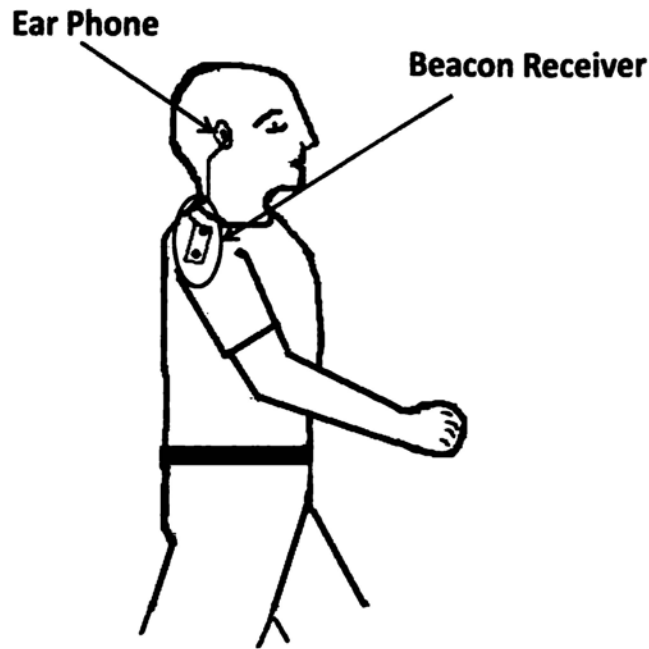
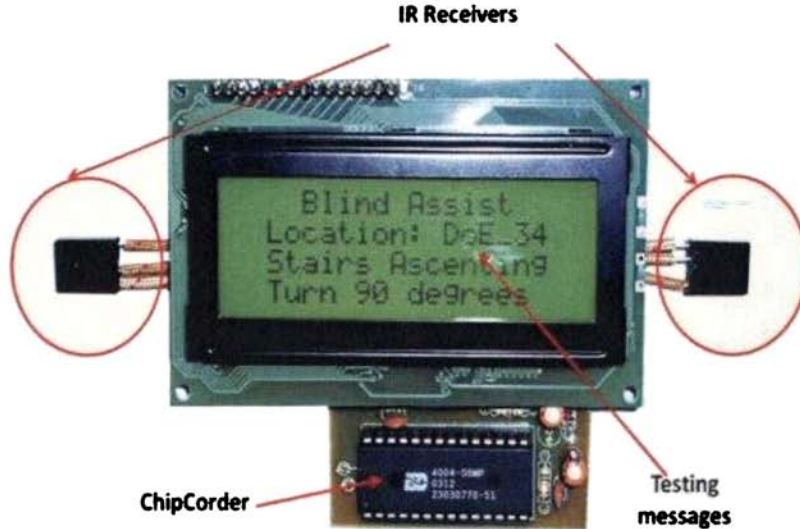


Figure 6.8 A typical posture of the shoulder unit and the footprint of the effective light sheet thickness (ELST)  $d$ . The heading angle  $\alpha$  is the angle between the ELST and the axis joining the beacon sensors  $S_1$  and  $S_2$ . The time delay  $t_d$  between the encoded signals reaching the sensors is also shown.



*Figure 6.9 Typical mounting scheme of the guidance and support system with an ear phone (shoulder unit).*

A typical posture of the shoulder unit under the beacon transmitter is shown in figure 6.9. The velocity of the moving personnel  $P_v$  has been estimated by the system in auto mode by measuring the beacon crossing time  $t_b$  or the ELST value  $d$  can be directly fed during initial configuration of the system. Microcontroller will compute the time  $t_d$  from the sensor readings. In a practical environment the sensor readings may be affected with the posture errors as well as the angle of incidence of the beacon. The resolution of the system is adequate in guiding visually impaired personnel. The photograph of a typical shoulder unit shown in figure 6.10 includes an LCD for easy debugging at the development stage, which can be detached later.



*Figure 6.10 Photograph of a typical shoulder unit with an LCD display for debugging.*

## 6C. Summary

A techniques for reducing the traffic congestions and location identification are introduced in this chapter. The need for an intelligent traffic control for the modern public transportation system has been well illustrated. The realization details of a traffic and transport control system using the existing GSM network are discussed. A flexible and friendly vehicle unit design has also been proposed.

The **DISLiB** based visually impaired personnel support system described in this chapter is simple, cost effective and provides less body gear without much computational burden or significant processing. The diverse ways of position estimation and support systems for differently-able people that are already in use have also been briefed. The natural language assisting capability of the system by incorporating a ChipCorder has also been addressed.

## CONCLUSIONS

---

7.1 Contributions .....	135
7.2 Highlights of the Work .....	136
7.3 Strengths and Limitations .....	138
7.4 Future Research.....	141
7.5 Summary .....	141

---

This chapter consolidates the design, features, results and applications of the system developed for the localization application. A comparison of the merits and demerits of the system is also carried out. Future enhancement and correction methods for improving the performance of the system are proposed. The extension of the use of the system to other applications is also suggested.

### 7.1 Contributions

This thesis is mainly concerned with an absolute and robust localization system for indoor mobile robots. The principal contributions of this thesis are as follows:

- Pioneered in developing an encoded digital infrared sheet of light beacon system especially suited for the localization and navigation of mobile

vehicles and personnel in a real world environment. This system incorporates a special assembly to produce the sheet of light and encode with position information, which is capable of finding the vehicle pose information.

- A novel approach to find the absolute position and attitude of the mobile robot vehicle with the help of DISLiB beacons with out any computational overhead. A single reading from the beacon computes the pose, so the line-of-sight restrictions can be minimized.
- Developed a scheme for networking of the beacons and establishing communication with mobile robot vehicles in a structured indoor environment.
- Developed an algorithm, which can improve the resolution of the localization achieved by the DISLiB system.
- The realization of a new technique to reduce the odometry error is achieved, which reduces the frequent absolute position updates.
- Developed a system for assisting the differently able personnel for their movement in a structured indoor and outdoor environment using the DISLiB.
- Also extended the same technique to establish a cost effective and efficient traffic and transportation system for roadways.

## **7.2 Highlights of the Work**

- (i) A new localization approach based on an encoded digital infrared sheet of light beacon (DISLiB) system to increase the navigational capabilities and object manipulation of autonomous mobile robots, which provides position errors smaller than 0.02m has been presented. To achieve this minimal



position error, a resolution enhancement technique has been developed by utilising inbuilt odometric/optical flow sensor information. This system respects strong low cost constraints by using an innovative assembly for the digitally encoded infrared transmitter. For better guidance of mobile robot vehicles, an online traffic signalling capability is also incorporated.

- (ii) A simple and efficient method, and its implementation in FPGA, for reducing the odometric localization errors caused by over count readings of an optical encoder based odometric system in a mobile robot due to wheel-slippage and terrain irregularities has been introduced. The detection and correction is based on redundant encoder measurements. The method suggested relies on the fact that the wheel slippage or terrain irregularities cause more count readings from the encoder than what corresponds to the actual distance traveled by the vehicle. The standard quadrature technique is used to obtain four counts in each encoder period. In this work a three-wheeled mobile robot vehicle with one driving-steering wheel and two fixed rear wheels in-axis, fitted with incremental optical encoders is considered. The CORDIC algorithm has been used for the computation of sine and cosine terms in the update equations. The results presented demonstrate the effectiveness of the technique.
- (iii) Two applications of DISLiB have been exploited. The first is the design, characterization and implementation of a digital encoded infrared sheet of light based beacon system for intelligent control of the public transportation system. The system consists of an encoded infrared sheet of light beacon, which can convey the current location and traffic information to the vehicles. The system is capable of receiving traffic status input through a GSM (Global System Mobile) modem. The vehicles have an infrared receiver and a

processor capable of decoding the information, and generating the audio and video messages to the driver.

- (iv) The second application is a guidance system based on DISLiB for assisting the visually impaired in structured indoor and partially outdoor environments. The system consists of a number of encoded infrared sheet of light beacons installed at appropriate locations and a small receiver module attached to the shoulder of the visually impaired person. The system is intended for use in indoor environments, such as home, office buildings, supermarkets, airports, etc.. The Digital Infrared Sheet of Light Beacons (**DISLiB**) transmit the encoded location information and an infrared receiver module decodes this data and the message is retrieved from the corresponding location in a voice recorder/playback chip. The orientation of the person can also be informed through natural language.

### 7.3 Strengths and Limitations

The **DISLiB** developed for mobile robot localization is a high resolution system which is simple, fast and accurate without much of computational burden or significant processing. Most of the localization research works are carried out in laboratory or room like environment. But most of the service mobile robot vehicles are employed in industries, warehouses, etc., where a particular path is defined for their movement. Most of the available beacon's performance in corridors and narrow passages are not satisfactory but the performance of **DISLiB** is very encouraging in such situations. The installation is not limited to corridors provided the vehicle crosses the light sheet for position update and error correction. Even in indoor applications the inclined paths cause localization errors, which are very difficult to eliminate. But by installing **DISLiBs** at appropriate locations one can easily reduce the same. An innovative assembly of the transmitter together with the

database in the receiver module eliminates the time consuming triangulation or trilateration algorithms, which is utilized by most of the existing systems for position estimation. The bit length used for position encoding can be easily increased for mapping large workspaces. Separate firmware for encoding different beacons can be eliminated by incorporating either configuration switch inputs to the system or a RS 485 type of network and a host computer. The wireless closed loop monitoring increases the overall efficiency of the system. For exterior mobile robot localization, the beacon systems can be organised on pillars in a side looking arrangement.

Normally the **DISLiBs** are fixed in such a way that the vehicle crosses the beacon with the angle between the light sheet footprint and the line joining the beacon receiver sensors equals to zero. As the DISLiB system requires a long baseline (the distance between the IR sensors) for better attitude estimation, this technique may not be appropriate for determining the attitude of small and micro vehicles. While crossing the very short distance of around 0.12 m (ELST), the system assumes uniform vehicle speed and accurate odometry. In order to guarantee this, the beacon installation points should be selected accordingly. The effective light sheet thickness depends on the light intensity, mounting height and receiver sensitivity. The non-uniform distribution of the beacon light intensity results in slight variations of light sheet thickness on the sides of the passage. This can be reduced using multiple infrared LEDs. The maximum resolution of the DISLiB is limited to the resolution of the odometry system. This system will obviate the inherent odometric and INS position errors.

The odometric error reduction and its implementation in FPGA is an efficient and effective technique. By using this system, one can reduce the odometric error so as to increase the travel distance between absolute position

updates and this results in lower installation and operating costs for the system. A change in the direction of motion of the robot vehicle inside a time window may cause error in the velocity measurement. This observation will be eliminated. With the use of this sub system, most of the odometric computational burden can be released from the control processor associated with the mobile robot vehicle. This approach may not be recommended for mobile robot vehicles having chances of frequent skidding during path execution. Under most situations this approach is quite satisfactory, simple and efficient.

The use of **DISLiB** based traffic control system is expected to improve the traffic operation and safety of the driver as well as vehicle, which will subsequently reduce congestion and congestion-related accidents. The number of beacons required and their distribution can be identified based on the roadway conditions and the traffic rate. The traffic signs like speed limit, no-horn, etc. can be automatically implemented and the associated devices can be enabled or disabled accordingly by suitably modifying the electronics associated with the vehicle. For establishing the communication among the beacon systems, traffic management center, Mobile control unit and traffic personnel, there is no need for any dedicated channel, as it can utilise the standard commercial channels. All these communications are protected against unauthorised access. The use of intelligent traffic management can result in reduction of total travel time, fuel consumption and thereby vehicle emissions too. The presence of any object that affects the visibility of the beacon to the infrared receiver module installed outside the vehicle may disrupt the functioning of the system. Under most situations this approach is simple, efficient and cost effective.

The **DISLiB** based visually impaired personnel support system is simple, cost effective and provides less body gear without much computational burden or

significant processing. The performance of **DISLiB** is very encouraging in corridors and narrow walkways. Normally the **DISLiBs** are fixed in such a way that the person crosses the beacon with zero degree heading angle. More bits can be used for encoding information for structuring in sizeable environment. For outdoor localization, the beacon systems can be organised on pillars or even one can consider the mounting of these on a street light masts. This system together with a conventional cane is a very helpful aid to visually impaired personnel.

## **7.4 Future Research**

Use of a Wi-Fi network instead of RS 485 network for the **DISLiB** together with robot control and managing station can be investigated. The intensity distribution at the edges of the light sheet may not be uniform. The correction algorithm for the same can be developed for improving the system performance.

The feasibility of **DISLiB** mounting in a side looking way in floating platforms for port vessel traffic management can be studied. Guidance of tourists and strangers in large hospitals or hotel buildings with the help of **DISLiB** system also offers further scope for research.

## **7.5 Summary**

This research work is carried out with an aim of developing a robust, cost effective and absolute position update system without much of computational burden. The proposed absolute localization method has been realized and tested. Two other applications of the system in intelligent traffic and transport control and differently able assist are also proposed. Thus, the work reported in this thesis provides an absolute localization system well suited for autonomous mobile robot navigation, and numerous other applications.

## A WEB BASED ROBOT MANIPULATOR CONTROLLER



---

A1.1 Introduction.....	144
A1.2 Robotic Workcell.....	146
A1.3 Robot Controller Design.....	147
A1.4 Control Program and User Interface .....	149
A1.5 Web Control Module .....	152
A1.6 Exercises .....	154
A1.7 Summary .....	156

---

This section presents the realization of a simple and flexible microcontroller based robot manipulator controller. A web control/server module has been developed for the networked access of this robotic system in a laboratory. The robot actuator control is designed around a microcontroller, which senses the motor speed, position and direction with the help of a quadrature decoder and generates PWM signals for the motor control H-bridge. The robot controller developed is suitable for SCARA/XR4 robot arms from Rhino Robotics Inc., USA. The robot manipulators, which are equipped with permanent magnet DC motors with inbuilt incremental optical encoders for driving the links, and the end-effector are considered for the study. The controller is capable of accepting the commands from a host computer through an RS232 serial port. The control software in the host computer has a user friendly graphical interface with teach-pendant like keys

and functions to control the manipulator arm. The computer can be replaced with a small web server implemented in another microcontroller, which is having a serial port to interact with the robot controller and an Ethernet interface for web access. The web pages stored in the program memory area are very similar to the host computer Graphical User Interface (GUI), through which the user can control and monitor the robot. Without any additional hardware or software any networked system can be programmed (teach the robot). Some of the laboratory exercises using the controller and manipulator are also discussed.

### **A1.1 Introduction**

The capability and simplicity of web based automation systems are stupendously expanding their use in industrial, household and robotic applications. Robotic control is an exciting and highly challenging research work in recent years. Several solutions to the implementation of digital control systems for robot manipulators and mobile robots are proposed in various literatures [152, 153]. In order to meet the demands of a flexible robot controller, the amazingly increasing computational capabilities of personal computer are envisaged. By utilizing the inbuilt standard interfaces and resources one can easily design a practical robot controller, which can be upgraded even in a day-by-day manner. The compatibility allows the user to work offline and online. The use of PC and existing communication interfaces help the efficient co-ordination or synchronization of multiple robots in a large workspace in an industrial environment. The analog control schemes like PI or PID loop can be easily implemented using the host computer. These flexibilities are very useful in a laboratory environment to study the characteristics of the robot and its controller.

The Robotic workstation described here has been developed in the Department of Electronics, Cochin University of Science and Technology, India by

utilizing the existing Rhino XR4 and SCARA Robot arms from Rhino Robotics Inc., USA. In 1988, the robotics laboratory was equipped with Rhino XR4 and Rhino SCARA robots with their own controller and *RoboTalk*, a high level robotic programming language, which is capable of establishing a serial communication with the host computer [154, 156]. In order to gain more control and low level access over the control strategies as well as to utilize the state of the art technologies available, the company supplied controllers have been replaced with the in house controllers designed in Cochin University of Science and Technology. The controller design has the same interface standard that is compatible with the existing mechanical arm. So the robot controller developed is suitable for SCARA/XR4 robots. It can also be used as a general purpose controller for any robot having compatible driving power for the actuator, by changing the interface connector and configuration settings like maximum and minimum count values for various motors etc.. The entire controller hardware is simplified by using more integrated components and the inbuilt teach pendant interface is also eliminated. The controller is capable of establishing communication with a standard PC through an RS232C Port and can receive the commands for various link actuators to manage its position, speed, direction and count increments. The controller is also capable of executing the *hard home* command and detecting the end points and stall conditions for self protection of the system. The H-bridge drivers for the motors are designed around an integrated motor control chip from National Instruments [104]. A fast serial link of 28.8 kbps has been established from the computer to the controller. The computer is provided with a very user friendly interface to support the teach pendant operations and a high level language to learn the robotic systems. For obtaining more flexibility, another module has been developed for interfacing the controller to the web through an Ethernet link. The control GUI stored in this single chip module can be accessed from anywhere in the



network. The technical details of the system and its implementation and use in the laboratory are described.

## A1.2 Robotic Workcell

The functional diagram of the setup is shown in figure A1.1. The Robotic Workcell consists of Rhino XR4 and SCARA Robot manipulators and a conveyor platform for robot to increase the freedom and flexibility of the robotic system. The XR4 is an educational robot having five axis articulated mechanical manipulator with an end effector or gripper. The robotic arm requires six motor drives for control and additional similar drives for actuating the moving conveyor robot platform and tilt rotator tables which necessitates auxiliary drive ports. The joint actuators are permanent magnet DC servomotors with inbuilt gear boxes and incremental optical encoders. The optical encoders mounted on the shaft of the drive motors result in high resolution position measurements. The shaft encoder pulses A and B (from Ch\_A and Ch\_B) are fed to the microcontroller to measure the position, speed and direction of rotation of the motor.

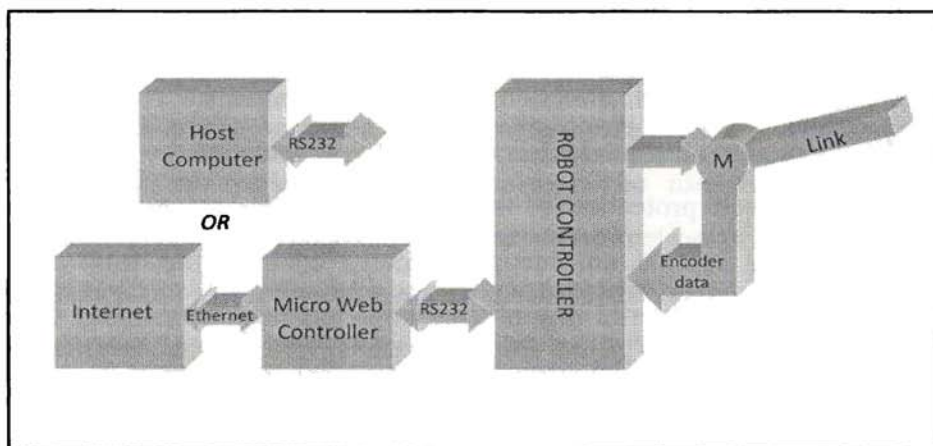


Figure A1.1 Functional diagram of the setup

Rhino SCARA robots are also equipped with the same types of servo motor drives having the same control interface. So the controller can be used with any one of the Rhino robots with appropriate configuration. The SCARA robot is a four axis servo controlled arm with an end effector or tool. The main characteristic of SCARA is its high precision, repeatability and speed. The basic SCARA geometry is a parallel structure and it incorporates one prismatic joint for vertical up and down movements.

### **A1.3 Robot Controller Design**

The robot controller uses PIC18F452 microcontroller, which can incorporate five link controllers. Each link controller consists of one direction control bit, one bit PWM signal and one bit brake signal. The link controller also uses two quadrature encoder inputs for finding the position, speed, direction of movement and stall condition of the link. The functional block diagram of the robot controller is shown in figure A1.2. It uses LMD18200 H-bridge driver IC from National Instruments [104] to drive and control the link actuator. The LMD18200 is a 3A H-bridge designed for motion control applications. It accommodates peak output currents up to 6A and operating supply voltages up to 55V. The chip is also having a thermal shutdown (outputs off) at 170°C which is very helpful in short circuit and overload conditions. The driver chip having a current sense output is not utilized in this design as one can easily identify the stall condition of the robot from the PWM status and the encoder inputs.

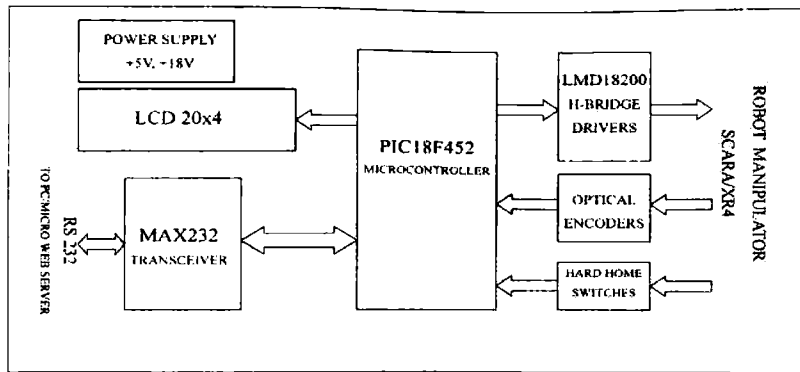
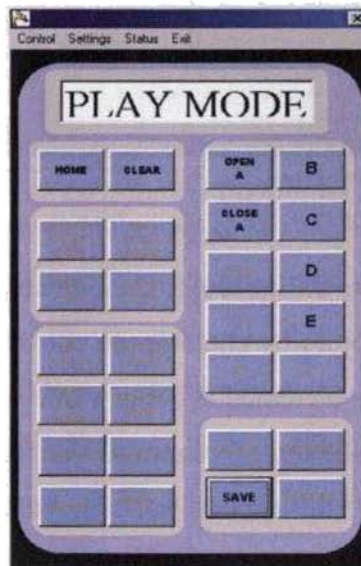


Figure A1.2. Block diagram of the robot controller

The optical incremental encoder attached to the motor shaft is capable of generating pulses A and B. The low level information provided in the form of two pulse trains A and B are  $90^{\circ}$  out of phase (quadrature) and depending on the direction of rotation, one of these pulses will lead or lag the other. From these signals the actual position, speed and acceleration information needed for the controller are computed. So a link control requires three output signals to control the motor and two input signals from the optical encoder and one input from a micro switch to sense the hard home position. The robot can achieve *hard home* position with the help of micro switch sensing. A 20x4 LCD module is interfaced for monitoring the control status of the robot arm. This will display the current position of the links and stall conditions if any. The control card is designed in such a way that if the system needs more than five control/auxiliary ports, an additional card can be stacked to incorporate more links/Aux ports. A serial communication link has been established using a MAX 232 level converter. The power supply requirements of the motors is +18V, 10A and that of the rest of the circuitry is +5V, 1A.

## A1.4 Control Program and User Interface

The user interface developed for the control program in the host computer is very flexible and modular and has three modes of operation. They are *play*, *online control* and *file/offline control*, which can be selected from the Control menu. From the Settings menu the *hard home* can be executed and the speed (PWM duty cycle) for the current step or program also can be set. The Status menu is helpful in monitoring the current motor count value and gripper status of the robot arm. The count values from the optical encoders are used for representing the position or angle of the link with respect to the reference or home position. The angle corresponding to the count value depends upon the number of pulses per revolution of the encoder and the gear ratio of the motor shaft. For a particular motor the number of pulses per revolution of the encoder and the gear ratio are constants, so the count value is a measure of the position or angle of the link.



*Figure A1.3 Screen shot in play mode*

In the play mode most of the teach pendant play mode functions of the Rhino Mark IV Controller are implemented. By using this GUI, all the motors can

be actuated individually and the movements can be saved by pressing the save button. The screen shot of the *play mode* GUI is shown in figure A1.3.

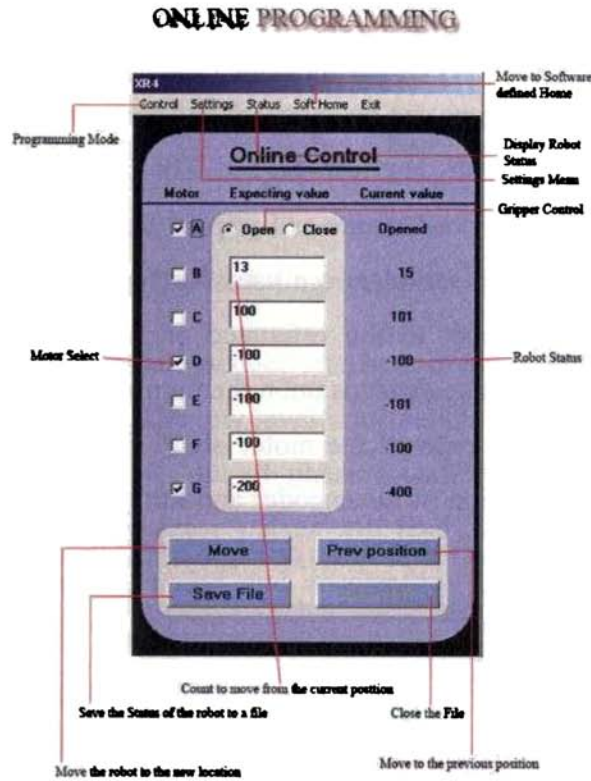
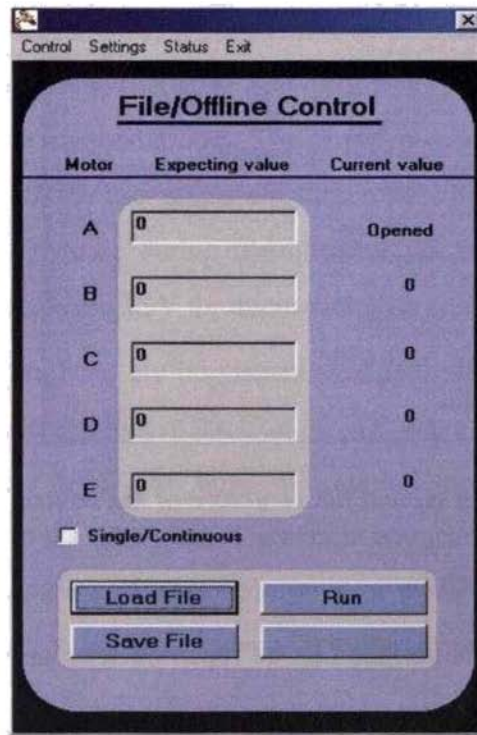


Figure A1.4 Details of the online control mode

Figure A1.4 shows the Online Control mode screen. In this mode the user can select the appropriate motors by clicking the corresponding check boxes. The operator write the destination incremental count value for the motors and pressing the move button key will guide the robot arm to the respective positions with the selected speed by displaying the current position values of each motors at the current value location of the GUI. By clicking the Save button the user can store these movement steps in a file. The advantage of this mode is that the user can fine turn the movements by feeding small count values and establishing up or down

movements by visualizing the robot arm actions. The previous position key is also very useful in developing the control program or teaching the robot.



*Figure A1.5 The GUI for the file/offline control mode*

The third mode is the file/offline control mode. In this mode the system can load a file containing several movements and other commands like PWM value, delay, home(hard home), soft home, switch sense etc. The program can be run by clicking the *run* button and editing is also possible with this mode. A single execution or repeated operation can be achieved by selecting the single/continuous check box. This mode is used for offline editing of the program as well as file execution of the robotic system. The GUI for this mode is shown in figure A1.5. The control file format is in plain ASCII text and the user can edit or merge the files using an editor like notepad. A typical file is shown in figure A1.6.

```

: SCARA robot control file 8/3/2007
4:25:38 PM
: MOTOR A, motor B, motor C, motor D, motor E
*****
home
0,0,-160,0,0.
0,0,0,300,400.
0,340,0,0,0.
1,0,0,200,700.
1,-570,0,0,0.
0,0,0,-200,-700.
0,570,0,0,0.
0,0,289,0,0.
1,0,0,0,0.
1,0,-289,0,0.
1,0,0,200,700.
1,-570,0,0,0.
1,0,349,0,0.
0,0,0,0,0.
delay 1000 -----time delay of 1sec.
0,0,-349,0,0.
0,0,0,-200,-700.
0,570,0,0,0.
0,0,349,0,0.
1,0,0,0,0.
1,0,-349,0,0.
1,0,0,200,700.
1,-570,0,0,0.
1,0,309,0,0.
0,0,0,0,0.
0,0,-309,0,0.
0,0,0,-200,-700.
0,570,0,0,0.
home

```

Figure A1.6 A typical file structure of the control program

## A1.5 Web Control Module

The dedicated PC interface can be replaced with any networked computer by using a web control module. This increases the flexibility of the system and the micro-web control/server module [159, 160] is designed around a PIC18F67J60 with inbuilt Ethernet peripheral module having 128k flash program memory, 8k Ethernet Tx/Rx buffer and more than 3k data memory [158].

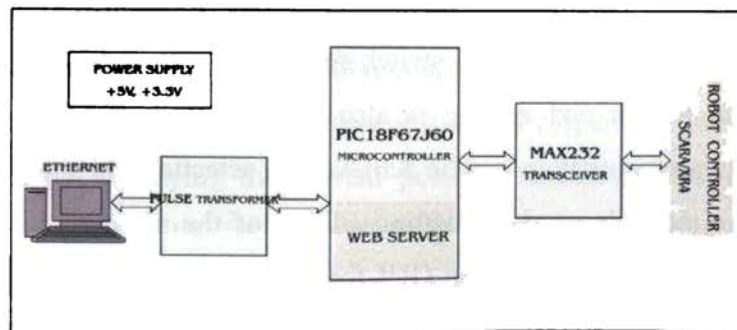


Figure A1.7 Block diagram of the Ethernet web control/server module

The functional block diagram of the system is shown in figure A1.7. The microcontroller is having all the features to implement the Ethernet interface. The only additional components required are the pulse transformer, associated resistors and capacitors. For establishing a communication link to the robot controller an RS232C interface is designed by using MAX232 level converter chip and the inbuilt serial peripheral module of the microcontroller. The program memory stores the code and web pages to interact with the user and control the robot arm. An IP number must be assigned to the control module during configuration of the system. Power supply requirements for the module are 3.3V for microcontroller and 5V for level converter.

All the control interfaces are implemented in web pages and is very similar to the dedicated GUI. The screen shot of the Control Web page for the file/offline control mode is shown in figure A1.8. The small web control/server module will generate appropriate commands to the controller. User login and password protections etc. are also implemented for security. The host computer or micro-web control module can send commands/parameters like *hard home*, position increments/decrement values, and duty ratio of PWM etc. to the robot controller.



Figure A1.8 The Control Web page for the file/offline control mode



## **A1.6 Exercises**

In order to learn the basics of robot manipulation and the fundamentals of robot motion the students must practice certain laboratory exercises like accuracy, precision and repeatability study, pick and place objects, manipulator characteristics study by learning the actuator response etc [155,157].

The motor A is used as gripper or hand actuator for the SCARA/XR4 robots. From the full gripper opening to closing the controller receives more than 50 pulse counts from the corresponding encoder. So the pulse count value can be used to sense whether the object or work piece is held by the gripper or not. If the gripper driver is actuated and the number of pulses received by the controller is less than that required for a close means that the object is held by the gripper. In practice by applying 5 to 10 percentage of PWM signal voltage, while the gripper holds the object, the tendency of the object to slip can be eliminated.

For the repeatability study the gripper holds a felt tipped pen above a drawing sheet on the work table. The robot is moved to draw arcs on the paper in such a way that we obtain multiple arc crossing points on the sheet. Then the arm is moved in a random fashion and the same movements are repeated to obtain another set of arc crossing point that may overlap the old points or slightly deviate from the earlier ones. The repeatability of the robotic system can be computed from the deviations by repeating the process.

To perform the pick and place exercise, students use a number of small wooden blocks of various sizes. The robot can be taught or programmed to pick and place the objects in the desired way. Executing the same program by changing the speed, students can learn the speed and acceleration problems associated with the arm. Trapezoidal and triangular velocity schemes can be studied. Analog control schemes like PID or PI can be implemented by properly setting the

parameters like delays, PWM values and increment counts for the respective motors. The photograph in figure A1.9 shows the finished view and inside view of the controller and a typical workcell.

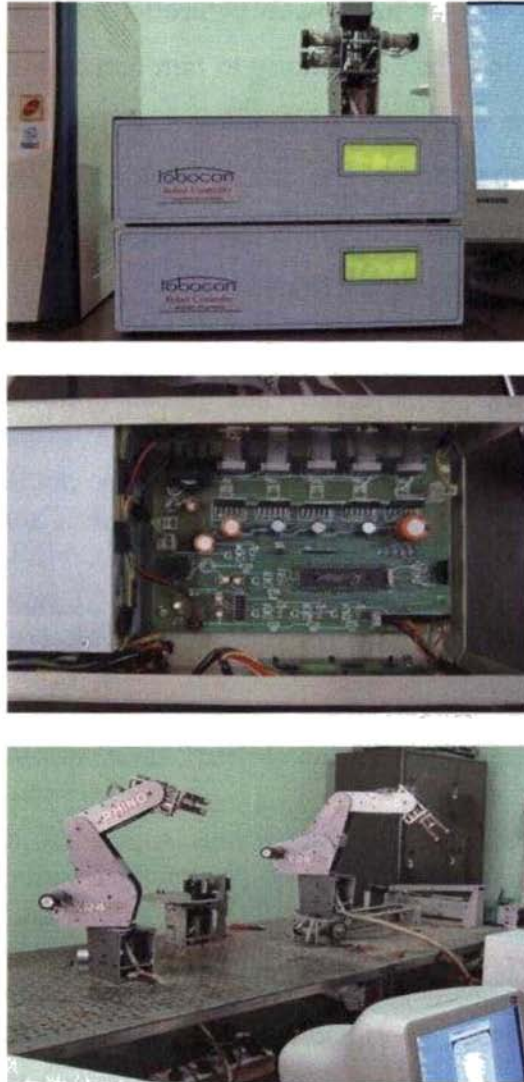


*Figure A1.9 Photographs of the finished view and inside view of the controller and a typical workcell*

## **A1.7 Summary**

The robot controller presented in this annexure replaces the existing XR4/SCARA robot controller from Rhino Robots Inc, USA and is capable of operating from a computer or micro-web controller system through Internet or Intranet. This setup is ideal for a laboratory to familiarize with the various control schemes and techniques associated with robotics. Solving the inverse kinematic equations and finding the pose of the arm is difficult to implement in the web control scheme. But in PC based controller approach, one can easily utilize the high level tools like Matlab for solving the same.

## REFERENCES

- [1] Siegel, M., Gunatilake, P., “Remote Inspection Technologies for Aircraft Skin Inspection”, IEEE Workshop on Emergent Technologies and Virtual Systems for Instrumentation and Measurement, Ontario, Canada, May 1997.
- [2] Prassler, E., Ritter, A., Schaeffer, C., Fiorini, P., “A Short History of Cleaning Robots”, *Autonomous Robots*, Special Issue on Cleaning and Housekeeping Robots, Vol. 9, Issue 3, December 2000.
- [3] Iborra, A., Pastor, J., Alvarez, B., Fernandez, C., Merono, J., “Robots in Radioactive Environments”, *IEEE Robotics and Automation Magazine*, December 2003.
- [4] Anthony Stentz, John Bares, Sanjiv Singh and Patrick Rowe, “A Robotic Excavator for Autonomous Truck Loadin”, *Autonomous Robots* 7, pp 175–186, 1999.
- [5] Rossetti, M. D., Kumar, A. and Felder, R., “Mobile Robot Simulation of Clinical Laboratory Deliveries”, *Proceedings of the Winter Simulation Conference*, 1998.
- [6] Montemerlo M, Pineau J, Roy N, Thrun S and Verma V, “Experiences with a Mobile Robotic Guide for the Elderly”, *Proceedings of the AAAI National Conference on Artificial Intelligence*, Edmonton, Canada, 2002.
- [7] R. Bahl. Object Classification using Compact Sector Scanning Sonars in Turbid Waters, *Proceedings of the 2nd IARP Mobile Robots for Subsea Environments*, Monterey, CA, volume 23, pages 303–327, 1990.
- [8] Anthony J. Healey, Application of Formation Control for Multi-Vehicle Robotic Minesweeping, *Proceedings of the IEEE CDC Conference*, 2001.

- [9] Everett, H.R., Gage, D.W., From Laboratory to Warehouse: Security Robots Meet the Real World, *International Journal of Robotics Research*, Special Issue on Field and Service Robotics, Vol. 18, No. 7, July 1999.
- [10] Pastore, T.H., Everett, H. R., and Bonner, K., *Mobile Robots for Outdoor Security Applications, American Nuclear Society 8th International Topical Meeting on Robotics and Remote Systems (ANS'99)*, Pittsburgh, PA, April 1999.
- [11] J. Borenstein, H. R. Everett, L. Feng, and D. Wehe “Mobile robot positioning sensors and techniques”, *Journal of Robotic Systems; Special Issue on Mobile Robots*, 14(4):231–249, 1997.
- [12] Lindsay Kleeman, “ Optimal Estimation of position and Heading for Mobile Robots Using Ultrasonic Beacons and Dead-reckoning”, *Proceedings of the IEEE International Conference on Robotics and Automation*, Nice, France, 1992.
- [13] J. J. Leonard and H. F. Durrant-Whyte. “Mobile Robot Localization by Tracking Geometric Beacons”. *IEEE Transactions on Robotics and Automation*, 7(3), pp. 376–382, 1991.
- [14] O. Wijk, H.I. Christensen, “Localization and navigation of a mobile robot using natural point landmarks extracted from sonar data” *Robotics and Autonomous Systems* 31, 31–42, 2000.
- [15] M. L ‘Opez-s’ Anchez, F. Esteva, R. L ‘Opez De M’ Antars and C. Silerra, “Map Generation by Cooperative Low-Cost Robots in Structured Unknown Environments”, *Autonomous Robots* 5, 53–61, 1998.
- [16] Salah Sukkarieh, Eduardo M. Nebot, and Hugh F. Durrant-Whyte, “A High Integrity IMU/GPS Navigation Loop for Autonomous Land Vehicle Applications”, *IEEE Transactions on Robotics and Automation*, VOL. 15, NO. 3, pp 572-578, 1999.
- [17] J. Borenstein and L. Feng. “Measurement and Correction of Systematic Odometry Errors in Mobile Robots”. *IEEE Transactions on Robotics and Automation*, 12(6), pp. 869–880, 1996.
- [18] B. Barshan and H. F. Durrant-Whyte. “Inertial Navigation Systems for Mobile Robots,” *IEEE Transactions on Robotics and Automation*, 11(3), pp. 328–342, 1995.
- [19] Sooyong Lee and Jae-Bok Song. “Robust Mobile Robot Localization using Optical Flow Sensors and Encoders”. *Proc. of the IEEE Int. Conf. on Robotics & Automation*, pp.1039-1044, April 2004.

- [20] J. J. Leonard, H. F. Durrant-Whyte, and I. J. Cox, "Dynamic map building for an autonomous mobile robot," *Int. J. Robotic Research*, vol. 11, No. 4, pp. 286–298, 1992.
- [21] A.H. Mishkin, J.C. Morrison, T.T. Nguyen, H.W. Stone, B.K. Cooper, and B.H. Wilcox, "Experiences with operations and autonomy of the mars pathfinder microrover", *Proceedings of IEEE Aerospace Conference*, volume 2, pp. 337–351. IEEE, 1998.
- [22] L. Whitcomb, D. Yoerger, H. Singh, and J. Howland, "Advances in underwater robot vehicles for deep ocean exploration: Navigation, control and survey operations", *The Ninth International Symposium on Robotics Research*, pages 346–353, 1999.
- [23] Ingemar j. cox "Balache-An Experiment in Guidance and Navigation of an Autonomous Robot vehicle", *IEEE Transactions on Robotics and Automation*, Vol.7, No. 2, pp 193-204, 1991.
- [24] Winton, P. and E. Hammerle (2000). "High resolution position estimation using partial pulses." *IEE, Electronics Letters*, 36(10), pp. 897-898, 2000.
- [25] Kai Lingemann, Andreas N"uchter, Joachim Hertzberg, Hartmut Surmann, "High-speed laser localization for mobile robots", *Robotics and Autonomous Systems* 51, pp 275–296. 2005.
- [26] P. Hoppenot, E.Colle and C. Barat. "Off line localization of a mobile robot using ultrasonic measures." *Robotica*, 18, pp. 315–323, 2000.
- [27] Youngjoon Han, Hernsoo Hahn, "Localization and classification of target surfaces using two pairs of ultrasonic sensors", *Robotics and Autonomous Systems* 33, 31–41, 2000.
- [28] F. Thomas and L. Ros. "Revisiting trilateration for Robot Localization." *IEEE Transactions on Robotics*, 21(1), pp. 93 - 101, 2005.
- [29] <http://www.evolution.com/products/>
- [30] <http://www.fujitsu.com/global/news/pr/archives/month/2005/20050913-01.html>
- [31] <http://asimo.honda.com>
- [32] R. Siegwart and I. R. Nourbakhsh, "Introduction to Autonomous Mobile Robots", Massachusetts Institute of Technology, 2004.
- [33] RD Instruments, "Workhorse Navigator Data Sheet "California, USA, <http://www.rdinstruments.com/products.html>.
- [34] Mohinder S. Grewal, Lawrence R. Weill, Angus P. Andrews, "Global Positioning systems, Inertial Navigation, and Integration", John Wiley & Sons, Inc. 2001.

- [35] P. H. Milne. *Underwater Acoustic Positioning Systems*. E and F N Spon Ltd, 1983.
- [36] Chenavier, F. and Crowley, J., 1992, "Position Estimation for a Mobile Robot Using Vision and Odometry." *Proceedings of IEEE International Conference on Robotics and Automation*, Nice, France, May 12-14, pp. 2588-2593.
- [37] Henkel S.L., "Optical Encoders: A Review." *Sensors*, September, pp. 9-12, 1987.
- [38] Jones, J. L. and Flynn, A., *Mobile Robots: Inspiration to Implementation*, A K Peters, Ltd. Wellesley, MA, 1993.
- [39] J. Borenstein, H. R. Everett, and L. Feng, "Where am I? Sensors and Methods for Mobile Robot Positioning", Chapter 3, The University of Michigan, April 1996.
- [40] Thomas Stork, "Electronic Compass Design using KMZ51 and KMZ52", Application Note: AN00022, Philips Semiconductors, Systems Laboratory Hamburg, Germany, 2000. [N10]
- [41] Data sheet "Sparton Digital Compass", <http://www.thedigitalcompass.com>
- [42] Barshan, B. and Durrant-Whyte, H.F., 1993, "An Inertial Navigation System for a Mobile Robot" *Proceedings of the 1993 IEEE/RSJ International Conference on Intelligent Robotics and Systems*, Yokohama, Japan, July 26-30, pp. 2243-2248.
- [43] Everett, H. R., 1995, *Sensors for Mobile Robots: Theory and Application*, A K Peters, Ltd., Wellesley, MA.
- [44] E. M Nebot, "sensors Used for Autonomous Navigation", Chapter 7, "Advances in Intelligent Autonomous Systems", Edited by Spyros G. Tzafestas, Kluwer, 2000.
- [45] S. F. Appleyard, R. S. Linford and P.J. Yarwood, "Marine Electronic Navigation", Routledge & Kegan Paul, 1997.
- [46] <http://en.wikipedia.org/wiki/Gyroscope>
- [47] V. Apostolyuk "Theory and design of micromechanical vibratory gyroscopes", MEMS/NEMS Handbook, Springer, 2006, Vol.1, pp.173-195.
- [48] John Geen and David Krakauer, "New iMEMS Angular Rate-Sensing Gyroscope", *Analog Dialogue* 37-03, 2003.
- [49] Data Sheet, "Programmable Low Power Gyroscope ADIS16251", 2007 Analog Devices, Inc. [www.analog.com](http://www.analog.com)

- 
- [50] E.N. Macleod and M. Chiarella, "Navigation and control breakthrough for automation technology", In *Proceedings of SPIE - The International Society for Optical Engineering*, pages 57-68, Boston, 1993.
- [51] M.I. Skolnik. *Introduction to Radar Systems*, McGraw-Hill, New York, 1980.
- [52] R.E. Kalman, "A new approach to linear filtering and prediction problems" *Transactions of the ASME Journal of Basic Engineering*, pages 35-45, March 1960.
- [53] R.E. Kalman and R.S. Bucy, "New results in linear filtering and prediction theory" *Transactions of the ASME Journal of Basic Engineering*, pages 95-108, March 1961.
- [54] P.S. Maybeck. *Stochastic Models, Estimation, and Control*, volume 1. Academic Press, 1979.
- [55] J.O. Berger. *Statistical Decision Theory and Bayesian Analysis*. Springer-Verlag, 1985.
- [56] Cohen, C. and Koss, F., "A Comprehensive Study of Three Object Triangulation." *Proceedings of the 1993 SPIE Conference on Mobile Robots*, Boston, MA, Nov. 18-20, pp. 95-106, 1992.
- [57] S.C. Crow and F.L. Manning. Differential GPS control of starcar 2. *Navigation: Journal of the Institute of Navigation*, 39(4):383-405, Winter 1992-93.
- [58] H. Evers and G. Kasties. Differential GPS in a real-time land vehicle environment – satellite based van carrier location system. *IEEE Aerospace and Electrical Systems Magazine*, 9(8):26-32, August 1994.
- [59] Getting, I. A., 1993, "The Global Positioning System," *IEE Spectrum*, December, pp. 36-47.
- [60] Hurn, J., 1993, *GPS, A Guide to the Next Utility*, No. 16778, Trimble Navigation, Sunnyvale, CA.
- [61] Ellowitz, H.I., 1992, "The Global Positioning System." *Microwave Journal*, April, pp. 24-33.
- [62] Hadaru Data Sheet "GPS Engine Module HPM103H-6 GPS Receiver rev.1.10", 2005.
- [63] Sure Electronics "GPS Demo Board User's Guide", [www.sure-electronics.net](http://www.sure-electronics.net)
- [64] Heale, A., Kleeman, L.: "A Real Time DSP Sonar Echo Processor," *Proceedings of the IEEE/RSJ International Conference on Intelligent Robots and Systems (IROS'00)*, Japan, October 31–November 5, 2000.



- [65] P. P. Smith. *Active Sensors for Local Planning in Mobile Robotics*, volume 26. World Scientific, Singapore, 2001.
- [66] <http://www.hokuyo-aut.jp/02sensor/07scanner/ubg.html>
- [67] M. I. Skolnik. *Radar Handbook*. 2 edition, McGraw-Hill, 1990.
- [68] L. Matthies, A. Kelly, and T. Litwin. Obstacle Detection for Unmanned Ground Vehicles: A Progress Report. *Seventh International Symposium of Robotics Research*, 1995.
- [69] P. Bhartia and I. J. Bahl. *Millimeter Wave Engineering and Applications*, John Wiley and Sons, 1984.
- [70] S. Scheduling, G. Brooker, M. Bishop, R. Hennessy, and A. Maclean. Terrain imaging millimetre wave radar. In *International Conference on Control, Automation, Robotics and Vision*, Singapore, November 2002.
- [71] Shuzhi Sam Ge and Frank L. Lewis, “*Autonomous Mobile Robots Sensing, Control, Decision Making and Applications*”, Taylor & Francis, 2006.
- [72] Shinichi Yamano *etal*. “76GHz Millimeter Wave Automobile Radar using Single Chip MMIC” *Fujitsu Ten Technichal Journal*, No.23(2004).
- [73] Critchlow, A.J., *Introduction to Robotics*, Macmillan Publishing Co., New York, 1985.
- [74] K. S. Fu, R. C. Gonzalez, and C. S. G. Lee, *Robotics- Control, Sensing, Vision and Intelligence*, McGraw-Hill, 1987.
- [75] C. Jennings and D. Murray. Stereo Vision Based Mapping and Navigation for Mobile Robots. In *Proceedings of the IEEE International Conference on Robotics and Automation*, pages 1694–1699. 1997.
- [76] Hager, G. and Atiya, S., 1993, “Real-Time Vision-Based Robot Localization.” *IEEE Transaction on Robotics and Automation*, vol. 9, no. 6, pp. 785-800.
- [77] Talluri, R., and Aggarwal, J., 1993, “Position Estimation Techniques for an Autonomous Mobile Robot - a Review.” in *Handbook of Pattern Recognition and Computer Vision*, World Scientific: Singapore, Chapter 4.4, pp. 769-801.
- [78] Hoppen, P., Knieriemen, T., and Puttkamer, E., 1990, “Laser-Radar Based Mapping and Navigation for an Autonomous Mobile Robot.” *Proceedings of IEEE International Conference on Robotics and Automation*, Cincinnati, OH, May 13-18, pp. 948-953.
- [79] Crowley, J., 1989, “World Modeling and Position Estimation for a Mobile Robot Using Ultrasonic Ranging.” *Proceedings of IEEE International*

- Conference on Robotics and Automation*, Scottsdale, AZ, May 14-19, pp. 674-680.
- [80] Buchberger, M., Jörg, K., and Puttkamer, E., 1993, "Laser radar and Sonar Based World Modeling and Motion Control for Fast Obstacle Avoidance of the Autonomous Mobile Robot MOBOT-IV." *Proceedings of IEEE International Conference on Robotics and Automation*, Atlanta, GA, May 10-15, pp. 534-540.
- [81] Courtney, J. and Jain, A., 1994, "Mobile Robot Localization via Classification of Multisensor Maps." *Proceedings of IEEE International Conference on Robotics and Automation*, San Diego, CA, May 8-13, pp. 1672-1678.
- [82] R. Smith, M. Self, and P. Cheeseman, "Estimating uncertain spatial relationships in robotics," in *Autonomous Robot Vehicles*, I.J. Cox and G.T. Wilfon, Eds, New York: Springer Verlag, 1990, pp. 167-193.
- [83] P. Moutarlier and R. Chatlia, "Stochastic multisensor data fusion for mobile robot localization and environment modeling," in *Int. Symp. Robot. Res.*, 1989, pp. 85-94.
- [84] J. Leonard and H. Durrant-Whyte, *Directed Sonar Sensing for Mobile Robot Navigation*. Boston, MA: Kluwer Academic, 1992.
- [85] M. W. M. Gamini Dissanayake, Paul Newman, Steven Clark, Hugh F. Durrant-Whyte, and M. Csorba "A Solution to the Simultaneous Localization and Map Building (SLAM) Problem" *IEEE Transactions on Robotics and Automation*, Vol. 17, No. 3, June 2001.
- [86] Graham Brooker, Mark Bishop, and Steve Scheduling. Millimetre waves for robotics. In *Australian Conference for Robotics and Automation*, Sydney, Australia, November 2001.
- [87] J. J. Leonard and H. J. S. Feder, "A computationally efficient method for large-scale concurrent mapping and localization," in *Proceedings IEEE Int. Symposium on Robotics Research*, 2000, pp. 169-176.
- [88] S. Thrun, "Robotic mapping: A survey," in *Exploring Artificial Intelligence in the New Millenium*, G. Lakemeyer and B. Nebel, Eds. Morgan Kaufmann, 2002.
- [89] A. Dunkin, "Automated guided vehicle systems: An introduction", *Industrial Engineering*, 26:47-53, August 1994.
- [90] T. Tsumura, "Survey of automated guided vehicle in Japanese factory", *IEEE International Conference on Robotics and Automation*, pages 1329-1334, 1986.

- [91] G. Giralt, R. Sobek, and R. Chatila. A multi-level planning and navigation system for a mobile robot: A first approach to Hilare. In *Sixth International Joint Conference on Robotics and Automation*, 1979.
- [92] M. Brady, S. Cameron, H. Durrant-Whyte, M. Fleck, D. Forsyth, A. Noble, and I. Page, "Progress towards a system that can acquire pallets and clean warehouses", *Fourth International Symposium of Robotics Research*, pages 359–374, 1987.
- [93] H.F. Durrant-Whyte. An autonomous guided vehicle for cargo handling applications. *International Journal of Robotics Research*, 15, 1996.
- [94] Datasheet "PIC12F675", <http://www.microchip.com>
- [95] Datasheet "TSOP1740", <http://www.Vishay.com>
- [96] Datasheet "GPIU58Y", <http://sharp-world.com/products/device/>
- [97] Datasheet "PIC16F630/676", <http://www.microchip.com>
- [98] Datasheet "MAX485", <http://www.maxim-ic.com>
- [99] Datasheet "PIC18F2550/4550", <http://www.microchip.com>
- [100] Datasheet "CYWUSB6935 Wireless USB LR 2.4-GHz DSSS Radio SoC, 2005", *Cypress Semiconductor Corporation*, <http://www.cypress.com>.
- [101] R. Peterson, R. Ziemer, D. Borth, *Introduction to Spread Spectrum Communication*, Prentice Hall, 1995.
- [102] Don Anderson, "*USB System Architecture (USB 2.0)*" Addison-Wesley Developer's Press, 2001.
- [103] John Hyde, "USB Design by Example - A Practical Guide to Building IO Devices", Intel University press, 2000.
- [104] Datasheet "H-bridge: LMD1800", *National Semiconductor Corporation*, [www.national.com/pf/LM/LMD18200.html](http://www.national.com/pf/LM/LMD18200.html), 2005.
- [105] Mariolino De Cecco, "Sensor fusion of inertial-odometric navigation as a function of the actual manoeuvres of autonomous guided vehicles", *IOP Measurement Science and Technology* **14**, 643-653, 2003.
- [106] M. Faccio, et al., "An embedded system for position and speed measurement adopting incremental encoders", *Proc. of the IEEE Ind. Appl. Conf.2* 1192–1199, 2004.
- [107] Ndubuisi Ekekwea, Ralph Etienne-Cummingsa and Peter Kazanzidesb, "A wide speed range and high precision position and velocity measurements chip with serial peripheral interface", *ELS. INTEGRATION, the VLSI journal* 41 297–305, 2008.

- [108] Bernard Hebert, Michel Brule, and Louis-A. Dessaint, "A High Efficiency Interface for a Biphase Incremental Encoder with Error Detection", *IEEE Transactions on Industrial Electronics*, Vol. 40, 1, 155-156, 1993.
- [109] Lauro Ojeda and Johann Borenstein, "Reduction of Odometry Errors in Over-constrained Mobile Robots" *Proceedings of the UGV Technology Conference SPIE AeroSense Symposium*, 2003.
- [110] Altera Corporation, "Cyclone II DSP Development Board Reference Manual", 101 Innovation Drive, San Jose, CA 95134, USA. <http://www.altera.com>
- [111] J. Volder, "The CORDIC Trigonometric Computing Technique," *IRE Trans Electronic Computing*, Vol. EC-8, pp330-334, Sept. 1959.
- [112] R. Andraka, "A survey of CORDIC algorithms for FPGA based computers," *Proceedings of the 1998 ACM/SIGDA sixth international symposium on Field Programmable Gate Arrays*, pp191-200, Feb. 22-24, 1998.
- [113] J. N. Lygouras. Memory reduction in look-up tables for fast symmetric function generators. *IEEE Transactions on Instrumentation and Measurement*, 48(6):1254–1258, Dec. 1999.
- [114] Jean Duprat and Jean-Michel Muller, "The CORDIC Algorithm: New Results for Fast VLSI Implementation", *IEEE Transactions on Computers*, Vol. 42, No. 2, pp.168-178, February 1993.
- [115] Herbert Dawid, and Heinrich Meyr, "The Differential CORDIC Algorithm: Constant Scale Factor Redundant Implementation without Correcting Iterations", *IEEE Transactions On Computers*, Vol. 45, No. 3, pp. 307-318, March 1996.
- [116] B. Parhami, "On the Implementation of Arithmetic Support Functions for Generalized Signed-Digit Number Systems," *IEEE Transactions on Computers*, vol. 42, no. 3, pp. 379-384, Mar. 1993.
- [117] J. Lee and T. Lang, "Constant-Factor Redundant CORDIC for Angle Calculation and Rotation," *IEEE Transactions on Computers*, vol. 41, no. 8, pp. 1,016-1,035, Aug. 1992.
- [118] J. Valls, M. Kuhlmann, and K. K. Parhi. "Evaluation of CORDIC algorithms for FPGA design". *Journal of VLSI Signal Processing*, vol. 32, no. 3, pp. 207-222, 2002.
- [119] S.W. Alexander, E. Pfann, R.W. Stewart, "An Improved Algorithm For Assessing The Overall Quantisation Error In FPGA Based CORDIC Systems Computing A Vector Magnitude", *Microprocessors and*

- Microsystems Special Issue on FPGA-based Reconfigurable Computing*, Jan 2007.
- [120] L. Wanhammar, K. Johansson, and O. Gustafsson, "Efficient Sine and Cosine Computation Using a Weighted Sum of Bit-Products", *ECCTD 2005 - European Conference on Circuit Theory and Design*, Cork Ireland, 29 August - 2 September 2005.
- [121] Altera Corporation, "Implementation of CORDIC-Based QRD-RLS Algorithm on Altera Stratix FPGA With Embedded Nios Soft Processor Technology", [www.altera.com](http://www.altera.com), 2004.
- [122] Peter R. Wilson, "*Design Recipes for FPGAs*", Newnes – Elsevier, 2007.
- [123] Z. Navabi, "*Digital Design and Implementation with Field Programmable Devices – Featuring Altera and Menter Graphics Verilog Simulation and Synthesis Tools*", Kluwer Academic Publishers, 2005.
- [124] Douglas L. Perry, "*VHDL: Programming by Example*", McGraw-Hill, 2002.
- [125] Jean-Pierre Deschamps, Gery Jean Antoine Bioul, Gustavo D. Sutter, "*Synthesis of arithmetic circuits: FPGA, ASIC and embedded systems*", John Wiley & Sons, Inc. 2006.
- [126] Steve Kilts, "*Advanced FPGA Design Architecture, Implementation and Optimization*" John Wiley & Sons, Inc. 2007.
- [127] David H. Roper, Goro Endo, "Advanced Traffic Management in California", *IEEE Transactions on Vehicular Technology*, Vol. 40, No. 1, February 1991.
- [128] Ken-ichi Aoyama, "Universal traffic System (UTMS) Management in Japan", *IEEE Vehicle Navigation & Information Systems Conference Recedngs*, 1994.
- [129] Joseph K. Lam, Jim Kerr, "Development of Compass - An Advanced Traffic Management System", *IEEE-IEE Vehicle Navigation & Information Systems Conference procedngs*, 1993.
- [130] John Murray, Yili Liu, "Hortatory Operations in Highway Traffic Management", *IEEE Transactions on systems, man, and cybernetics—part a: systems and humans*, Vol. 27, No. 3, May 1997.
- [131] John F. Gilmore, Khalid J. Elibiary, "Harold Forbes, Intelligent Control in Traffic Management", *IEEE Vehicle Navigation & Information Systems Conference procedngs*, 1994.
- [132] D. Bowen Tritter, John Zietlow, "Designing a Traffic Management Communication System to Accommodate Intelligent Vehicle Highway

- Systems”, *IEEE-IEE Vehicle Navigation & Information Systems Conference procedngs*, 1993.
- [133] B. G. Heydecker, “Objectives, Stimulus and Feedback in Signal Control of Road Traffic”, *Journal of Intelligent Transportation Systems*, 8:63–76, 2004.
- [134] M. F. Medeiros, “Advanced Traffic Management System Automation”, *Proceedings of the IEEE*, Vol. 77, No. 11, November, 1989.
- [135] C. Collier and R. Weiland, “Smart cars, smart highways,” *IEEE Spectrum*, vol. 31, no. 4, Apr. 1994.
- [136] M. Sugimoto, K. Aoyama, A. Kongoh, “Improvement of Traffic Control System by means of Infrared Beacon Two-way Communication”, *Proceedings of the IEEE Intelligent Transportation Systems Conference*, Dearborn (MI), USA October 1-3, 2000.
- [137] H. Kazama, A. Hokazono, K. Goshima and T. Tajima, “Field Experiment With Logistics Mobile Operation Control Systems Using Infrared Beacons”, *Proceedings of the IEEE Intelligent Transportation Systems Conference*, Dearborn (MI), USA October 1-3, 2000.
- [138] Benjamin J. M, Ali N. A and Schepis A. F, “A Laser cane for the blind”, *Proceedings of San Diego Medical Symposium*, 1973.
- [139] Bissitt D and Heyes A, “An application of biofeedback in the rehabilitation of the blind”, *Applied Ergonomics* **11(1)** 31–33, 1980.
- [140] Shoal S, Borenstein J and Koren Y, “In Mobile robot obstacle avoidance in a computerized travel for the blind”, *IEEE Transactions on Biomedical Engineering*, **45(11)**, 1998.
- [141] Vladimir Kulyukin, Chaitanya Gharpure, John Nicholson and Grayson Osborne, “Robot-assisted wayfinding for the visually impaired in structured indoor environments”, *Autonomous Robot*, **21** 29–41, 2006.
- [142] Morgen E Peck, “RFID Tags Guide the Blind”, *IEEE spectrum magazine*, January, 2008.
- [143] Mori H and Kotani S, “Robotic travel aid for the blind: HARUNOBU-6”, *Second European Conference on Disability, Virtual Reality, and Assistive Technology*, Sweden, 1998.
- [144] J. A. Brabin, “New developments in mobility and orientation aids for the blind,” *IEEE Transactions on Biomedical. Engineering*, vol.29, pp. 285–290, April, 1982.

- [145] T. Harada, Y. Kaneko, Y. Hirahara, K. Yanashima, K. Magatani, "Development of the navigation system for visually impaired", *Proceedings of the 26th Annual International Conference of the IEEE EMBS*, San Francisco, CA, USA. September 1-5, 2004.
- [146] D. Kavradi and N. Bourbakis, "Intelligent assistants for disable peoples' independence: A case study," *Proceedings of IEEE Symposium on Intelligent Systems*, Baltimore, MD, pp. 337-344, Nov. 1996.
- [147] N. Bourbakis, "Sensing Surrounding 3D Space for Navigation of the Blind", *IEEE Engineering In Medicine And Biology Magazine*, pp. 49-55, January/February, 2008.
- [148] Datasheet, "ChipCorder Voice Record and Playback IC", <http://www.winbond-usa.com>.
- [149] Mark Samuels, "PIC a Compact Flash Card", *CIRCUIT CELLAR*, February, 2001.
- [150] Marnix Nuttina and Victor Claesb, "Design and development of a new sensor system for assistive powered wheelchairs", *IOS Press, Journal of Technology and Disability* **19**, pp. 7-15, 2007.
- [151] Giulio E. Lancionia, Mark F. O'Reillyb, Nirbhay N. Singhc, Jeff Sigafosd, Doretta Olivae, Sandro Bracalente and Gianluigi Montironie, "Orientation systems to support indoor travel by persons with multiple disabilities: Technical aspects and applicability issues", *IOS Press, Journal of Technology and Disability* **19**, pp. 1-6, 2007.
- [152] M. Kabuka, P. Glaskowsky and J. Miranda, "Microcontroller-based Architecture for Control of a Six Joints Robot Arm," *IEEE Trans. on Industrial Electronics*, vol. 35, no. 2, 1988, pp.217-221.
- [153] G. Yasuda, "Microcontroller Implementation for Distributed Motion Control of Mobile Robots," *Proceeding of International workshop on Advanced Motion Control*, 2000, pp. 114-119.
- [154] *Rhino XR-4 Series Service Manuals*, Rhino Robots, Inc., 308 South State Street, Champaign, IL 61820 USA.
- [155] Schilling, R., J., "*Fundamentals of Robotics: Analysis and Control*", Prentice Hall, New Jersey, USA, 1990.
- [156] Mrad, F., T., "Extending the utility of the Rhino Educational Robot", *IEEE Transactions on Education*, vol. 40, no. 3, pp. 184-189, Jun.1997.
- [157] Krotkov, E., "Robotics Laboratory Exercises", *IEEE Transactions on Education*, vol.39, no. 1, pp. 94-97, Feb. 1996.

- [158] Datasheet “PIC18F67J60”, <http://www.microchip.com>
- [159] Nilesh Rajbharti, “*The Microchip TCP/IP Stack -AN833*”, Microchip Technology Inc.USA, 2002.
- [160] Jan Axelson, “*Embedded Ethernet and Internet Complete Designing and Programming Small Devices for Networking*“, Lakeview Research LLC, 2003.



# LIST OF PUBLICATIONS

## List of Publications in the area of Doctoral Work

- 1 James Kurian and P.R. Saseendran pillai “An Infrared Sheet of Light Beacon Based Intelligent Traffic and Transport Control system”, *International Review of Automatic Control (I.R.A.CO.)*, Vol.1, No.2, July 2008.
- 2 James Kurian and P.R. Saseendran pillai “Design and Realization of a Web Based Controller for Laboratory Robot Manipulator”, *Proceedings of the National Conference on Machine Intelligence (NCMI-2008 )* Jagadhri, INDIA, PP141-145, August 2008.
- 3 James Kurian and P.R. Saseendran pillai “An FPGA Sub System for Terrain Irregularity Corrections by Reducing Odomrtric Localization Errors in Wheeled Mobile Robots”, *Proceedings of the National Conference on Machine Intelligence (NCMI-2008 )* Jagadhri, INDIA, PP285-293, August 2008.
- 4 James Kurian and P.R. Saseendran pillai “An Encoded Infrared Sheet of Light Beacon System for Precise Localization of Indoor Mobile Robot Vehicles”, *Communicated to: Journal of Automation, Mobile Robotics and Intelligent Systems*
- 5 James Kurian and P.R. Saseendran pillai “ A DISLiB based Natural Language Guiding System for Assisting Visually Impaired in Indoor Structured Environment”, *Communicated to: IOS Press, Journal of Technology and Disability* .
- 6 James Kurian and P.R. Saseendran pillai “Realization of an FPGA Sub System for Reducing Odomrtric Localization Errors in Wheeled Mobile Robots”, ”, *Communicated to: International Review of Automatic Control* .

## Other Publications

- 1 James Kurian, K.A. Jose, K. G. Balakrishnan, and K.G. Nair, Nair, "Microwave Non-Destructive Flaw/Defect Detection System for Non-Metallic Media Supported by Microprocessor Based Instrumentation" *International Journal of Microwave Power and Electromagnetic Energy*. Vol.24 No.2, 1989, pp. 74-78.
- 2 P. Ramakrishnan, James Kurian and K.G Balakrishnan "Dynamic Characteristic And Transmission Studies of Ferroelectric Liquid Crystal: 4'(n-Octyl benzoxy)-4-(2-Octyloxy)-biphenyl , *FERROELECTRICS*, Vol.113, 1991, pp.395-403.
- 3 James Kurian, K.G. Balakrishnan, and K.G. Nair "A Simple Regulated Power Supply for Characteristics Studies of Klystron Oscillators" *Journal of Physics E: Meas. Sci.Technol.* Vol.3 (1992) pp-1146-1148.
- 4 James Kurian, K.A. Jose, K. G. Balakrishnan, and K.G. Nair, "Microwave Non-Destructive Flaw/Defect Detection System for Non-Metallic Media Supported by Microprocessor Based Instrumentation" *Indian RUBBER & PLASTICS AGE*, Vol. 27 No.4, April, 1991, pp.43-48.
- 5 James Kurian and K.G Balakrishnan "Under/Over Voltage Protection Circuit With Delay", *Electronics For You*, May 1989, pp 97-98.
- 6 Mariamma Chacko, James Kurian, P.R.S. Pillai, and Paulose Jacob, "An onboard operation support Information system and data logger for sea going vessels with an Ethernet interface", *Journal of Shiptechnic Vol XVIII*, 2002 pp 85 – 94.
- 7 James Kurian P. Ramakrishnan and K.G Balakrishnan "Microprocessor Interfaced Noiseless Heater Power Controller" *National Symposium on Instrumentation (NSU-13)*, Mysore 25-28, Nov. 1988.
- 8 James Kurian, K.A. Jose, K. G. Balakrishnan, and K.G. Nair, "An Instrumentation for Flaw / Defect Detection in Tyres" *National Symposium on Instrumentation (NSU-13)*, Mysore 25-28, Nov. 1988.
- 9 James Kurian, K.A. Jose, K. G. Balakrishnan, and K.G. Nair, "Microprocessor Based Microwave Non- Destructive Testing System For Non- Metallic Media" *National Seminar on Microwave Propagation & Antennas Dec.15-17, Department of Electronics, Cochin University of Science and Technology, Cochin, 1988.*
- 10 James Kurian, K.A. Jose, K. G. Balakrishnan, and K.G. Nair, "Microwave Non-Destructive Flaw/Defect Detection System For Non Metallic Media

- Backed Up by a Microprocessor based Instrumentation". *Proceedings of the First KERALA SCIENCE CONGRESS February, 1989, pp 325-327.*
- 11 James Kurian, K.A. Jose, K. G. Balakrishnan, and K.G. Nair, "A Novel Instrumentation for Flaw/Defect Detection Using Microwaves" , *National Seminar on Instrumentation Nov: 7-9 , Department of Physics, Cochin University of Science and Technology, Cochin-22, 1989.*
  - 12 P. Ramakrishnan, James Kurian and K.G Balakrishnan "Ferroelectric Liquid Crystals For a Better Dynamic Display", *NACONES-89, Proceedings of the National Conference on ELECTRONICS CIRCUITS and SYSTEMS, (Nov.2-4, 1989, Roorkee), Tata McGraw Hill, New Delhi, 1989, pp 160-162.*
  - 13 James Kurian, Ajayakrishnan V, Santhosh Arvind, Gopikakumari R and Sridhar C.S, "Modelling and Processing of Sonar Echo Supported by an Efficient Data Base management System", *Proceedings of SYMPOL '91 (National Symposium on OCEAN ELECTRONICS), Department of Electronics, Cochin University of Science and Technology, Cochin, 1991, pp 76-78.*
  - 14 James Kurian, K.A. Jose, K. G. Balakrishnan, and K.G. Nair, "Microwave Non-Destructive Flaw/Defect Detection System for Non-Metallic Media", *RUB-PLAS-91, seminar on Rubber and Plastics DEC: 18-20, 1991, Nehru Center, BOMBAY. Won RUBPLAS 91 EXCELLENCE AWARD FOR PROCESS INNOVATION in 1991.*
  - 15 Mariamma Chacko, James Kurian, and Paulose Jacob, "Design and Implementation of a Microcontroller Based Onboard Cockpit Display and Data Logger for Sea Going Small Crafts", *Proceedings of SMART 2000, International Conference on SHIP AND MARINE -TECHNOLOGY. Dec.19-20, Cochin ,2000, pp123-130.*
  - 16 James Kurian, K. G. Balakrishnan, and K.G. Nair, "A PC Based Non-Destructive Microwave Imaging System for Detection of Flaws/Defects in Non-Metallic Media", *Proceedings of National Conference on Technology Convergence for Information Communications & Environment (NICE 2001) conducted by IETE , Feb:23-24, Cochin, 2001, pp 213-220.*
  - 17 James Kurian, Supriya M.H & P.R.S. Pillai "Design and Implementation of a Computer Controlled Transducer Positioning system for an acoustic tank". *Proceedings of National Conference on Technology Convergence for Information Communications & Environment (NICE 2001) conducted by IETE , Feb:23-24, Cochin, 2001, pp 221-224.*

- 18 James Kurian, Supriya M.H and P.R.S. Pillai. "Design and Implementation of a Computer Controlled Transducer Positioning System for an Underwater Test Facility" *Proceedings of SYMPOL 2001 (National Symposium on OCEAN ELECTRONICS, Department of Electronics, Cochin University of Science and Technology, Cochin, December. 18-19, 2001, pp 84-88.*
- 19 Anil Kumar C.P, Sajith N Pai, Soniraj, James Kurian, Supriya M.H, C Madhavan, and P.R.S. Pillai, "Studies of Target Strengths of Fishes Under Captive Conditions", *SYMPOL 2001 National Symposium on OCEAN ELECTRONICS), Department of Electronics, Cochin University of Science and Technology, Cochin, December 18-19, 2001, pp 124-129.*
- 20 Anil Kumar C.P., Sajith N Pai, Soniraj N, P.R.Saseendran Pillai, James Kurian, C Madhavan, Supriya M.H, & T.K.Mani, "Studies on Geometrical Backscattering Models of Marine Bodies" , *The 145<sup>th</sup> Meeting of the Acoustical Society of America ; Nashville, Tennessee, USA, April 28<sup>th</sup> 2003 – May 2<sup>nd</sup> 2003.*
- 21 T.K.Mani, P.R.Saseendran Pillai, James Kurian & Supriya M.H. "Rain Parameter Estimation Using Impact Generated Low Frequency Acoustic Signals", *The 145<sup>th</sup> Meeting of the Acoustical Society of America ; Nashville, Tennessee, USA, April 28<sup>th</sup> 2003 – May 2<sup>nd</sup> 2003.*
- 22 James Kurian and P.R. Saseendran pillai, "Design and Development of a remotely operated underwater multi-robot manipulator controller", *IEEE, Oceans 2003 proceedings Vol. 1 2003 p. 355. (Marine Technology and Ocean Science Conference Sep 22-26 , San Diego, CA.)*
- 23 Binu George, Anand Raj, M.H. Supriya, James Kurian and P.R. Saseendran pillai. "Development of a spread spectrum communication system for underwater telemetry applications" *Proc on Ocean Electronics, 55-61, 2003, Allied Publishers Pvt. Limited, New Delhi.*
- 24 Sajith N. Pai, C.P.Anil Kumar. N. Soniraj, S. Balu, M.H. Supriya, James Kurian C. Madhavan and P.R. Saseendran pillai "Backscattering models of Sardines", *Proc. on Ocean Electronics, 146-149, 2003, Allied Publishers, PVT. Limited, New Delhi.*
- 25 Anil Kumar.C.P., Sajith.N.Pai, Soniraj.N., Balu.N., Supriya.M.H., James Kurian, Madhavan.C., and Saseendran Pillai.P.R "Development of an Algorithm for Biomass Estimations", *Proc. SYMPOL-2003 (National Symposium on Ocean Electronics), Allied Publishers Pvt. Ltd., New Delhi, 2003, pp.150-156.*

- 26 C.P. Anil Kumar, Sajith N. Pai, N. Soniraj, S. Balu, M.H. Supriya, James Kurian C. Madhavan and P.R. Saseendran pillai Numerical analysis for geometrical backscattering of selected marine specie “, *Proc. on Ocean Electronics, 157-161, 2003, Allied Publishers, PVT. Limited, New Delhi.*
- 27 Binu George, Anand Raj, M.H. Supriya, James Kurian and P.R. Saseendran pillai “Doppler Compensated Underwater Acoustic Communication System” *J. Acoust. Soc. Am. 115(5/pt.2) 2004, p.2507.*
- 28 Anil Kumar, C.P., Sajith. N. Pai, Soniraj. N., Supriya. M. H., James Kurian, Madhavan. C. and Saseendran Pillai. P. R. “An Echo Analysis Technique for Estimating the Fish Population” *J. Acoust. Soc. Am. 115( 5, Pt. 2 ), 2004, p. 2584.*

# INDEX

## A

Absolute, 2  
Accelerometers, 2, 4, 15, 22, 23, 29, 98  
Acoustic, 45, 54, 55  
Active ranging, 14, 42  
Actuators, 73, 145, 146  
Asimo, 11  
Attitude, 1, 3, 4, 5, 8, 9, 10, 12, 15, 22, 32, 60, 65, 69, 71, 91, 92, 93, 94, 95, 96, 97, 103, 104, 106, 107, 110, 127, 136, 139  
Automated guided vehicles, 1  
Autonomous, 1, 2, 5

## B

Beacon identification number, 65, 79, 80  
Beacons, 14, 65, 66, 79, 82, 115, 121, 124, 126, 128, 138  
Brush encoders, 14

## C

Capacitive encoders, 14  
CCD/Cmos camera(s), 14  
ChipCorder, 129, 130, 133  
Cluttered, 12, 71  
Cognition, 72  
Compass, 14, 21  
CORDIC, 9, 98, 107, 109, 110, 111, 112, 113, 137

## D

Dead reckoning, 2, 4, 21  
Detectors, 18, 74, 118, 126  
Development board, 63  
DGPS, 6, 40, 127  
Differently-able, 10, 66, 115, 127, 128, 133  
DISLiB, 9, 10, 61, 65, 66, 78, 79, 82, 86, 87, 89, 90, 91, 92, 93, 95, 115,

120, 121, 124, 126, 128, 130, 133, 136, 137, 138, 139, 140, 141

Doppler sonar, 14, 55

DSSS, 65, 83

## E

Echo, 43, 44, 48, 50

Electromagnetic, 37, 42, 48, 51, 54, 55

ELST, 64, 75, 76, 87, 88, 89, 90, 120, 124, 130, 131, 132, 139

Encoder, 97, 99, 100, 103, 111, 112

Enhancement, 69, 89

Error reduction, 9, 61, 66, 67, 106, 139

Ethernet, 143, 145, 152, 153

Exteroceptive, 13, 15, 16

## F

Flowchart, 91

FPGA, 9, 61, 66, 98, 106, 107, 109, 111, 113, 137, 139

## G

Geometry, 56, 91, 146

Givens rotation, 107

GPS, 14, 16, 34, 36, 37, 39, 40, 41, 42, 69, 127

GSM, 10, 61, 66, 116, 118, 119, 122, 133, 137

Gyros, 2, 4, 22, 24, 26, 29, 98

Gyroscopes, 13, 14, 24

## H

Hard home, 145, 148, 149, 151, 153

H-bridge, 84, 85, 143, 145, 147

Heading sensors, 14

## I

Implementation, 97, 106

Inclinometers, 14

Indoor, 2, 4, 6, 7, 8, 12, 19, 58, 61,  
66, 69, 71, 77, 82, 83, 86, 126, 127,  
135, 136, 138

Inductive encoders, 14

Inertial navigation system, 2, 23, 73,  
98

Infrared beacons, 14

Intelligent control, 10, 66, 115, 116,  
137

## **K**

Kalman filter, 7, 33, 58

Kinematics, 91, 103

## **L**

Lambertian scattering, 62, 75, 120,  
121

Landmarks, 2, 5, 6, 16, 56, 72

Laser, 7, 24, 26, 27, 28, 32, 42, 43,  
45, 46, 47, 48, 52, 55, 69, 81, 126

Laser rangefinder, 14

LCD display, 84, 133

Localization, 1, 4, 5, 6, 13, 14, 31, 32,  
69, 71, 74, 115, 128

## **M**

Magnetic encoders, 14

Map-matching, 2, 5

MEMS, 27, 29

Microcontroller, 63, 132

Micro-switches, 14

Millimeter wave, 32

Mobile robots, 2, 3, 5, 8, 13, 14, 16,  
29, 42, 43, 44, 60, 70, 72, 74, 97,  
127, 135, 136, 144

Motion sensors, 14

## **N**

Navigation, 2, 4, 5, 6, 8, 12, 14, 15,  
17, 21, 22, 23, 24, 26, 28, 31, 33,  
41, 59, 65, 67, 71, 72, 86, 91, 103,  
107, 126, 127, 128, 129, 130, 135,  
141

Northstar, 7

## **O**

Obstacle avoidance, 3, 10, 55, 57, 73,  
115, 126

Odometric, 9, 13, 14, 17, 60, 97, 98,  
99

Odometry, 2, 4, 15, 17, 24, 30, 31,  
73, 94, 95, 97, 136, 139

Optical encoders, 13, 14, 17

Optical or rf beacons, 14

Outdoor, 2, 5, 6, 40, 66, 126, 127,  
136, 138, 141

## **P**

Performance, 69, 87

Period mode, 100, 101

Position, 15, 69, 91, 97, 103, 115,  
130

Proprioceptive, 2, 4, 5, 14, 15, 17, 89,  
97

Proximity sensors, 14

Pulse mode, 100, 102

PWM, 62, 142, 147, 149, 151, 153,  
154, 155

## **R**

Radar, 14, 48, 51, 54

Radio frequency, 7, 69, 74, 81, 119

Rangefinder, 43, 45

Realization, 97, 111

Receiver, 9, 32, 33, 36, 37, 38, 40,  
43, 46, 47, 50, 53, 54, 61, 64, 65,  
66, 67, 70, 76, 78, 80, 83, 84, 86,  
87, 88, 90, 92, 94, 116, 118, 119,  
120, 123, 126, 128, 129, 130, 137,  
138, 139, 140

Redundant, 66

Reflective beacons, 14

Reflectors, 62, 75, 120

Relative, 2, 14, 19, 27, 35, 53, 54, 57,  
59, 72, 82, 97, 102

Roadmap, 1, 8

- 
- Robot vehicles, 1, 4, 8, 9, 12, 29, 57,  
60, 66, 70, 90, 97, 115, 136, 137,  
138, 140
- Robotalk, 145
- S**
- Satellite, 38
- SCARA, 143, 145, 146, 147, 154,  
156
- Sensors, 13, 14, 15, 17, 21, 53, 55, 73
- SLAM, 6, 9, 59, 60
- Sonar, 14, 43, 54
- Spacecraft, 3
- SPI, 21, 29, 61, 66, 83, 107, 111, 112,  
124, 129
- Steering, 9, 17, 84, 91, 92, 93, 94, 95,  
96, 99, 103, 106, 137
- Structured light, 13, 14, 52
- T**
- Tactile sensors, 13, 14, 16
- Traffic control, 10, 55, 61, 85, 115,  
117, 119, 123, 133, 140
- Transmitter, 61, 64, 79
- Transportation, 10, 66, 115, 116, 117,  
118, 133, 136, 137
- Triangulation, 32, 35
- Trilateration, 32, 33, 34
- U**
- UART, 21
- Ultrasonic beacons, 14
- V**
- Vision sensors, 14
- Visual guidance system, 13, 57
- Visually impaired, 10, 61, 67, 115,  
126, 127, 128, 129, 130, 132, 133,  
138, 140
- X**
- XR4, 143, 145, 146, 154, 156